

Residence time distribution studies in a reactor with recycle

Thesis submitted
in partial fulfillment for the award
of the degree
of

Doctor of Philosophy

in

CHEMICAL ENGINEERING

By

Arghya Datta
(Registration No.: 901501004)

Under the guidance of

Dr. Raj Kumar Gupta
Professor
Department of Chemical Engineering,
Thapar Institute of Engineering &
Technology, Patiala

Dr. Haripada Bhunia
Professor
Department of Chemical Engineering,
Thapar Institute of Engineering &
Technology, Patiala



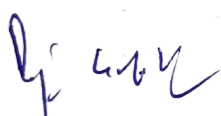
DEPARTMENT OF CHEMICAL ENGINEERING
THAPAR INSTITUTE OF ENGINEERING & TECHNOLOGY
(Deemed to be University)
PATIALA-147004, PUNJAB, INDIA

June 2021

Certificate

This is to certify that thesis entitled “**Residence time distribution studies in a reactor with recycle**” being submitted by **Mr. Arghya Datta** to the Department of Chemical Engineering, Thapar Institute of Engineering & Technology (Deemed to be University), Patiala for the award of degree of **Doctor of Philosophy** is a record of bonafide research work carried out by him. **Mr. Arghya Datta** has worked under our guidance and supervision. He has fulfilled the requisite standard for the submission of the thesis.

To the best of our knowledge, the matter embodied in this thesis has not been submitted to any other university/institute for the award of any degree or diploma.



Dr. Raj Kumar Gupta
Professor
Department of Chemical Engineering,
Thapar Institute of Engineering &
Technology, Patiala, Punjab, India



Dr. Haripada Bhunia
Professor
Department of Chemical Engineering,
Thapar Institute of Engineering &
Technology, Patiala, Punjab, India

Acknowledgments

I express my deep and sincere gratitude and profound regards to **Prof. Raj Kumar Gupta**, and **Prof. Haripada Bhunia**, Department of Chemical Engineering, Thapar Institute of Engineering and Technology (Deemed to be University) for providing me an opportunity to work under their guidance. Their wide knowledge, expertise, valuable suggestions, encouragement and freedom of independent work provided a platform for learning and performing research. Their enthusiasm and optimism made this experience both rewarding and enjoyable. Their feedback and editorial comments were also valuable for the writing of this thesis.

I am extremely thankful to **Prof. Prakash Gopalan**, Director, **Shri. Gurbinder Singh**, Registrar, **Prof. Rafat Siddique**, Dean of Research and Sponsored Projects, **Prof. Satvinder Singh Bhatia**, Dean of Academic Affairs, and **Prof. Haripada Bhunia**, Head, Department of Chemical Engineering, Thapar Institute of Engineering and Technology (Deemed to be University) for giving necessary approvals and kind support to perform this research work.

I would like to thank my doctoral committee members **Dr. Sanjeev Kumar Ahuja**, Associate Professor, Department of Chemical Engineering, **Dr. Sudhir Kumar Singh**, Associate Professor, Department of Chemical Engineering, and **Dr. Amit Dhir**, Associate Professor, School of Energy and Environment, Thapar Institute of Engineering and Technology (Deemed to be University) for their guidance and support throughout the duration of this work. I would also like to express my sincere gratitude to **Dr. Pramod Kumar Bajpai**, Ex-Distinguished Professor, for providing guidance and support for successfully conducting this work.

I would like to thank **all the faculty members** of the Department of Chemical Engineering, Thapar Institute of Engineering and Technology (Deemed to be University) for encouraging me to write the thesis report. I would also like to thank **all the staff members** of the Department of Chemical Engineering, Thapar Institute of Engineering and Technology (Deemed to be University) for their everlasting support.

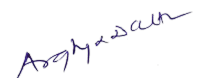
I am extremely thankful to **Dr. Harish Jagat Pant** and his team members **Dr. Vijay Kumar Sharma**, and **Dr. Sunil Goswami**, Isotope and Radiation Applications Division, Bhabha

Atomic Research Centre for providing radiotracer and valuable guidance and support during industrial experiments.

I sincerely thank **DAE-BRNS, Government of India** and **Thapar Institute of Engineering and Technology (Deemed to be University), Patiala** for providing necessary financial support.

I express my deep sense of gratitude to my family. I am thankful to my parents **Mrs. Dipa Datta** and **Mr. Rasamay Datta** for their great support throughout my life. I would also like to thank my sister **Mrs. Jaya Datta Kayet** for her prayers and love.

I would like to thank all my colleagues and friends **Dr. Metali Sarkar, Dr. Meenakshi, Dr. Dev Kumar Mandal, Dr. Kamaljeet Singh, Dr. Deepak Tiwari, Mr. Saudagar Dongare** and **Mr. Sunil Sable** for their support and encouragement in carrying out my research smoothly.


Arghya Datta

Abstract

Residence time distribution (RTD) studies are of immense importance in process industries as they provide valuable information regarding the flow behavior in process equipment and can help with their real time diagnosis. In the present work, two sets of RTD studies were carried out in an industrial-scale ethyl acetate reactor system consisting of two reactors in series with a large recycle ratio and recirculation as a mean of external mixing. ^{82}Br as ammonium bromide was used as the radiotracer for the RTD experiments. The individual reactors and the reactor system were modeled using basic RTD building blocks, like, continuously stirred tank reactor (CSTR) and plug flow reactor (PFR) to map the experimental RTD curves. RTD experiments were also performed on a laboratory-scale reactor system to study the effect of recirculation and recycle on the flow behavior.

In the first set of industrial RTD studies, the results showed that the recirculation rate had a significant effect on the flow mixing behavior and mean residence time (MRT) in the reactor system. The experimental RTD curves showed that there was bypassing (12% - 22%) of the fluid in the first reactor at different operating conditions. MRT of the reactor system 1 (comprising of reactor R1 and reactor R2), decreased from 17 h to 10 h with decrease in recirculation flow. A stagnant volume of 40% inside the first reactor, exchanging fluid with the active volume, gave the best fit between experimental and model predicted RTD curves. The second reactor, however, behaved very closely to a CSTR at different operating conditions. Before the second set of RTD experiments was conducted, the reactor system was modified by the industry to accommodate any future increase in the production capacity of the plant. In the new reactors system (reactor system 2), reactor R1 had a horizontal orientation and reactor R2 had vertical orientation. Flow rates, working volume and other process parameters were kept the same as for the reactor system 1.

The second set of industrial experiments was performed on the new reactor system (reactor system 2). The results showed the presence of bypassing (18% - 32%) of process fluid in the first reactor, and bypass of 2% - 15% was observed in the second reactor, at different operating conditions. MRT for the reactor system 2, decreased from 26 h to 18 h when the recirculation to both the reactors decreased. The model results predicted the presence of stagnant volume (with fluid exchange) in both the reactors corresponding to the best fit between the experimental and model predicted RTD curves. In the first reactor, 5%-15%, and in the second reactor, 5%, stagnant volumes (with fluid exchange) were predicted

corresponding to the best fit between the experimental and model predicted RTD data at different operating conditions.

In the laboratory-scale reactor system, RTD experiments were performed with varying recycle and recirculation rates to see their effect on mean residence time (MRT), flow bypassing and stagnant volume in the reactor. A computer program was developed to solve the model equations using fourth-order Runge-Kutta method. A low bypass flow (<5%) was observed from the experimental RTD curves obtained at different operating conditions. A change in the MRT from 1.2 h to 1.8 h was observed at different recycle and recirculation rates. At maximum recycle and maximum recirculation, in the study ranges, a 37% stagnant volume (with exchange) was predicted. In the absence of recycle and recirculation, a 53% stagnant volume (with exchange) was predicted corresponding to the best fit of the experimental RTD data. The results of the laboratory-scale RTD studies were also compared qualitatively with the results obtained from industrial RTD experiments.

Fig. 1 shows the schematic of the methodology followed for overall thesis.

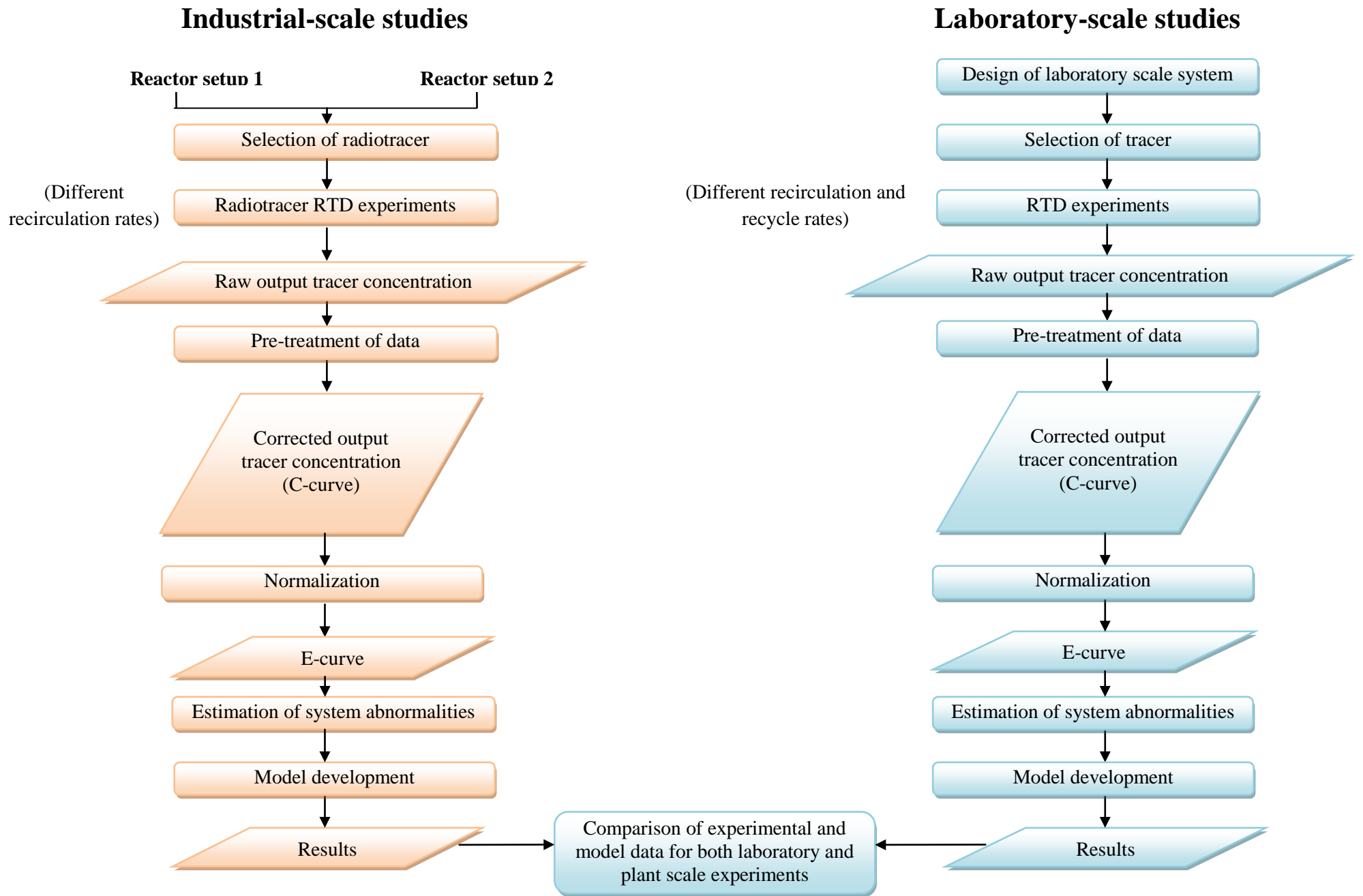


Fig. 1 Schematic of the methodology of residence time distribution studies in a reactor with recycle

Table of contents

CERTIFICATE	ii
ACKNOWLEDGMENTS	iii
ABSTRACT	v
TABLE OF CONTENTS	viii
LIST OF FIGURES	xi
LIST OF TABLES	xiv
LIST OF SYMBOLS	xvi
LIST OF ABBREVIATIONS	xx
Chapter-1 Introduction	1
1.1 Recycling and its importance	3
1.2 Mixing by recirculation	3
1.3 Residence time distribution	4
1.3.1 Suitability of tracers	5
1.3.2 Conventional tracers	6
1.3.3 Radiotracers	7
1.3.3.1 Advantages of using radiotracers	7
1.3.3.2 Safe handling of radiotracers	8
1.3.3.3 Tracer technique	9
1.3.3.4 Pre-treatment of data	9
1.3.4 Characteristics of RTD	10
1.4 Thesis motivation and objectives	10
1.5 Thesis overview	11
Chapter-2 Literature review	13
2.1 Experimental RTD studies on various systems	14
2.1.1 Fluidized beds	14
2.1.2 Packed beds	16
2.1.3 Trickle beds	18
2.1.4 Micro-reactors	19
2.1.5 Bio-reactors	20
2.1.6 Polymer and glass production systems	22
2.1.7 Pilot-scale systems	23
2.2 Experimental RTD studies on recycle systems	24

2.3	RTD theories on recycle systems	25
Chapter-3 Materials and methods		30
3.1	Materials	31
3.1.1	Software used	31
3.2	Methodology	32
3.2.1	Selection of the tracer	32
3.2.2	RTD experiments	32
3.2.2.1	Industrial RTD experiments	32
3.2.2.2	Laboratory-scale RTD experiments	34
3.3.3	Data pre-treatment	35
Chapter-4 RTD experiments on industrial reactor system 1		37
4.1	Plant/process description	38
4.2	Pre-treatment of the radiotracer data	40
4.3	RTD analysis	44
4.4	Reactor R1	45
4.4.1	Model conceptualization	45
4.4.2	Effect of recirculation on MRT, bypassing and stagnant volume	46
4.5	Reactor R2	48
4.5.1	Model conceptualization	48
4.5.2	Data convolution	49
4.5.3	Effect of recirculation on MRT, bypassing and stagnant volume	49
4.6	Reactor system 1	51
4.6.1	Model conceptualization	51
4.7	Uncertainty analysis	54
Chapter-5 RTD experiments on industrial reactor system 2		55
5.1	Pre-treatment of the radiotracer data	58
5.2	RTD analysis	61
5.3	Reactor R1	61
5.3.1	Model conceptualization	62
5.3.2	Effect of recirculation on MRT, bypassing and stagnant volume	62
5.4	Reactor R2	65
5.4.1	Model conceptualization	65
5.4.2	Data convolution	66

5.4.3 Effect of recirculation on MRT, bypassing and stagnant volume	66
5.5 Reactor system 2	68
5.5.1 Model conceptualization	68
5.6 Uncertainty analysis	71
Chapter-6 RTD experiments on laboratory system	72
6.1 Process flow description	73
6.2 RTD analysis	75
6.3 Model development	75
6.3.1 Model equations and solution	77
6.4 Effect of recirculation and recycle on MRT	85
6.5 Effect of recirculation and recycle on bypassing	86
6.6 Effect of recirculation and recycle on stagnant volume	87
6.7 Statistical analysis	88
6.8 Uncertainty analysis	91
Chapter-7 Conclusions and recommendations	92
7.1 Conclusions	93
7.2 Recommendations for future work	94
References	96
List of publications	103

List of figures

Figure No.	Title	Page No.
1	Schematic of the methodology of residence time distribution studies in a reactor with recycle	vii
4.1	Schematic of industrial reactor system 1 showing the detector positioning	39
4.2	Reactor R1 (a) and reactor R2 (b) of industrial reactor system 1	40
4.3	Raw and pre-treated tracer counts for detector D2 (Run 1)	41
4.4	Raw and pre-treated tracer counts for detector D5 (Run 1)	41
4.5	Raw and pre-treated tracer counts for detector D2 (Run 2)	42
4.6	Raw and pre-treated tracer counts for detector D5 (Run 2)	42
4.7	Raw and pre-treated tracer counts for detector D2 (Run 3)	43
4.8	Raw and pre-treated tracer counts for detector D2 (Run 3)	43
4.9	Conceptual model of reactor R1	46
4.10	Comparison of experimental and model predicted RTD curves for reactor R1 (Run 1)	47
4.11	Comparison of experimental and model predicted RTD curves for reactor R1 (Run 2)	47
4.12	Comparison of experimental and model predicted RTD curves for reactor R1 (Run 3)	48
4.13	Conceptual model of reactor R2	49
4.14	Comparison of experimental and model predicted RTD curves for reactor R2 (Run 1)	50
4.15	Comparison of experimental and model predicted RTD curves for reactor R2 (Run 2)	50
4.16	Comparison of experimental and model predicted RTD curves for reactor R2 (Run 3)	51
4.17	Conceptual model of reactor system 1	52
4.18	Comparison of experimental and model predicted RTD curves for reactor system 1 (Run 1)	52
4.19	Comparison of experimental and model predicted RTD curves for reactor system 1 (Run 2)	53
4.20	Comparison of experimental and model predicted RTD curves for	

	reactor system 1 (Run 3)	53
5.1	Schematic of industrial reactor system 2 showing the detector positioning	57
5.2	Reactor R1 (a) and reactor R2 (b) of industrial reactor system 2	57
5.3	Raw and pre-treated tracer counts for detector D2 (Run 1)	58
5.4	Raw and pre-treated tracer counts for detector D5 (Run 1)	59
5.5	Raw and pre-treated tracer counts for detector D2 (Run 2)	59
5.6	Raw and pre-treated tracer counts for detector D5 (Run 2)	60
5.7	Raw and pre-treated tracer counts for detector D2 (Run 3)	60
5.8	Raw and pre-treated tracer counts for detector D5 (Run 3)	61
5.9	Conceptual model of reactor R1	62
5.10	Comparison of experimental and model predicted RTD curves for reactor R1 (Run 1)	63
5.11	Comparison of experimental and model predicted RTD curves for reactor R1 (Run 2)	64
5.12	Comparison of experimental and model predicted RTD curves for reactor R1 (Run 3)	64
5.13	Conceptual model of reactor R2	66
5.14	Comparison of experimental and model predicted RTD curves for reactor R2 (Run 1)	67
5.15	Comparison of experimental and model predicted RTD curves for reactor R2 (Run 2)	67
5.16	Comparison of experimental and model predicted RTD curves for reactor R2 (Run 3)	68
5.17	Conceptual model of reactor system 2	69
5.18	Comparison of experimental and model predicted RTD curves for reactor system 2 (Run 1)	69
5.19	Comparison of experimental and model predicted RTD curves for reactor system 2 (Run 2)	70
5.20	Comparison of experimental and model predicted RTD curves for reactor system 2 (Run 3)	70
6.1	Laboratory-scale reactor system	74
6.2	Schematic of the laboratory-scale reactor system	74

6.3	Calibration curve for sodium chloride	75
6.4	Conceptual model of the laboratory-scale reactor system	76
6.5	Comparison between experimental and model predicted RTD curves for run 1-4 at recycle rate of 120 l/h	80
6.6	Comparison between experimental and model predicted RTD curves for run 5-8 at recycle rate of 80 l/h	80
6.7	Comparison between experimental and model predicted RTD curves for run 9-12 at recycle rate of 40 l/h	81
6.8	Comparison between experimental and model predicted RTD curves for run 13-16 at recycle rate of 0 l/h	81
6.9	Effect of recirculation rate on MRT of reactor system at different recycle rates	86
6.10	Effect of recirculation rate on bypass percentage of reactor system at different recycle rates	87
6.11	Effect of recirculation rate on stagnant volume fraction of main reactor at different recycle rates	88

List of tables

Table No.	Title	Page No.
2.1	RTD studies in fluidized beds	15
2.2	RTD studies in packed beds	17
2.3	RTD studies in trickle beds	19
2.4	RTD studies in micro-reactors	20
2.5	RTD studies in bio-reactors	21
2.6	RTD studies in polymer and glass production systems	23
2.7	RTD studies in pilot-scale systems	24
2.8	RTD studies in recycle systems	25
2.9	Theoretical RTD studies on recycle systems	29
3.1	Conditions for RTD experiments on industrial reactor system 1	33
3.2	Conditions for RTD experiments on industrial reactor system 2	34
3.3	Conditions for RTD experiments on laboratory-scale reactor system	35
4.1	Results of the RTD model of reactor R1	48
4.2	Results of the RTD model of reactor R2	51
4.3	Results of the RTD model of reactor system 1	54
5.1	Experimental and model predicted MRT for reactor R1	65
5.2	Model predicted bypass parameters for reactor R1	65
5.3	Model predicted stagnant volume parameters for CSTR A	65
5.4	Model predicted recycle parameters for reactor R1	65
5.5	Model predicted parameters for reactor R2	68
5.6	Experimental and model predicted MRT for reactor system 2	71
5.7	Model predicted bypass parameters for reactor system 2	71
5.8	Model predicted stagnant volume parameters for reactor system 2	71
5.9	Model predicted recycle parameters for reactor system 2	71
6.1	Comparison of experimental, model predicted and theoretical MRT for reactor system	82
6.2	Model predicted bypass parameters for reactor system	82
6.3	Model predicted parameters for stagnant volume in main reactor	82
6.4	Model predicted parameters for active volume in main reactor	83
6.5	Model predicted parameters for recirculation in main reactor	83

6.6	Model predicted parameters for stagnant volume of reactor in recycle line	84
6.7	Model predicted parameters for active volume of reactor in recycle line	84
6.8	Statistical analysis of MRT (s) for reactor system	89
6.9	Statistical analysis of the bypass percentage for reactor system	89
6.10	Statistical analysis of the fraction of stagnant volume of main reactor to the total volume of main reactor	90

List of symbols

^{198}Au	Gold with mass number 198
^{82}Br	Bromine with mass number 82
c_0	Concentration of the fresh feed tracer impulse input (laboratory system)
c_1	Output concentration of the reactor system and also input to active volume of the reactor in recycle line (laboratory system)
^{14}C	Carbon with mass number 14
C1A-B	Distillation columns 1A and 1B in the ethyl acetate plant (industrial system)
$\text{C}_2\text{H}_5\text{OH}$	Ethanol
c_b	Concentration of the output stream from bypass CSTR (laboratory system)
c_d	Output concentration of flow from stagnant volume entering active volume of the main reactor (laboratory system)
$\text{CH}_3\text{COOC}_2\text{H}_5$	Ethyl acetate
CH_3COOH	Acetic acid
c_m	Output concentration from the active volume of main reactor (laboratory system)
CO_2	Carbon dioxide
^{60}Co	Cobalt with mass number 60
c_r	Concentration of the output stream of active volume of the reactor in recycle line (laboratory system)
c_{rc}	Output concentration of flow from recirculation pump volume entering the active volume of the main reactor (laboratory system)
c_{rd}	Output concentration of the flow from stagnant volume to active volume of the reactor in recycle line (laboratory system)
^{137}Cs	Cesium with mass number 137
c_y	Concentration of the input stream to bypass CSTR (laboratory system)
c_z	Concentration of the input stream to the active volume of main reactor (laboratory system)
D1-8	Nal(Tl) detectors No. 1 to 8 (industrial system)
D1-2	Detectors 1 and 2 (conductivity meter probes) used in laboratory system
$E(t)$	Normalized tracer concentration
H_2O	Water

${}^3\text{H}$	Hydrogen with mass number 3
HCl	Hydrochloric acid
He	Helium
${}^{131}\text{I}$	Iodine with mass number 131
KCl	Potassium chloride
${}^{140}\text{La}$	Lanthanum with mass number 140
LiCl	Lithium chloride
${}^{56}\text{Mn}$	Manganese with mass number 56
${}^{24}\text{Na}$	Sodium with mass number 24
NaCl	Sodium chloride
NaI(Tl)	Sodium iodide doped with thallium
NaOH	Sodium hydroxide
$n_c(t)$	Corrected tracer concentration (gamma count) at any time t
$n_m(t)$	Original tracer count (gamma count) at any time t
O_3	Ozone
RI-2	Ethyl acetate reactor No. 1 and 2 (industrial system)
R^2	Regression coefficient
SiC	Silicon carbide
T	Random time variable
\bar{t}	Experimental mean residence time
$T_{1/2}$	Half life of the radiotracer used
${}^{99}\text{Tc}$	Technetium with mass number 99
${}^{99m}\text{Tc}$	Technetium (meta-stable) with mass number 99
V	Volume of the reactor system(laboratory system)
v_0	Fresh feed flow rate(laboratory system)
v_a	Flow rate of the stream entering the active volume of main reactor(laboratory system)
V_A	Volume of the active region of the main reactor (laboratory system)
v_b	Flow rate of the stream entering the bypass CSTR(laboratory system)
V_B	Bypass CSTR volume (laboratory system)
v_d	Flow rate of the stream from active volume to the stagnant volume of the main reactor (laboratory system)
V_D	Stagnant volume of main reactor (laboratory system)

v_d'	Flow rate of the stream from the stagnant volume to the active volume of main reactor (laboratory system)
v_r	Recycle flow rate(laboratory system)
V_R	Active volume of the reactor in recycle line (laboratory system)
v_{rc}	Recirculation flow rate (laboratory system)
V_{RC}	Volume of the recirculation CSTR (laboratory system)
v_{rd}	Flow exchange rate between stagnant volume and active volume of the reactor in recycle line (laboratory system)
V_{RD}	Stagnant volume of the reactor in recycle line (laboratory system)
$X(t)$	Input tracer count curve
$Y(t)$	Output tracer count curve

Greek letters

α	Ratio of flow rate of the stream entering the active volume of main reactor and fresh feed flow rate(laboratory system)
β	Ratio of flow rate of the stream entering the bypass CSTR and fresh feed flow rate(laboratory system)
γ	Ratio of flow rate of the stream from active volume to the stagnant volume of the main reactor and fresh feed flow rate(laboratory system)
δ	Ratio of recycle flow rate and fresh feed flow rate (laboratory system)
ε	Ratio of active volume of main reactor and total reactor volume(laboratory system)
η	Ratio bypass volume of main reactor and total reactor volume(laboratory system)
θ	Ratio of stagnant volume of main reactor and total volume of the reactor system (laboratory system)
κ	Ratio of stagnant volume in the main reactor and main reactor volume(laboratory system)
λ	Ratio of active volume of the reactor in recycle line and total volume of the reactor system (laboratory system)
μ	Ratio of volume of the recirculation CSTR and total volume of the reactor system (laboratory system)
π	Ratio of flow rate from stagnant volume to active volume of main reactor and fresh feed flow rate(laboratory system)
ρ	Ratio of flow exchange rate between active volume and stagnant volume in reactor in recycle line and fresh feed flow rate(laboratory system)
τ	Theoretical mean residence time of the reactor system (laboratory system)
φ	Ratio of stagnant volume of the reactor in recycle line and total volume of the reactor system (laboratory system)
ω	Ratio of recirculation flow rate and fresh feed flow rate (laboratory system)

List of abbreviations

ACS	American Chemical Society
ALARA	As low as reasonably possible – safety principle to handle radioisotopes
ANOVA	Analysis of variance
BARC	Bhabha Atomic Research Centre
CFD	Computational fluid dynamics
CSTR	Continuous stirred tank reactor
CTD	Cycle time distribution
EXPT.	Experimental
F-Crit	Critical F-value
IAEA	International Atomic Energy Agency
IOLCP	IOL Chemicals and Pharmaceuticals Limited, Barnala, India
L/D	Ratio of length to diameter of a vessel
MRT	Mean residence time
MSMPR	Mixed-suspension, mixed-product-removal
OFAT	One factor at a time
PFR	Plug flow reactor
RMSE	Root mean square error
RSS	Root sum squared
RTD	Residence time distribution
Sv	Sievert (derived S.I unit of ionizing radiation dose)
TRAM	Tubular reactor vessel with axial mixing
THEO.	Theoretical
TRRTD	Total regional residence time distribution
VFD	Variable Frequency Drive

CHAPTER-1

Chapter-1 Introduction

Chemical Industries are the backbone of any major economy. They transform natural raw materials into a wide variety of products used for the betterment of mankind [1,2]. In chemical industries, the raw materials undergo a series of steps that include physical treatments and chemical reactions to finally give desirable product(s) [1]. In order to keep the manufacturing process economical and cause less harm to the environment, it is very important to know and rectify abnormalities in the process equipment [3,4]. RTD studies can prove to be very beneficial in detecting and quantifying these abnormalities. RTD is a statistical method based on stimuli-response experiments to prepare a distribution of residence time of the particles of the process fluid, which in turn gives a quantitative idea of the deviation from ideality in the reactor [5].

In order to achieve a total conversion of reactants, recycling a part of the reactor product is performed in most of the process industries. Recycling of the process material has become a prevalent practice in process industries today due to its usefulness in saving precious energy and resources. Also, one of the other important factors in any process industries is the use of proper mixing techniques in reactors. Good mixing techniques also help with energy and resource economy as it increases the conversion of reactants to products. Generally, internal mixing techniques like impellers and agitators are used in process industries but in some cases like in bioreactors, the use of external mixing techniques like recirculation is preferred. Recycling and mixing techniques can affect the flow behavior inside a reactor. RTD techniques can help to determine the changes in flow behavior due to recycling and mixing techniques.

Conducting industrial RTD studies with conventional tracers without hampering the manufacturing process and the quality of the product is one of the most important problems faced by engineers. Conventional tracers can cause problems in such cases as they have low detection capabilities and also can hamper the quality of the product. Radiotracers are beneficial in such circumstances as they have high detection capabilities and they can be used in minute quantities without hampering the product quality. Also, due to radioactive decay, the radiotracer concentration automatically falls below the accepted level in process material in a short time which keeps the product quality at an acceptable level.

In the present work, industrial RTD studies were performed at the ethyl acetate plant of IOL Chemicals and Pharmaceuticals Limited, Barnala, Punjab, India. Ethyl acetate is an organic compound with a fruity smell and widely used as an extraction solvent in the production of surface coatings and thinners, antibiotics, food flavors, and essences, polyester films, etc [6,7]. It has low solubility in water and high solubility in other organic solvents. The reactors at the ethyl acetate plant receive a large recycle from the bottom product of the distillation columns following the reactors. Also, the external mixing technique of recirculation is used to cause mixing inside the ethyl acetate reactors. In this work, RTD studies were performed to see the effect of recirculation and recycle on the flow behavior of reactors. Also, laboratory-scale RTD experiments were performed to study the effect of recirculation on reactor behavior at various recycle rates.

1.1 Recycling and its importance

Recycling in the chemical industry is the process where a portion of the outlet of a process unit is combined with fresh feed and sent into the same unit again. Recycling of reactor contents is a prevalent practice in many industrial processes. Recycling has many advantages and is the most practical way to achieve full conversion taking into consideration the reaction thermodynamics and kinetics [2]. Recycling is beneficial in cases of side (successive or parallel) reactions to achieve maximum conversion [2]. In addition, recycling of reactor products helps to properly utilize the heat generated during the reaction at other parts of the plant [2]. Thus recycling help decrease the cost of equipment, the area of plant required, fuel costs among other expenditures considerably. Generally, in the process industries recycle flow is kept as a fraction of the feed flow. A recycle flow larger than the feed flow becomes necessary when there are more unreacted feed components in the product. The reactors at the ethyl acetate plant of IOLCP Ltd., Barnala, India receive a large recycle flow (recycle/feed ratio = 3.57) from the bottom product of two parallel distillation columns. The bottom product of the distillation columns contains mostly unreacted feed along with the catalyst and recycling helps increasing the conversion of unreacted feed into ethyl acetate.

1.2 Mixing by recirculation

Generally, in industries internal mixing mechanisms with impellers (radial and axial) like Rushton, hydrofoil mixers, etc. are used to cause mixing inside reactors. But in certain cases where contamination from physical agitators could pose a problem, external mixing

mechanisms are used. Recirculation is a type of external mixing in reactors where the reactor contents are returned to the reactor at high flow rates to cause turbulence inside the reactor and thereby help with mixing. Recycling varies from recirculation in the way that recycle flow can be brought back to the reactor from any other process equipment outflow but recirculation flow is always taken from the reactor where it is supposed to cause turbulence. Recirculation is generally performed by strategically placing branches of jet sprayer or nozzles inside the reactor in various geometry which forces (using recirculation pumps) jets or fast-moving stream of reactor content into the slow-moving liquid [8], thus facilitating mixing. Turbulence caused by recirculation of the reactor contents decreases the chance of contamination inside the reactor which is of utmost importance in bio-reactors [9,10]. Recirculation can also be beneficial for solid suspension, e.g. leaching or crystallization, liquid blending, and gas-liquid mass transfer [10]. Also, unlike impellers and other agitators, the absence of moving components on the interior of the reactor makes it easier to maintain and thereby economical as compared to other forms of mixing [9,10]. Mixing by recirculation is used in the ethyl acetate reactors at IOLCP Ltd., Barnala, India to mix the contents inside the reactors. A recirculation pump forces the reactor contents back to the reactor through a system of nozzles inside the reactor which causes the turbulence.

1.3 Residence time distribution

The choice of reactors for any chemical process is one of the basic tasks that a process design engineer has to undertake even before planning the recycling of reactor product(s). Chemical reactors are vessels where the chemical reactions take place. A reactor is designed to behave either as a plug flow reactor (PFR) or as a continuously stirred tank reactor (CSTR) depending upon the process and kinetics of the reaction(s) [5,11]. The reactors are always designed as ideal reactors, but in actual operating conditions the flow patterns deviate from the designed ideal flow patterns due to the occurrence of abnormalities such as bypassing, stagnant zones, channeling, etc. [11]. These abnormalities cause deviation in the flow patterns and eventually lead to deterioration in product quality and reduction in process efficiency causing a significant economic loss for the industry and can even pose a threat to the environment [3,4].

Measurement and analysis of RTD of process material is an important approach for identifying the aforementioned abnormalities, and to investigate hydrodynamics of process equipment in the chemical process industry. The approach is very reliable and provides

valuable information about the performance of process equipment like reactors, columns, etc. [5,12]. The approach is also used for evaluation or optimization of the design of the laboratory or pilot-scale system. RTD is a statistical operation where the distribution of residence time of the particles inside the reactor gives a clear idea of the behavior of the process fluid. The distribution can accurately calculate bypassing flow, stagnant volume and the actual mean residence time of the reactor.

RTD studies can prove to be a very important tool in industrial systems where the accurate real-time knowledge of abnormalities in the reactor can prove to be economical and safe. RTD studies had been successfully performed in many industries namely oil and gas, pharmaceutical, bioprocess, polymer, etc. to accurately find out different abnormalities in the process equipment [13]. In this study, RTD studies were performed on-site at the ethyl acetate plant of IOLCP Ltd., Barnala, Punjab, India to see the effect of recirculation flow in the flow behavior inside the reactors. RTD studies were also performed at a laboratory-scale recycle reactor with recirculation setup to find out the effect of recycle, and recirculation on the flow behavior of the reactor system.

1.3.1 Suitability of tracers

The choice of tracer is the first and most important component of any RTD experiment [5]. A perfect tracer should be able to completely mimic the properties of the process fluid and get detected easily. Broadly, there are two types of tracers that are used in the RTD experiments - conventional tracers and radiotracers [14-16]. Conventional tracers can be of various types e.g. dyes, salts, acids, bases, etc. Radiotracers are radioactive isotopes of different elements that are produced artificially in nuclear reactors, particle accelerators, etc.

Before a tracer is used in an RTD experiment, it is examined for its suitability. Among the many criteria, the most important is that the tracer should be non-reactive and easy to detect [11]. Tracer is also expected to mimic the physical properties of the process fluid and should be highly soluble in it [11]. Also, the tracer should be non-adsorbing i.e. shouldn't stick to the reactor or pipe surfaces causing loss of tracer [11].

For radiotracers, in addition to the earlier mentioned suitability criteria, a radiotracer is also chosen based on its half-life, type, energy, specific activity and handling of the radiotracer [16]. In systems, where the RTD experiments can continue for a long time e.g. in industrial systems, or where radiotracer needs to be transferred to a remote location, it is important to

have a radiotracer with half-life compatible to the duration of RTD experiments to prevent unnecessary decay loss. Type, energy and specific activity of a radiotracer are also important depending upon the method of detection. In industrial experiments generally, gamma-emitting radiotracers above 140 keV are used as they can be detected via scintillation detectors from outside the pipe-lines and reactors [16]. Gamma radiation can easily penetrate the thick construction material from which the process plant equipment and pipelines are made.

1.3.2 Conventional tracers

Conventional tracers are used extensively in laboratory setups. There are mainly three types of conventional tracers used in RTD experiments:

- Dyes – Use of dye as a tracer is based on the principle that the absorbance of light by the dye is proportional to the concentration of dye in the liquid sample. Once a small amount of tracer is introduced into the system, the output concentration of the tracer can be calculated via the absorbance of light measured by a spectrophotometer. Using dye as a tracer poses some problems such as at low concentrations dyes can give unsatisfactory results, high fluorescent dye concentration can be carcinogenic and at high pH or at any other conditions the dye can lose their molecular integrity and give erroneous results to name a few [17].
- Acids/bases – Acids/bases are generally used as a tracer in those systems where a small change in pH doesn't affect the working of the system [17]. The output pH of the outflow from the system is proportional to the concentration of acid/base (tracer) and can be used to calculate the RTD of the system.
- Salts –Salts or electrolytes are the most commonly used tracers for RTD experiments. They are easier to handle and cheap. They can also be detected in small quantities [17]. The conductivity of the output flow is proportional to the concentration of the salt (tracer) and can be used to get the system's output tracer concentration to calculate the RTD.

Conventional tracers are relatively cheap and their safety protocols are simple as compared to radiotracers. Conventional tracers and their data acquisition systems are also comparatively

cheap and not as complex as the radiotracers. In the present work, RTD studies performed at the laboratory-scale reactor system used sodium chloride (NaCl) as a tracer.

1.3.3 Radiotracers

Radioisotopes are broadly classified into two categories - natural and artificial. Artificial radioisotopes are generally made in particle accelerators and nuclear reactors. Generally, artificial radioisotopes are used as radiotracers in RTD experiments as they have shorter half-lives compared to naturally occurring radioisotopes. Shorter half-lives are helpful for the natural and safe disposal of the radiotracer.

Depending upon the usage, radiotracers are classified into intrinsic and extrinsic tracers. In situations where the tracer is required to have a similar chemical identity of the traced substance, intrinsic radiotracers are used. They are mostly used in kinetics studies of a reaction, solubility studies, vapor pressure experiments, etc. [16]. $^1\text{H}^3\text{HO}$ to trace H_2O , $^{24}\text{NaOH}$ to trace NaOH , $^{14}\text{CO}_2$ for CO_2 , etc. are a few examples of intrinsic radiotracers. In situations, where the radiotracer is only expected to mimic the physical properties of the traced substance, like in RTD experiments or to trace the flow of water in a water canal, extrinsic radiotracers are used [16]. Some commonly used extrinsic radiotracers are ^{24}Na , ^{198}Au , ^{82}Br etc. In the present study, ^{82}Br in the form of ammonium bromide was used as the radiotracer for the RTD experiments performed on-site at the ethyl acetate plant of IOLCP Ltd., Barnala, India.

1.3.3.1 Advantages of using radiotracers

There are several advantages of using radiotracers over conventional tracers for RTD studies. Radiotracers can be detected even at minuscule concentrations for instance 1 Ci of ^{131}I weighs only $8\mu\text{g}$ [16]. A radiotracer that emits gamma radiation can also be used for online RTD studies in industries as it can be detected from outside of pipelines and vessels [16]. As radiotracers undergo radioactive decay along with the advantage of having to use an extremely small quantity (concentration) they don't disturb the dynamics of the process of any system and also allow repeatability of the experiments [16]. Radiotracers have their characteristic radiation signatures and this trait can be used in cases where there is a need to use more than one tracer. Spectroscopy, in this case, helps with measuring the emissions (e.g. gamma) from these radiotracers [16]. These characteristics of radiotracer make it an extremely viable candidate as a tracer to be used for RTD study in the industries where it is

imperative not to disturb the process, product, and environment in any way. Although there are many advantages of using radiotracers, there are a few disadvantages as well. Radiotracers should always be handled by trained professionals. Radiotracers are not as cheap as compared to dyes and salts. Proper disposal of waste needs to be taken care of after radiotracer use.

1.3.3.2 Safe handling of radiotracers

Radiotracers can be potentially hazardous to health as they emit ionizing radiation. Thus, adequate measures should be taken to protect personnel from its harmful effects. In order to restrict the exposure of harmful radiation from radiotracers, the most fundamental rules of decrease in time spent by the personnel near the ionizing source, increase in the distance between personnel and the ionizing source and increase in the thickness of the shielding between personnel and the ionizing source are followed [16]. Except in cases, where a person is exposed to ionizing radiation for medicinal purposes, the radiation dose rate, the number of people exposed to radiation and the probability of getting exposed by ionizing radiation ALARA (As Low As Reasonably Achievable) principle is followed.

Before any radiotracer investigation, to ensure minimum with no unnecessary exposure to ionizing radiation following steps are taken [16]:

- Radiotracers should be able to be detected at minute concentrations even through a considerable width of pipelines and vessels.
- Radiotracers should have a shorter half-life unless it is absolutely necessary to use a radiotracer with a longer half-life.
- Process flow rates should be taken into consideration before considering the radiotracer concentration at the time of introduction to the system so that the radiotracer can be diluted to an acceptable concentration level
- There should be no room for personnel and environmental hazards.
- During the transport of radiotracer, adequate care should be taken so that the dose rate is not any higher than 2mSv/h.
- The residual radioactivity in the process fluid should be at an acceptable concentration level as decided by the regulating authorities.

- The radiation dose rate should be monitored for personnel so that the radiotracer investigation doesn't add to the acceptable radiation dose rate prescribed by the regulating authorities.
- Proper permission should be taken from regulating authorities before the radiotracer investigations.
- ALARA principle should be followed in every step without any room for error.

IAEA (International Atomic Energy Agency) published multiple reports like [18,19] regarding the safety in the handling of radiotracers. These reports have important and necessary guidelines, instructions, standards and policies which are followed around the world by the member states of IAEA for safety in handling radiotracers.

1.3.3.3 Tracer technique

After the choice of tracer for RTD studies, the next important step is to choose the method of tracer introduction. There are a variety of tracer introduction techniques functions like pulse, step, periodic, random, etc. However, pulse and step input are generally used as they are easy to interpret [5]. In an impulse input, a minute volume of tracer is introduced in the system in an extremely small time-step such that it approaches the Dirac-Delta function [11]. Step input, on the other hand, requires the tracer to be introduced at a constant rate at any fixed time till the concentration of tracer in the feed stream and outlet stream is equal [11]. Step input is generally used in smaller laboratory-scale setups and when the tracer is very cheap. Step input is not used with radiotracers as radiotracers are expensive to produce and require extensive precaution to handle. Also, in order to obtain RTD of the system with step input, the data needs to be differentiated first which can sometimes lead to large errors [11]. In the present study, radiotracer (^{82}Br as ammonium bromide) was introduced to the reactor system in the ethyl acetate plant of IOLCP Ltd., Barnala, India as an impulse input.

1.3.3.4 Pre-treatment of data

Post tracer selection and input, RTD experiments are performed in the concerned system. However, data produced from the RTD experiments cannot be analyzed unless it is treated first to eliminate the background errors and noise. Data generated from RTD experiments using radiotracers generally contain more errors and need more treatment than conventional tracers. Radiotracer data generally has four types of errors which should be corrected before analysis to provide accurate analysis: background radioactivity, radioactive decay, actual

starting time, and incomplete experimentation. Normalization of data is performed after the pre-treatment of the raw radiotracer data.

1.3.4 Characteristics of RTD

After the normalization, the data is ready to be analyzed. The most basic analysis is done by calculating the moments. Moments help understand the RTD functions with statistical parameters. Zero moment is the area under the E-curve (normalized) which is equal to 1. The first moment is the mean residence time which is the average time a fluid particle spends inside the system under consideration. The second moment of RTD is called Variance. It informs about the extent of the spread of the RTD. The more the variance is the greater the distribution is spread around the mean.

Although there are other moments like variance (third moment) which gives an idea about the expanse of the distribution, skewness (fourth moment) which is an idea about the inclination of the distribution in a particular direction, etc. [11]. The first and second moments are widely used.

Moments give an immediate idea about the system under consideration but in order to have a clear idea about the abnormalities in the system bypass and stagnant volume are found out. Bypassing in the system can be recognized by a sharp peak in the RTD curve (E-curve) and the area under the peak gives the bypass fraction in the system. Bypassing is the phenomenon when a part of the feed flow short-circuits to the output without spending adequate time inside the reactor. It leads to incomplete reaction causing higher concentration of unreacted feed components in the product. Similarly, the stagnant volume can be found out by comparing the difference between experimental mean residence time and actual mean residence time. Stagnant volume are pockets which form inside a reactor where mixing doesn't take place appreciably, leading to less or no fluid flow inside it. Stagnant volume can cause low product quality by not allowing the feed components to take part in the reaction and reduces the effective volume.

Using all the aforementioned information, an RTD model is hypothesized and its validity is checked. An RTD model can be a simple model like a CSTR or PFR or it can be complex multi-compartmental like CSTR and stagnant volume with an exchange or CSTR and stagnant volume with exchange along with bypass, etc. [11,5,15,16].

1.4. Thesis motivation and objectives

Industrial-scale RTD data is very scarce in literature due to the limitations conventional tracers pose while used in RTD studies in operational plants. Radiotracers provide an opportunity to study the flow behavior and diagnose the ills of the process equipment without affecting its normal plant operation. Recycling of the process fluid is a prevalent practice in chemical processing industries to increase conversion and to minimize waste. Therefore, RTD experiments on reactors with recycle are of interest to many processing industries.

The overall objective of the Ph.D. thesis is to conduct and analyze the results of RTD experiments on a reactor with recycle. To reach the main objectives the following sub-objectives were proposed:

- To study the residence time distribution (RTD) in a reactor vessel with recirculation by varying the operating conditions like feed, recirculation and recycle flows using conventional tracers (dyes or salts).
- To analyze RTD data, develop a model and estimate model parameters for recycle reactor.
- To perform RTD experiments in an industrial reactor with recycle using radiotracer.
- To estimate RTD model parameters for industrial reactor.

1.5 Thesis overview

The presented thesis is divided into 7 chapters:

CHAPTER-1 deals with the background of the present work. It covers the importance of recycling and recirculation in reactor systems. It also covers the background information of RTD studies, different kinds of tracers used in the RTD studies, and the advantages of using radiotracers over conventional tracers. The chapter also covers the general procedure of performing RTD experiments.

CHAPTER-2 covers the literature study of experimental RTD studies in various systems including pilot scale systems. It also includes experimental and theoretical RTD studies in systems with recycle.

CHAPTER-3 focuses on materials and methods used in conducting radiotracer RTD experiments in the industrial-scale reactor system and in a laboratory-scale reactor system with recycle.

CHAPTER-4 deals with the first set of industrial RTD experiments in the ethyl acetate reactor system. This chapter discusses the results of the experiments performed. It describes in detail the effect of recirculation on bypassing, stagnant volume and MRT of the reactor system. It describes the RTD model developed to simulate the experimental RTD curves. The results of the uncertainty analysis are also described in this chapter.

CHAPTER-5 deals with the second set of industrial RTD experiments in the revamped ethyl acetate reactor system. This chapter discusses the results of the experiments performed. It describes in detail the effect of recirculation on bypassing, stagnant volume and MRT of the reactor system. It describes the RTD model developed to simulate the experimental RTD curves. The results of the uncertainty analysis are also described in this chapter.

CHAPTER-6 deals with the RTD experiments performed on the laboratory-scale system of reactor with recycle. This chapter describes in detail the effect of recirculation and recycle flow rate on bypassing, stagnant volume and MRT of the reactor system. It also describes the RTD model developed to simulate the experimental data. Statistical and uncertainty analysis are also described in this chapter for the laboratory-scale reactor system.

CHAPTER-7 gives an overall conclusion to the present body of work and recommendations for future work.

In the end, cited references in this thesis and publications from this work are listed.

CHAPTER-2

Chapter-2 Literature review

RTD experiments are beneficial to properly measure the abnormalities in any process equipment. Proper knowledge of the working of process equipment can lead to better design and economic gains. RTD studies in industrial systems are generally performed with the help of radiotracers as they can be detected online without disturbing the process. In this chapter, experimental RTD analysis of various systems and theories on recycle systems are summarized.

2.1 Experimental RTD studies on various systems

2.1.1 Fluidized beds

Fluidized beds had been investigated numerous times via RTD experiments to determine the flow behavior of the particles in the bed. Hua et al. [20] performed RTD experiments on a gas-solid fluidized bed with baffles. They used RTD analysis and CFD analysis to describe the fluid behavior in the system. They used the plug flow model and the tank-in-series model to simulate the experimental RTD curves. Anitha et al. [21] investigated the RTD of a liquid-solid tapered fluidized bed. They performed RTD experiments on systems with different angle of tapering and liquid velocity. They simulated the experimental RTD curves with an RTD model comprising of a plug flow component and a CSTR in series. Bachmann and Tsotsas [22] performed RTD studies using radiotracers on horizontal fluidized beds. They tried to fit the experimental data with three different RTD models namely, method of moments, tank-in-series and dispersion. The best fit was achieved by the dispersion model. Goswami et al. [23] measured the mixing time and solid holdup in a gas-solid fluidized bed with the help of radiotracers. They measured the mixing time by plotting the variance with respect to tracer concentration at homogenization as a function of time. They also observed that there was a decrease in the mixing time as the fluidization velocity is increased to a limit. The mixing time was also observed to be higher for higher bed heights. The solid hold up was observed more near the walls as compared to the column center and also decreased following a linear trend with the increase in the gas velocity. A system of pressurized fluidized bed gasifier was studied by Rao et al. [24]. They used the tank-in-series model to represent the system with the value of the model parameter i.e. tank number. It proved the presence of bypassing in the system. The information received from the RTD analysis helped in improving the design of the system. Pant et al. [25] determined MRTs for different sections

of the fluidized catalytic cracking unit. The axial dispersion model suitably simulated the measured RTD data. The results of the investigation were then used to design a pilot scaled FCCU and optimize the performance of industrial-scale FCCU and thereby increasing the efficiency and quality of the product. Pant et al. [26] performed RTD studies on circulating fluidized bed system to calculate coal circulation rate and time. The study was intended to use the results of the study to optimize the behavior of already existing coal gasifiers. Pant et al. [27] studied the RTD for a fluidized bed gasifier used in the coal gasification process. The RTD showed the presence of bypassing of coarser coal particles which lead to their improper mixing inside the gasifier. The tank-in-series model adequately described the process. Santos and Dantas [28] studied the transit time and RTD to comprehend the flow pattern in a riser of FCCU. They showed that centre of mass technique is most suitable for transit time calculation. Centre of mass method had statistically fewer deviations than methods of maximum point and electronic watch recording. Plug flow with dispersion was able to represent the system according to them. Gauthier and Flamant [29] performed RTD studies on a perforated plate fluidized bed with three stages. They developed one-parameter and two-parameter models to simulate the experimental RTD curves. Wolf and Resnick [30] performed RTD studies on single-stage and multi-stage fluidized bed. They studied the effect of plates with perforation and plates fitted with a downcomer on the RTD of the fluidized bed. The RTD studies on fluidized beds discussed here are compiled in Table 2.1.

Table 2.1 RTD studies in fluidized beds

System	Tracer	Model	Work done	Reference
Gas-solid dense fluidized bed with baffles	Acid red 18 (dye)	1. 1D plug flow 2. Tank-in-series	The effect of solid rate and baffle on solid RTD was studied	[20]
Liquid-solid tapered fluidized bed	NaOH (base)	PFR and CSTR in series	The effect of the angle of taper and liquid velocity was studied	[21]
Horizontal fluidized bed	Solid particle	Tank-in-series	The extent of dispersion is determined	[22]
Gas-solid fluidized bed	^{198}Au (radioisotope)	N/A	Mixing time at different bed height and gas velocities was determined	[23]
Pressurized fluidized bed gasifier	^{140}La (radioisotope)	Tank-in-series	MRT at different operating conditions was determined	[24]
Fluidized catalytic cracking unit riser	1. ^{140}La 2. ^{24}Na (radioisotope)	Axial dispersion	MRT of the catalyst, degree of axial and radial dispersion in the riser was determined	[25]

Circulating fluidized bed system	¹⁹⁸ Au (radioisotope)	N/A	Circulation time and rate was determined for the coal particles in the bed	[26]
Fluidized bed gasifier	1. ¹⁴⁰ La 2. ²⁴ Na (radioisotope)	Tank-in-series	MRT of the coal particles at different operating conditions was determined	[27]
Fluidized catalytic cracking unit riser	1. ⁶⁰ Co 2. ⁸² Br (radioisotope)	N/A	Transit time was measured	[28]
Multi-stage fluidized bed	SiC (solid particle)	Tank-in-series with back mixing and bypass	A two-parameter RTD model was developed and compared with one-parameter model	[29]
Multi-stage fluidized bed with baffles	Magnetic particle	Two-parameter model containing mixing efficiency and system phase shift as parameters	Solid RTD at different gas velocities and kind of baffle for single and multi-stage was determined	[30]

Gamma-ray densitometry is another technique like RTD experiments that provides valuable information about flow behavior inside process systems. Veluswamy et al. [31] used CFD analysis along with gamma-ray densitometry technique to simulate the working of a laboratory-scale FCC (Fluidized Catalytic Cracking) stripper unit. The CFD model was able to validate the abnormalities in the stripper as obtained from the experimental analysis. Veluswamy et al. [32] performed gamma-ray densitometry technique to study the hydrodynamics of the stripper unit. They observed extensive solid segregation and a decrease in holdup with an increase in air flow rate. They also observed the presence of stagnant zones near the baffles.

2.1.2 Packed beds

There are numerous RTD studies performed on packed bed reactors over the years. Abdulmohsin and Al-Dahhan [33] studied the RTD of a pebble bed packed reactor used in nuclear reactors. The gas-phase of the system was described by the axial dispersion model. They also studied the effect of gas velocity and bed structure on the mixing characteristics of the packed bed. Gupta and Bansal [34] studied the RTD of a packed bed reactor with visco-elastic and visco-inelastic process fluid. They observed that Bodenstein number (liquid)

increased with liquid flow rate and consistency index for both kinds of non-Newtonian fluid. Gupta and Bansal [35] studied the effect of packed bed arrangement on the dispersion (represented by Peclet and Bodenstein number) in the bed. They simulated the experimental RTD curves with one-parameter axial dispersion RTD model. Experiments to study RTD were done on a packed bed column by Furman et al. [36]. They determined the flow parameters under unsteady state and steady for the system. van Gelder et al. [37] performed RTD experiments in a concurrent up-flow packed bed reactor to determine the extent of mixing at low Reynold's number and high pressure. They used the model of plug flow with axial mixing to explain the RTD of the system. Swaaij et al. [38] performed experimental RTD studies on a packed column under trickle flow conditions to describe the mixing behavior of the system. They performed the experiments for various diameters of Raschig rings. They were able to describe the behavior of the system with the RTD model of cascade of CSTR. The RTD studies on packed beds described here are listed in Table 2.2.

Table 2.2 RTD studies in packed beds

System	Tracer	Model	Work done	Reference
Packed bed pebble reactor	He (gas)	Axial dispersion	Degree of mixing and dispersion of the gas phase was determined	[33]
Packed bed reactor	KCl (Salt)	Axial dispersion	Degree of axial dispersion for visco-inelastic and visco-elastic fluid was determined	[34]
Packed bed reactor	KCl (salt)	Axial dispersion	Effect of bed arrangement on RTD was determined	[35]
Packed column	Radioisotope	Axial dispersion	RTD of the system at steady state and unsteady state was determined	[36]
Gas-liquid packed column	⁸² Br (radioisotope)	1D plug flow with dispersion	Liquid and gas rate and degree of dispersion at different height of the bed was determined	[39]
Co-current up-flow packed bed reactor	LiCl (salt)	Plug flow with axial dispersion	RTD parameters of the system were determined using weighted moments method	[37]
Packed column	NaCl (salt)	Plug flow with axial dispersion	RTD was determined at trickle flow condition for different sizes of packing (Raschig rings)	[38]

Gamma-ray densitometry technique was applied by Upadhyay et al. [40] to determine the variation in the gas holdup (radial) at different heights of a bubble column. Also, they

performed RTD analysis and modeled the bubble column with the axial dispersion model. Finally, they compared the experimental results with a two-fluid Euler-Euler model.

2.1.3 Trickle beds

Trickle bed reactors had been studied extensively through RTD experiments to observe the process flow behavior. Pant and Sharma [41] performed RTD experiments to determine the RTD of a trickle bed reactor at different operating conditions. They used axial dispersion with an exchange model with multi parameters to simulate the experimental RTD curves. Bittante et al. [42] performed RTD experiments to determine RTD of a laboratory-scale trickle bed reactor at different gas flow rates, liquid flow rates, and bed arrangement. They used the axial dispersion model in series with a total backmixed CSTR to simulate the experimental RTD data. Desulphurization is an important and necessary part of any crude oil refining plant [43]. Prokešová et al. [44] performed RTD studies on a laboratory-scale hydrodesulfurization trickle bed reactor to determine the flow behavior at different operating conditions. They used the axial dispersion model to simulate the experimental RTD curves. Wanchoo et al. [45] measured axial dispersion in a laboratory-scale trickle bed reactor. They used the axial dispersion model with Peclet number and Bodenstein number as its two parameters to describe the RTD of the liquid phase of the trickle bed reactor. They were determined from the RTD data using the first and second moment. After determining the model parameter values at different operating conditions it was observed that at low interaction or trickle flow regime Bodenstein number increases with an increase in liquid phase velocity independent of gas flow velocity. In the regime of high contact between the liquid and gas phase, Bodenstein number (liquid) and Reynold's number (liquid) showed an oscillatory trend. Kulkarni et al. [46] performed RTD studies on a trickle bed reactor and a monolith concurrent downflow contactor to compare the RTD and selectivity for the product (2-butene-1,4-diol). They observed that both the reactors presented similar RTD behavior but the monolith CDC had better selectivity towards the product. Pant et al. [47] measured the liquid holdup in trickle bed reactors. They observed that there was no significant malfunction radially. Liquid holdup increased with increasing liquid flow rate but the gas flow rate did not have any influence on it. They observed that axial dispersion model was suitably able to represent the system. They also observed that liquid holdup and Peclet number, which is a representation of the axial mixing of liquid, was greatly influenced by the shape and size of

the catalyst particle. The RTD experiments on fluidized beds discussed here are listed in Table 2.3.

Table 2.3 RTD studies in trickle beds

System	Tracer	Model	Work done	Reference
Trickle bed reactor	⁸² Br (radioisotope)	Multi-parameter axial dispersion with exchange	Liquid phase RTD was measured at different operating conditions	[41]
Laboratory-scale trickle bed reactor	HCl (acid)	Axial dispersion model in series with a total backmixed CSTR	RTD was determined at different gas flow rate, liquid flow rate, and bed arrangement	[42]
Hydrodesulfurization trickle bed reactor	KCl (salt)	Axial dispersion	Axial dispersion, liquid holdup, and MRT was determined for different operating condition	[44]
Downward co-current trickle bed reactor	KCl (salt)	Axial dispersion	Hydrodynamic behavior of the reactor was determined	[45]
Trickle bed reactor and monolith co-current downflow contactor	KCl (salt)	N/A	Comparison of the hydrodynamic behavior of the two types of reactors	[46]
Trickle bed reactor	⁹⁹ Tc (radioisotope)	Two-parameter axial dispersion model	MRT, axial dispersion of liquid, and liquid holdup was determined	[47]

2.1.4 Micro-reactors

RTD of micro-reactors to determine their flow behavior is getting a lot of attention in recent years. Bošković and Löbbecke [48] studied RTD on three different kinds of micro-mixers. They used the axial dispersion model and developed another empirical model to simulate the RTD of the micro-mixers. Bošković and Löbbecke [49] performed RTD studies on one split-and recombine micro-mixer. They modeled the experimental RTD curves with the help of the axial dispersion model and with empirical models. Commenge et al. [50] studied RTD for falling film gas-liquid micro-reactors. They modeled the gas phase of the micro-reactor with the help of a series of CSTR with Reynold's number (gas) as the parameter. The experimental results were also validated with a CFD model. Trachsel et al. [51] performed RTD experiments on a rectangular microchannel. They determined the RTD for various capillary

numbers. They used the axial dispersion model to simulate the experimental RTD curves. The RTD experiments on micro-reactors discussed in this section are shown in Table 2.4.

Table 2.4 RTD studies in micro-reactors

System	Tracer	Model	Aim	Reference
Micro-fluidic reactor	Basic blue 3 (dye)	Plug flow with axial dispersion	RTD was measured for three different kinds of micro-reactor for different flow rates	[48]
Micro-mixer	Basic blue 3 (dye)	1D plug flow with axial dispersion	RTD was measured for different flow rates	[49]
Falling film micro-reactor	O ₃ (gas)	Low and high dispersion tank-in-series	RTD was measured for different flow rates	[50]
Micro-channel reactor	Fluorescent dye	Plug flow with dispersion	RTD was measured for single-phase and multiphase flow	[51]

2.1.5 Bio-reactors

Bio-reactors had also been studied extensively by RTD experiments to observe the flow behavior. Sarkar et al. [52] performed RTD experiments on an aeration tank and secondary clarifier in a wastewater treatment plant. They determined the abnormalities in the system at different process parameters. They developed an empirical RTD model to simulate the experimental RTD curves. Sievers et al. [53] performed RTD experiments on a thermochemical biomass pretreatment reactor to see the effect of biomass feed rate and tube fill fraction on the residence time of the system. They developed a semi-empirical model to simulate the experimental RTD curves. Royae and Sohrabi [54] performed RTD studies on an impinging streams reactor. They studied the flow behavior of the slurry phase of the system. Pant et al. [55] investigated a rotary fluidized bed bio-reactor used in a wastewater treatment plant. They performed RTD experiments in the reactor and were able to determine that there were no bypassing and stagnant zones in the reactor. Tank-in-series model was used to model the system accurately. Borroto et al. [56] investigated an opaque anaerobic digester to measure the RTD of the liquid phase. They were able to model the system with the help of a few CSTR in series with backmixing and a parallel line of few CSTR in series with a low flow rate. The first line represented the presence of baffles and the second line in parallel depicted a short-cut. Shin et al. [57] investigated the presence of a stagnant region and the extent of bypassing with the help of RTD studies in a submerged bio-reactor in waste water treatment plant. The Levenberg-Marquardt algorithm was used to determine the

optimal parameters. The results from the model matched the experimental results satisfactorily. Prokop et al. [58] studied a continuous tower fermentor. They studied the RTD of the fluid which was the continuous phase and the microorganisms which was the dispersed phase. Non-ideality in the form of fluid backflow and sedimentation of the dispersed phase was observed. They drew conclusion that superficial air velocity was the main parameter which dominated the difference between the RTD of dispersed and continuous phase. Also, the superficial air velocity controlled the gas hold up for any particular design of plate. The RTD studies on bio-reactors discussed here are compiled in Table 2.5.

Table 2.5 RTD studies in bio-reactors

System	Tracer	Model	Aim	Reference
Aeration tank and secondary clarifier in an activated sludge process	LiCl (salt)	1. Tank-in-series with backmixing for aeration tank 2. Tank-in-series with backmixing with an axial dispersion plug flow in series for activated sludge process	RTD was measured and the abnormalities in the system were determined	[52]
Thermochemical biomass pretreatment reactors	NaCl (salt)	Plug flow	RTD was determined for different operating conditions	[53]
Photo impinging streams reactor	Reactive black (dye)	Three-parameter compartmental model with 5 CSTR and 1 PFR	RTD was determined for different operating conditions	[54]
Rotary fluidized bioreactor	⁸² Br (radioisotope)	Two-parameter tank-in-series	RTD was determined for different liquid and air flow rate	[55]
Opaque anaerobic digester	^{99m} Tc (radioisotope)	Compartmental model with multiple CSTR in different orientation	RTD was determined for different operating condition	[56]
Submerged bioreactor	¹³¹ I (radioisotope)	CSTR with exchange	RTD parameters were determined for different operating conditions	[57]
Multistage tower fermentor	³ H (radioisotope)	Tank-in-series with backflow and bypass	RTD was determined at different air-liquid flow rates	[58]

2.1.6 Polymer and glass production systems

There are some RTD studies available in the literature which were performed on polymer and glass production systems (Table 2.6). Bogatykh and Osterland[59] performed RTD experiments on a plug flow reactor which are used in polymerization processes. They developed an RTD model considering that the abnormalities in the system can lead to improper impulse output in the RTD of a plug flow reactor. Onyemelukwe et al. [60] performed RTD experiments on a steady-state MSMR reactor used in the crystallization of glycine. They compared the RTD results of the system with plug flow reactors and determined the effect of RTD on the size distribution of α -glycine. Pant et al. [61] studied the hydrodynamics of a glass production unit with the help of radiotracer experiments. They performed radiotracer experiments in the tank furnace and forehearth of the glass production unit. They were able to detect stagnant volumes in both the furnace and forehearth but with a higher percentage in the former. It suggested that there was a stagnant layer of molten glass at the bottom of the furnace. They also found out the accurate homogenization time with the help of radiotracer experiments which helped the industry in finding out the time taken before they receive uniform glass composition and undertake quality control steps efficiently. They were able to model the unit as a PFR followed by two parallel streams of multiple CSTR in series with poor intermixing between the parallel streams. Puaux et al. [62] performed RTD experiments on a twin-screw extruder used in polymer process plants. They determined the change in stagnant volume inside the extruder at different screw speeds. They simulated the experimental RTD curves with the help of one and two-parameter RTD models. The experimental RTD curves were accurately simulated by the two-parameter RTD model of delayed tank-in-series with internal recirculation. Hornsby et al. [63] determined the RTD of a polymer processing setup. They described two different methods namely neutron activation analysis and ashing technique to perform RTD experiments. Finally, the methods were tested to characterize polymer RTD of twin-screw extrusion and injection molding unit. In neutron activation analysis a tracer was introduced as a pulse function to the feed stream and the tracer got distributed in the product. A sample from the product was taken at regular times and was irradiated by neutron source. The tracer decayed into a different element and released energy in the form of gamma rays. The gamma rays were counted henceforth and the count provided information about the homogenization of the product. Ashing technique was fairly easy to perform but it had low accuracy at low tracer concentrations. In this technique, a known amount of inert mineral filler was mixed with the feed stream of the polymer

processing apparatus and the concentration of the tracer in the extrudate was calculated by measuring the amount of tracer present after ashing it at fixed time intervals.

Table 2.6 RTD studies in polymer and glass production systems

System	Tracer	Model	Aim	Reference
Plug flow reactor	KCl (salt)	Axial dispersion	RTD of a plug flow reactor was determined when the variation in the impulse output is considered	[59]
Steady state MSMPR reactor	NaCl (salt)	Axial dispersion	RTD of a single stage and multi stage MSMPR reactor is determined and compared with RTD of tubular reactor	[60]
Furnace, forehearth, and annealing section in a glass production unit	¹⁴⁰ La (radioisotope)	Compartment model containing PFR and tank-in-series	RTD parameters and degree of uniformity of the glass produced at different operating conditions were determined	[61]
Co-rotating twin-screw extruder	Iron powder (solid)	1. Delayed tank-in-series with internal recirculation 2. Delayed axial dispersion	RTD was determined at different operating conditions	[62]
Twin-screw extruder and injection molder	1. ⁵⁶ Mn (radioisotope) 2. Fordabar barites (solid)	N/A	Comparison of radiotracer and solid tracer for RTD experiments, MRT at different screw speed and degree of mixing was determined	[63]

2.1.7 Pilot-scale systems

There are a few RTD experiments reported in literature which were performed on pilot-scale systems over the years (Table 2.7). Sharma et al. [64] performed RTD experiments on a pilot-scale soaker to see the flow behavior of petroleum residues. They used tank-in-series model with backmixing to simulate the experimental RTD behavior. They also found that baffles in the soaker decrease backmixing in the system. Pant et al. [65] performed RTD experiments on a pilot-scale poison tank used in nuclear plants as a part of the safety mechanism. They were able to determine the amount of stagnant volume inside the reactor at operating conditions. They were able to simulate the experimental RTD data with the help of an axial

dispersion model with high backmixing. Pant et al. [66] investigated the flow behavior in a pilot-scale continuous leaching reactor which is generally used in uranium extraction. They used the tank-in-series model to simulate the experimental RTD data. Jafari and Mohammadzadeh [67] performed RTD studies on a pilots-scale gas-liquid contactor. They investigated the effect of various operating parameters on the RTD of the system. Burkhardt et al. [68] performed radiotracer RTD experiments on a pilot-scale hydrotreating plant. They found the values of liquid velocity and the dispersion coefficient (axial) using a dynamic axial piston model with dispersion and used Danckwert's boundary conditions.

Table 2.7 RTD studies in pilot-scale systems

System	Tracer	Model	Aim	Reference
Soaker	⁸² Br (radioisotope)	Tank-in-series with backmixing	RTD was measured and the degree of backmixing was determined at different operating conditions	[64]
Poison tank	⁸² Br (radioisotope)	1. Axial dispersion with backmixing 2. Tank-in-series with backmixing	RTD was measured, the degree of backmixing was determined at different operating conditions	[65]
Continuous leaching reactor	⁸² Br (radioisotope)	Two-parameter tank-in-series	RTD was measured for liquid phase at different liquid flow rates	[66]
Gas-liquid contactor	KCl (salt)	CSTR with stagnant volume and bypassing	Effect of various operating parameters on the RTD of the system was determined	[67]
Hydrotreati ng plant	⁸² Br (radioisotope)	Axial dispersion	RTD was measured and degree of axial mixing in downflow mode and up- flow mode was compared	[68]

2.2 Experimental RTD studies on recycle systems

There are very few experimental RTD studies reported on recycle systems over the years to determine the effect of recycle on their flow behavior. Meibodi et al. [69] performed RTD experiments on a rotating packed bed reactor with recycle producing calcium carbonate nanoparticles. They studied the effect of gas-liquid flow rates, packing type, rotation speed on the synthesis of the nanoparticles. They also simulated the experimental RTD curves with a CSTR with recycle. Sánchez et al. [70] performed RTD experiments on an activated sludge reactor with recycle at a wastewater treatment plant to determine the abnormalities inside the reactor. They also developed three different analytical RTD models with recycle with

different assumptions to simulate the experimental RTD curves. Martinov et al. [71] performed RTD experiments on a fibrous fixed bed biofilm reactor with recycle used in wastewater treatment at different fluid velocities. They simulated the experimental RTD curves with a tank-in-series model. The RTD experiments on recycle systems discussed in this section are listed in Table 2.8.

Table 2.8 RTD studies in recycle systems

System	Tracer	Model	Aim	Reference
Rotating packed bed reactor	KCl (salt)	CSTR with recycle	RTD was determined and effect of various operating parameters on the production of CaCO ₃ nanoparticles	[69]
Activated sludge reactor	LiCl (salt)	Axial dispersion model and analytical models	RTD model was developed	[70]
Fibrous fixed bed reactor	NaCl (salt)	One-parameter tank-in-series	RTD was determined for different operating conditions	[71]

2.3 RTD theories on recycle systems

One of the very first papers on RTD of recycle systems was written by Haddad et al. [72]. They described the RTDs of closed-loop systems where the system input was influenced by the output. They derived equations for RTD function for step input for recycle in ideal systems and real systems. In ideal systems, they considered the cases of continuously stirred tank reactors (CSTR) in series and plug flow reactor (PFR). In real systems, they considered the cases of with and without lag in the recycle stream. Sinclair and McNaughton [73] developed a theory to calculate the RTD of a complex system for an impulse tracer input by combining the constituent elementary flow regions of the system. They derived RTD equations for five different types of systems in succession of complexity. They started with the basic system where there was a direct transfer of process fluid particle from input to output. Then they described multiple systems in series and in parallel. Finally, they described a system with a recycle stream and derived a general equation for a complex system comprising of systems in parallel and in series with a recycle stream. They used the concept of additive and multiplicative (principle of convolution) property of probability density function (or in this case, RTD) of process fluid particle passing through the constituent parts of a complex system. Rippin [74] derived RTD for a recycle reactor, where a no recycle

condition, transformed the RTD function to that of a PFR and an infinitely large recycle converted the RTD function to that of a CSTR. He made an analogy between the RTD model of recycle reactor with tank-in-series model and longitudinal diffusion based on equality of coefficient of variation of these three models. He also calculated the Danckwert's degree of segregation for the recycle reactor. From the degree of segregation calculation, it was noticed that at no recycle condition (or as a PFR) degree of segregation becomes 1 or the recycle reactor becomes completely segregated. On the other hand, at high recycle rates (or as a CSTR), the degree of segregation becomes zero and the recycle reactor undergoes complete micromixing. Further inspection showed that recycle reactor was a maximum mixedness reactor as the degree of segregation in the case of maximum mixedness reactor was the same as the degree of segregation in case of the recycle reactor. Hopkins et al. [75] showed for an imperfect impulse input, transfer function (ratio of output to input tracer concentration curve) for a recycle system along with different systems like CSTR, PFR, CSTR in series, etc. They found out that at low values of τp (τ is the mean residence time and p is the Laplace operator) all models including complex recycle system gave the same transfer function. Hochman and McCord [76] investigated the RTD for a system with a relatively high L/D (ratio of the length and the diameter of the reactor) with axial flow agitation. The models described before did not satisfactorily describe the RTD of systems where there was a simultaneous change in concentration gradient (due to cross mixing) between the up-flow and downflow streams. They developed a generalized two-parameter (exchange coefficient and recycle rate) model which could describe any reactor including a reactor with a high L/D ratio. They considered four cases depending upon the higher and lower limits of the two parameters described before. The model converted to a plug flow reactor with high radial mixing when the exchange coefficient was infinitely high and in case of no exchange coefficient, the model behaved like a normal recycle reactor with plug flow components in both the feed and recycle stream. When there was a high recycle, the complete system responded as an ideal stirred tank and in absence of recycle, the model got reduced to a plug flow reactor with a stagnant volume exchanging material between them. Fu et al. [77] derived the RTD function of recycle system using the first passage time distribution. The derived equation for RTD was in the form of a Volterra integral equation (second kind). The derived equation for RTD function was solved for three recycle systems namely, PFR with recycle, n number of CSTR in series with recycle and a combination of both the system. Mah [78] studied the case represented by Hochman and McCord [76] and modified their model by including an extra parameter of number of stages in the two flows (up-flow or recycle and down-flow) in the

reactor. Due to the introduction of the extra parameter, the model proposed by Hochman and McCord [76] became flexible and elaborate. When the number of stages was infinite, the model proposed by Mah [78] simplified the model proposed by Hochman and McCord. Dohan and Weinstein [79] developed a general model that could explain an infinite number of micro-mixing states for a particular macro-mixing state. Their theory was an improvement above the model developed by Rippin[74] which stated that plug flow reactor with a recycle could explain macro-mixing but it also suggested that it was a maximum mixedness (high micro-mixing) reactor. In Dohan and Weinstein's [79] model there were two parameters namely, the number of reactors and recycle rate. They showed that at any constant level of macro-mixing (first and second moment of RTD function are fixed) any variation in the recycle rate and number of reactor in series gave rise to infinite permutations of micro-mixing states (from complete segregation to completely mixed). Mann and Crosby [80] described a way to determine the flow behavior in systems where there was not a throughput i.e. a circulating system. A circulating system as defined by them was a closed system in which all elements of the flowing fluid pass periodically through at least one specified cross-section. As RTD is based on the distribution of output tracer concentration of the system, it's not possible to determine the RTD of such circulating system. They defined the concept of cycle time distribution (CTD), in such cases, as a replacement for the concept of RTD of systems with a throughput. Cycle time is the time passed between two passages or cycles of a fluid element crossing a particular cross-section (all fluid particles pass through this cross-section periodically). According to Mann and Crosby [80] the flow behavior inside a flow region in such a system would influence the cycle time and the distribution of the cycle time would represent the flow patterns inside the flow region. They derived the CTD function for circulating systems. They also made a relation between RTD of individual flow regions in cases of circulating systems with more than one flow region in parallel, and CTD of the complete systems. Nauman [81] developed a theory of recycle systems by treating it as a limiting case of the theory developed by Mann and Crosby [80] for circulating systems. They considered two cases: 1. when the CTD function of a system was known and RTD function was to be determined and 2. when the RTD of a system was known and CTD of a system was to be determined. For the second case, they described two methods to calculate the moments of CTD when the moments of RTD were known. First method was applicable only to open system (or systems with recycle) and when the recycle rate was fairly low. This method was also applicable to system where the input was introduced to the system as a step or an impulse function. The second method was applicable for both open and closed (systems with

no throughput or pure circulating systems) systems but was only applicable when there was a pure impulse introduction of the tracer. It was believed before that RTD of a recycle system tends to be in exponential form when the recycle was increased indefinitely. Buffman and Nauman [82] developed a theory that said RTD of recycle systems tends to be in exponential forms at high recycle ratio only when there were two limiting cases. The first case was when the normalized RTD function becomes independent of the recycle flow after a finite value of recycle flow rate. The second case was when all the moments of the normalized RTD functions were bounded. Nauman and Buffman[83] portrayed a case where they showed that it was possible to have a limiting distribution of exponential systems even when both the prerequisites described by Buffman and Nauman [82] had not been satisfied. In addition, they also showed that it was possible to have a limiting distribution in a recycle system other than exponential. Rubinovitch and Mann [84] proved a theory stating that RTD of a recycle system converged to an exponential distribution but only when there was no stagnant volume at the limit. Mann et al. [85] developed a theory for recycle systems introducing three concepts – number of cycles distribution, RTD, and total regional RTD. Mathur and Weinstein [86] developed a two-parameter RTD theory for tubular reactor vessel with axial mixing (TRAM) with recycle. They developed the equations for the moments of RTD with recycle ratio and Peclet number as the two parameters. Mann and Rubinovitch[87] developed an extension of an earlier theory [85] but in this case, for a system of a series of recycle reactors by introducing the concept of number of cycles a particle completed in a system, the total time it resided in the system, and the total time it resided in a part of the system. It was found that number of cycle distribution (NCD) depended on recycle ratio and number of recycle systems in series. RTD, and total regional RTD (TRRTD), depended on recycle ratio, number of recycle systems in series, and one pass RTD between two consecutive reactors in the system. Buffham and Nauman [88] found out that at high recycle ratio, the RTD was exponential only if there was no considerable volume where the material passing rate was similar to or smaller than the throughput of the system. If there was a considerable volume inside the reactor where the material passing rate was similar to throughput, then the RTD would be significantly different than exponential. On the other hand, if there was a sizeable volume inside the reactor where the material passing rate was substantially lower than the throughput of the system, then the RTD was deemed defective and that volume was regarded as “bypassed”. Fan et al. [89] generated RTD models for various systems including systems with recycle using a stochastic model called Markov chain. They also verified the results with the results developed by Mann et al. [85] for a system with recycle. This stochastic approach

to generate RTD for various systems was particularly helpful when the system was very complex e.g. petrochemical and hydrocarbon systems. Waldram[90] developed a theory in which all the possible recycle rates were considered around a plug flow system. He developed RTD function for $R \geq 0$ (general recycle flow), $R < -1$ (system with bypass flow and reverse main flow) and $-1 < R < 0$ (system with bypass flow and normal main flow). Battaglia et al. [91] developed a procedure to calculate single-pass RTD of recycle systems. They also verified the theory by conducting a laboratory experiment. Table 2.9 reports the RTD theories on recycle systems discussed here.

Table 2.9 Theoretical RTD studies on recycle systems

Work done	Reference
Models developed for systems with multistage recycle systems:	[72]
1. Ideal system (no lag in recycle)	
2. Real systems (with and without lag in recycle)	
It was shown for complex fluid flow systems that the overall model can be obtained from continuous probability functions of individual units including recycle systems	[73]
It was shown that recycle reactor is a type maximum mixedness reactor	[74]
Laplace transformation was used to determine RTD of various systems	[75]
RTD was developed for recycle systems with crossmixing between output and recycle flow	[76]
RTD model developed for recycle systems using Volterra integral (2 nd kind)	[77]
RTD model was developed for a discrete recycle systems with crossmixing	[78]
RTD of a recycle system was obtained based on the principle that a system can be assumed as a infinite stages of micromixing for a particular macromixing stage	[79]
CTD were obtained for closed circulating systems and linked to the RTD of individual systems comprising of such systems	[80]
It was proved that closed circulating systems are a limiting case of open systems with recycle	[81]
Different outcomes were determined when recycle rate is increased keeping a constant output	[82]
More detailed outcomes were determined when recycle rate is increased keeping a constant output	[83]
Different outcomes were determined when recycle ratio tends to be infinite	[84]
RTD of a recycle system was developed taking into account number of cycles distribution, RTD and TRRTD	[85]
RTD of a cascade of recycle systems was developed	[87]
RTD was developed for high recycle ratio systems at constant output	[88]
Markov chain (a stochastic principle) was used to determine RTD of various systems including systems with recycle	[89]
RTD was developed for PFR with positive and negative recycle	[90]
A methodology was devised to obtain one-pass RTD of any system with recycle from experimental RTD experiments	[91]

CHAPTER-3

Chapter-3 Materials and methods

Two sets of residence time distributions studies were performed in the industry on two ethyl acetate reactor setups. A laboratory-scale RTD study was also performed on a recycle reactor with recirculation as a mean of mixing. Different materials were used and different methodologies were applied to conduct the RTD experiments in industry and in the laboratory.

3.1 Materials

^{82}Br (half-life: 36 h, gamma energies: 0.55 MeV (70%), 1.32 MeV (27%)) as ammonium bromide with approximately 5 mCi activity was used as the radiotracer and was sourced from Bhaba Atomic Research Centre, Mumbai, India. Eight-channel pulse processing system, counter unit for eight-channel multi-input data acquisition system, 2" x 2" NaI (Tl) detectors, voltage divider, and cables were supplied by Electronic Enterprises (India) Private Limited, Mumbai, India.

For laboratory-scale RTD experiments, the feed, recirculation and recycle pumps (centrifugal) were supplied by Roto Pumps Limited, Noida, India. The flow control system for the pumps was supplied by ABB India Limited, Chandigarh, India. Electrical conductivity transmitter, data logger for conductivity meter, panel box for conductivity meter and software for data acquisition and data download were supplied by Spectrum Technology, Ambala, India. NaCl used as the tracer for laboratory-scale RTD studies were procured from Rankem (ACS grade), Thane, India.

3.1.1 Software used

RTD modeling software DTSPRO V4.21 developed by PROGEPI, LSGC-CNRS-ENSIC, Nancy, France was used to model the industrial RTD data. C-program developed for modeling the laboratory-scale RTD data was prepared on Dev C++ open platform developed by Free Software Foundation, Incorporated, Massachusetts, United States of America.

3.2 Methodology

In order to conduct the RTD experiments, the following methodology was applied:

3.2.1 Selection of the tracer

After careful study, ^{82}Br (half-life: 36 h, gamma energies: 0.55 MeV (70%), 1.32 MeV (27%)) as ammonium bromide with approximately 5 mCi activity was used as the radiotracer for industrial-scale RTD experiments. Sodium chloride (5.13 N) was used as the tracer in the laboratory-scale RTD experiments.

3.2.2 RTD experiments

RTD studies were performed for both industrial-scale and laboratory-scale reactor system.

3.2.2.1 Industrial RTD experiments

Two sets of industrial RTD experiments were performed on ethyl acetate reactor (reactor R1 and reactor R2) system at IOLCP Ltd., Barnala, India. The plant produced 60 tons per day of ethyl acetate using esterification reaction in the presence of an acid catalyst between acetic acid and ethanol with water as the byproduct. The plant consisted of two reactors (R1 and R2) connected in series, two independent distillation columns (C1A and C1B) and a common decanter. The geometric volumes of the reactor R1 and R2 were 45.6 m^3 and 57.6 m^3 respectively. The fresh feed comprising of acetic acid and ethanol was fed into the reactor R1 at a mass flow rate of about 8900 kg/h ($\pm 5\%$), whereas the mass flow rate of recycle product stream from the bottom of the columns ranged from 35150 - 38850 kg/h. The output of the reactor R1 was fed into the reactor R2 to further complete the reaction. Two independent pumps of 3.7 kW and 11.2 kW were used to recirculate the reactants within the two respective reactors. After the first set of RTD studies, the reactor system was replaced by a new set of reactors by the industry to accommodate any future increase in the production capacity of the plant. Reactor R1 was replaced with a horizontal vessel, whereas, a vertical vessel was used as reactor R2 keeping all other process parameters same. The detailed process description of the plant is described in detail in chapter 4 and 5 for more clarity.

Before the RTD experiments were performed, the planning for the experiments was done. Several pre-plant visits took place and meetings were conducted with process engineers working in the plant. The working of the plant was discussed. Also, the physical properties of

the process fluid were studied which was needed in choosing the appropriate radiotracer. The feed line for the reactor R1 was checked for an appropriate position where the radiotracer was to be injected during the RTD experiments. Also, a specially designed injection system for radiotracer as described in a paper by Pant et al. [92] was fabricated which was to be used during the RTD experiments. Finally, a safe workplace was designated in consultation with the BARC scientists where the radiotracer was to be handled by the BARC scientists during the RTD experiments.

RTD studies using radiotracer were performed on the aqueous phase of the reactors R1 and R2 in series. Activity of 5mCi of ^{82}Br (half-life: 36 h, gamma energies: 0.55 MeV (70%), 1.32 MeV (27%)) in the form of ammonium bromide was used for the RTD experiments. Three experiments with different recirculation rates were performed as shown in Table 3.1 (reactor system 1) and Table 3.2 (reactor system 2). Recirculation flow rate corresponding to the 100% pump capacity was 20000 kg/h for the reactor R1 and 15000 kg/h for the reactor R2. Recirculation rate was varied to see its effect on the mean residence time of the reactor system as well as stagnant volume and bypassing inside the reactors. The recirculation rate was varied after careful deliberation and consultation with plant personnel. For carrying out RTD experiments at various recirculation rates, the pump throughput was varied using variable frequency drive (VFD). A VFD varies the frequency and voltage of the power supply to the pump causing a change in the speed of the impeller which in turn varies the pump throughput.

The specially designed pulse injection mechanism introduced the radiotracer into the feed line of reactor R1. The radiotracer activity was recorded at various spots using collimated NaI (TI) scintillation detectors. One detector was placed just after the injection point in the feed line to record the pulse input of the tracer. Two detectors to record the output tracer data were positioned at the outlet of the first and second reactors. The activity of the injected radiotracer was also recorded at 7 other strategically planned positions in the plant. The schematic of the plant showing the tracer injection point and positions of the detectors are described in detail in chapter 4 and 5 (Fig. 4.1 and 5.1).

All the detectors were connected to a data acquisition system controlled by a computer to record data points (counts) at a time interval of 20 seconds. The tracer count data was documented as a function of time and was saved in the memory of the computer for data pre-treatment and analysis. The duration of each experimental run in the first set of industrial

RTD experiments was around 20-25 hours and 40-45 hours in the second set of industrial RTD experiments. The data acquisition system was setup in an appropriate safe space inside the plant for observation and recording. Due to the large scale status of the experiments, a team of 3-4 persons was required to assist with the setup and observation of the data acquisition system and the detectors. The data acquisition system was kept under constant monitoring at all times even during the night in case of any unforeseen problem occurring during any of the experimental runs.

Table 3.1 Conditions for RTD experiments on industrial reactor system 1

Run	Recirculation Pump	Capacity	Mass flow rate (kg/h)
Run 1	1. Reactor 1 (5hp)	100%	20000
	2. Reactor 2 (15hp)	100%	15000
Run 2	1. Reactor 1 (5hp)	50%	10000
	2. Reactor 2 (15hp)	50%	7500
Run 3	1. Reactor 1 (5hp)	0%	NIL
	2. Reactor 2 (15hp)	25%	3750

Table 3.2 Conditions for RTD experiments on industrial reactor system 2

Run	Recirculation Pump	Capacity	Mass flow rate (kg/h)
Run 1	1. Reactor 1 (5hp)	100%	20000
	2. Reactor 2 (15hp)	100%	15000
Run 2	1. Reactor 1 (5hp)	50%	10000
	2. Reactor 2 (15hp)	50%	7500
Run 3	1. Reactor 1 (5hp)	0%	NIL
	2. Reactor 2 (15hp)	0%	NIL

3.2.2.2 Laboratory-scale RTD experiments

Before the RTD experiments were performed, the planning for the experiments was done. The dimensions of the tank were conceived to be proportional to the reactors used during the first set of industrial RTD experiments. The process description for the reactor system is described in detail in chapter 6. Tap water as the process fluid for the laboratory-scale reactor system was chosen as it matched the physical properties of the process fluid in the ethyl acetate reactors at the industry. Preliminary experiments were performed with different dyes and salts to check their efficiency during RTD measurements. Salt tracers, particularly NaCl, proved helpful to be used as the tracer in the RTD experiments as it was cheaper than dyes, highly soluble in water at room temperature and the conductivity meter to measure the conductivity of the salt in water was inexpensive as compared to the spectrophotometer used to measure the absorbance of the dyes. The feed line for the reactor was checked for the appropriate position where the impulse of the salt tracer was to be introduced during the RTD

experiments. The schematic of the reactor system showing the tracer injection point and positions of the detectors is described in chapter 6 (Fig. 6.2).

Sodium chloride (5.13N) was used as the tracer for the RTD studies as it was cheap, non-reactive and has a high solubility in tap-water (process fluid) at room temperature. The tracer was introduced instantaneously mimicking an impulse input into the fresh feed line of the reactor. The output tracer conductivity was measured and recorded every 8 seconds with the help of an online conductivity meter. Also, a calibration curve was prepared for NaCl concentration vs conductivity which was used to convert the output conductivity into concentration so that the data could be analyzed properly.

Experimental runs were performed on the reactor system with different recirculation and recycle rates at a fixed feed flow rate of 30 l/h. The recycle and recirculation pump throughput was varied using variable frequency drive (VFD) as well. Runs were performed at random to eliminate any error that might have crept in due to systematic experimentation [93]. For the ease of understanding, the runs are represented systematically in Table 3.3.

Table 3.3 Conditions for RTD experiments on laboratory-scale reactor system

Run	Feed rate (l/h)	Recycle rate (l/h)	Recirculation rate (l/h)
1	30	120	150
2	30	120	100
3	30	120	50
4	30	120	0
5	30	80	150
6	30	80	100
7	30	80	50
8	30	80	0
9	30	40	150
10	30	40	100
11	30	40	50
12	30	40	0
13	30	0	150
14	30	0	100
15	30	0	50
16	30	0	0

3.3.3 Data pre-treatment

Raw RTD data obtained from the Na-I scintillation detectors in the industrial RTD experiments were treated before any RTD analysis was performed on it. Four treatments which were performed on the RTD data using radiotracers are as follows:

Background correction

Prior to the injection of radiotracer into a system, it was necessary to measure the background radiation level, which was then subsequently subtracted from the experimental data.

Starting point correction

The gamma counts before the time of the introduction of the impulse input of radiotracer were eliminated.

Radioactive decay correction

Since radioisotope tracers decay exponentially with time, it was necessary to apply decay correction to the measured data (otherwise, more weight could have been unduly given to early measurements). Hence, the experimental data were corrected with an exponential decay function considering the half-life of ^{82}Br following Eq. 3.1.

$$n_c(t) = n_m(t) \exp\left(\frac{0.693 \cdot t}{T_{1/2}}\right) \quad (3.1)$$

where, $n_c(t)$ is the corrected gamma count at any time t , $n_m(t)$ is the original count at any time t and $T_{1/2}$ is the half-life of the radiotracer used. In the present case radiotracer used was ^{82}Br which has a half-life of 36 hours.

Extrapolation or tail correction

Data extrapolation is needed when the end of the measured tracer curve is incomplete for some reasons (large RTD, long tail, data acquisition system problems, etc). The regular tracer test assumes the count rates go back to zero at the end of the data acquisition. Mostly extrapolation is performed mathematically using exponential decay function. In the industrial and laboratory-scale RTD studies, experimental RTD curves were extrapolated using around the last 40% data points of the experimental data and regressing it with an exponentially decaying function.

After the radiotracer data was pretreated, normalization of the data was done and RTD analysis was performed on them as described in chapters 4 and 5.

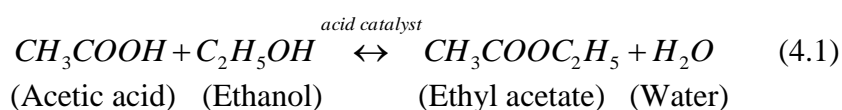
CHAPTER-4

Chapter-4 RTD experiments on industrial reactor system 1

The first set of industrial RTD experiments were performed on the ethyl acetate reactor system at the IOLCP Ltd., Barnala, India. The plant operation was kept undisturbed for the complete duration of the RTD experiments.

4.1 Plant/process description

The plant produces 60 tons per day of ethyl acetate using esterification reaction in the presence of an acid catalyst between acetic acid and ethanol with water as the byproduct. The stoichiometric representation of the chemical reaction is shown in Eq. 4.1.



The schematic of the ethyl acetate plant is shown in Fig. 4.1. The plant consisted of two reactors (R1 and R2) connected in series, two independent distillation columns (C1A and C1B) and a common decanter. The R1 had an internal diameter of 4.4 m and a height of 3 m, whereas the diameter and height of the reactor R2 were 3.8 m and height of 5.08 m, respectively. The geometric volumes of the reactor R1 and R2 were 45.6 m³ and 57.6 m³ respectively. But only about 80% of the geometric volume of each reactor was working volume. The reactor R1 and R2 are shown in Fig. 4.2.

Fresh feed and bottom product of both the distillation column were fed into the reactor R1. The fresh feed comprising of acetic acid and ethanol was fed into the reactor R1 at a mass flow rate of about 8900 kg/h ($\pm 5\%$), whereas the mass flow rate of recycle product stream from the bottom of the columns ranged from 35150 - 38850 kg/h. The output of the reactor R1 was fed into the reactor R2 to further complete the reaction. Two independent pumps of 3.7 kW and 11.2 kW were used to recirculate the reactants within the two respective reactors. The outlets and inlets of the pumps were connected to the specially designed flow distributors to achieve adequate recirculation in the reactors. During operation, the pressure inside the reactors was maintained between 11.77-15.70 kPa for reactor R1, and 19.61-39.22 kPa for reactor R2 and the temperature was maintained between 375- 378K.

The output of the reactor R2 was divided into two streams. One of the streams, with a mass flow rate of 27000-30000 kg/h entered column C1A, while, the other stream entered column C1B, with a mass flow rate of 16000-18000 kg/h. The column C1A and C1B were reactive

distillation columns where the reaction and product separation took place simultaneously thus driving the reaction in the forward direction. The product drawn from the top of the columns C1A and C1B, was fed into a decanter (volume = 4 m³) with a cumulative mass flow rate of 31000-32000 kg/h. The decanter separated the ethyl acetate rich aqueous layer and acetic acid-rich organic layer. An organic phase with a mass flow rate of 22650-23650 kg/h and an aqueous phase with a mass flow rate of 1350-1400 kg/h were obtained as an output from the decanter. The aqueous layer was sent for further purification and a part of the organic layer was sent back to column C1A and C1B as reflux.

Detector D1 was mounted at the inlet of the reactor R1 just after the injection location. This detector was mounted to record the time of the entry of the radiotracer into the reactor. Detectors D2 and D5 were mounted at the outlet of the reactor R1 and R2 respectively, to record the tracer concentration curves. Detector D4 was mounted at the inlet of the decanter, whereas the detectors D3 and D8 were mounted at the outlet streams of the decanter. Detectors D6 and D7 were mounted at the recycle streams to the reactor R1. The position of the detectors during the first set of industrial RTD experiments is shown in Fig. 4.1.

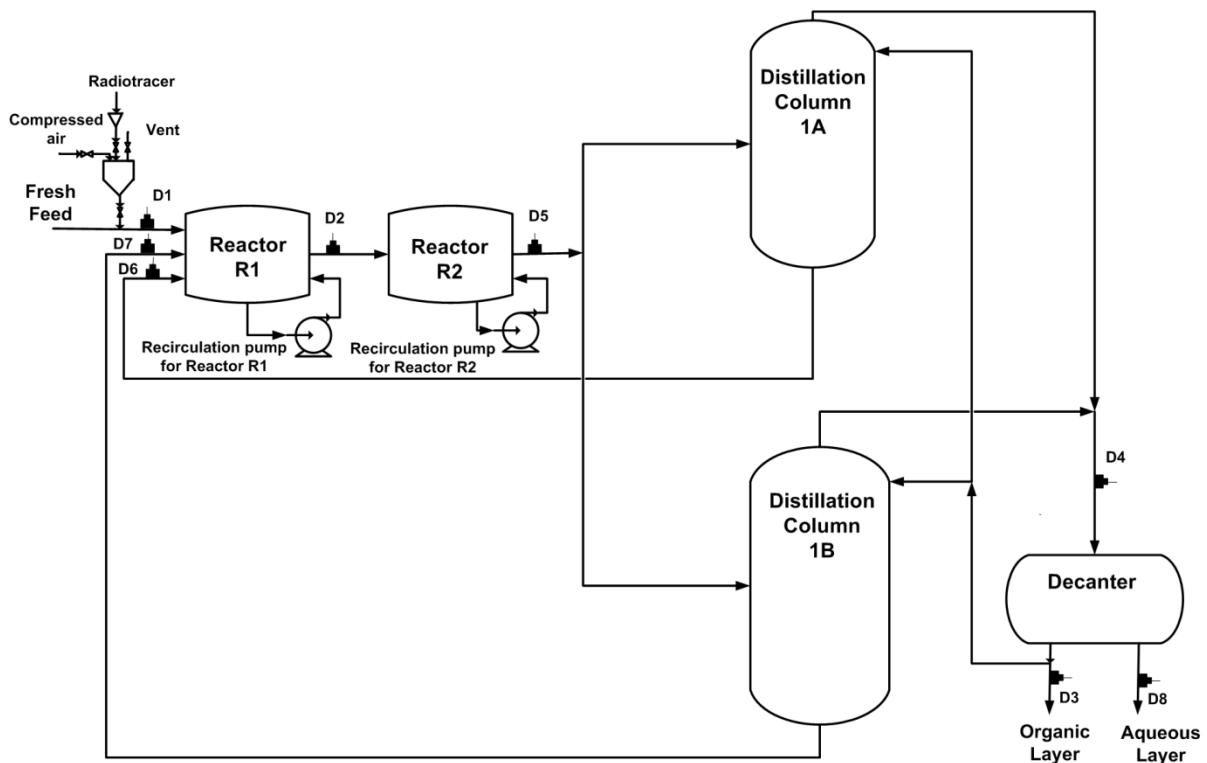


Fig. 4.1 Schematic of industrial reactor system 1 showing the detector positioning



Fig. 4.2 Reactor R1 (a) and reactor R2 (b) of industrial reactor system 1

Three experiments with different recirculation rates were performed as shown in Table 3.1. These experiments mapped with the sub-objective 3 of the thesis. After the RTD experiments pre-treatment of the radiotracer data was performed.

4.2. Pre-treatment of the radiotracer data

The raw output tracer count data was corrected for errors namely, starting point, background radioactivity, and radioactive decay before extrapolating the tail of the tracer count curve. After the correction, the output tracer count data was normalized. Figures 4.3-4.8 shows the comparison between the output tracer curve before and after pre-treatment for detector D2 (mounted in the output line of reactor R1) and D5 (mounted in the output line of reactor R2) for different runs. The difference in magnitude observed between the raw and pre-treated tracer counts was due to the background radiation present around the plant.

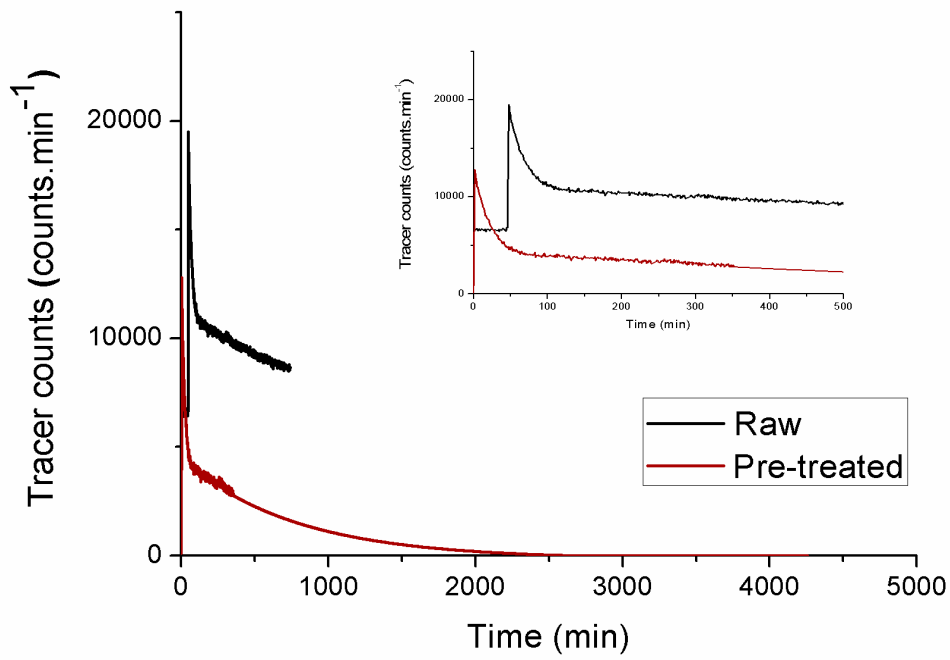


Fig. 4.3 Raw and pre-treated tracer counts for detector D2 (Run 1)

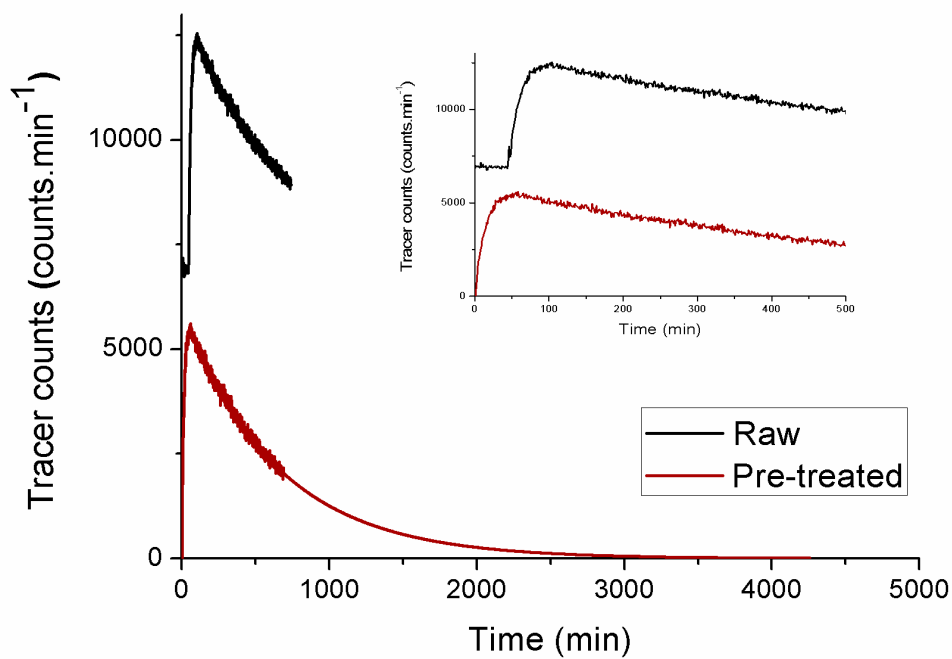


Fig. 4.4 Raw and pre-treated tracer counts for detector D5 (Run 1)

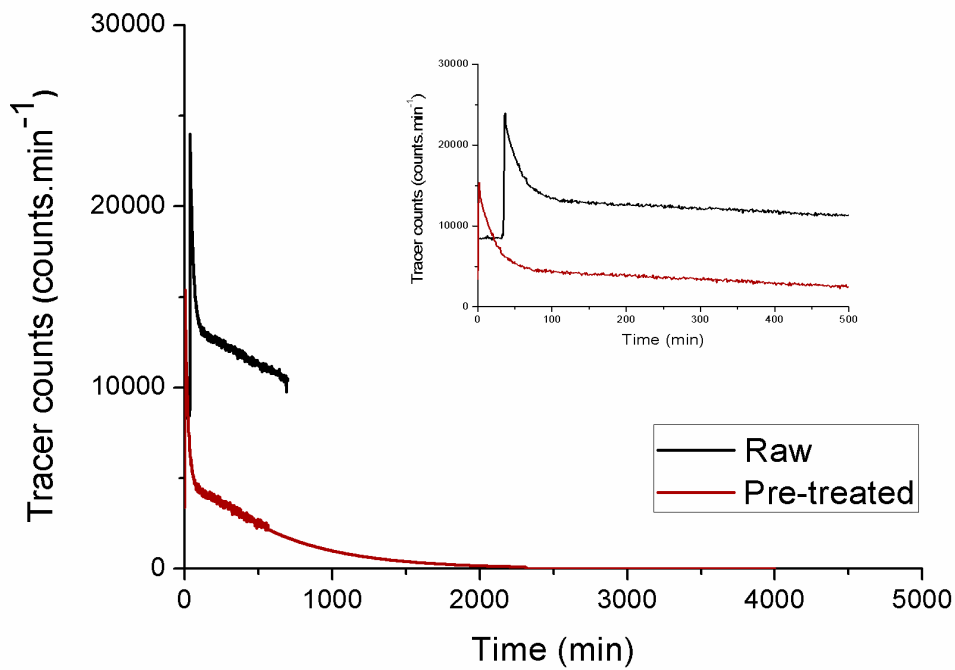


Fig. 4.5 Raw and pre-treated tracer counts for detector D2 (Run 2)

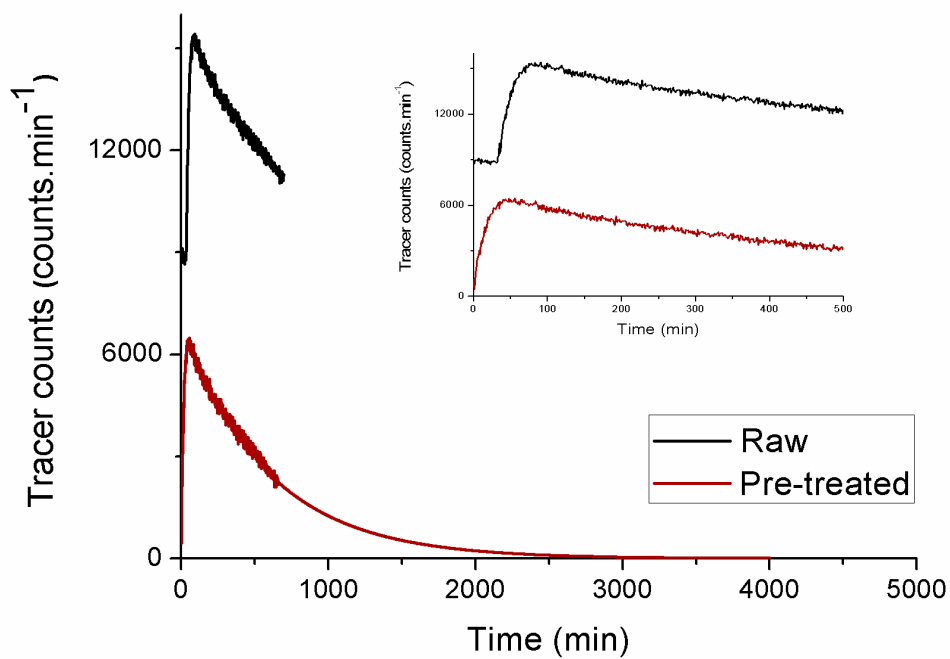


Fig. 4.6 Raw and pre-treated tracer counts for detector D5 (Run 2)

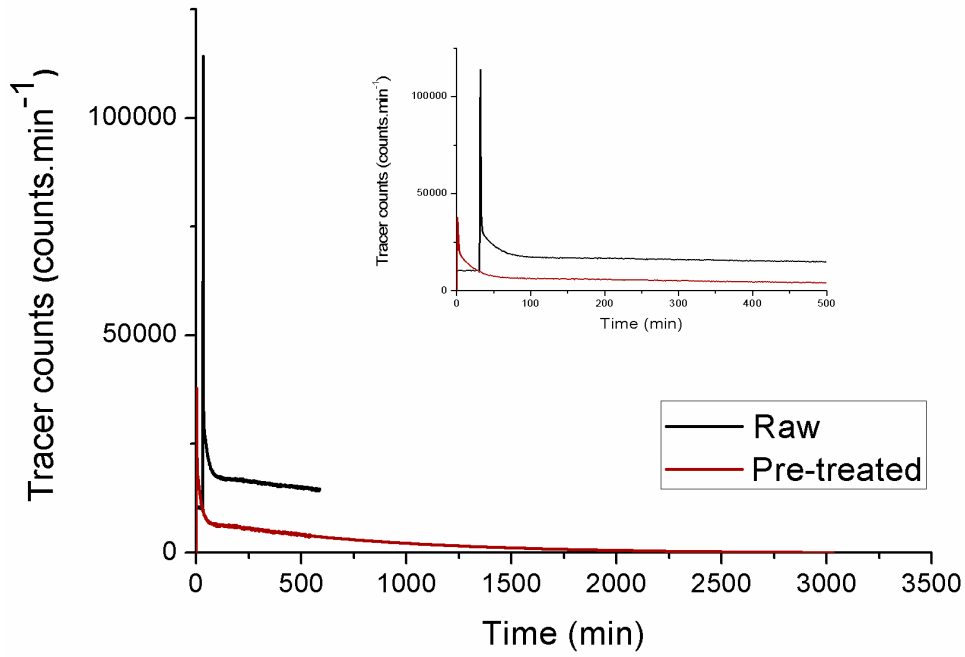


Fig. 4.7 Raw and pre-treated tracer counts for detector D2 (Run 3)

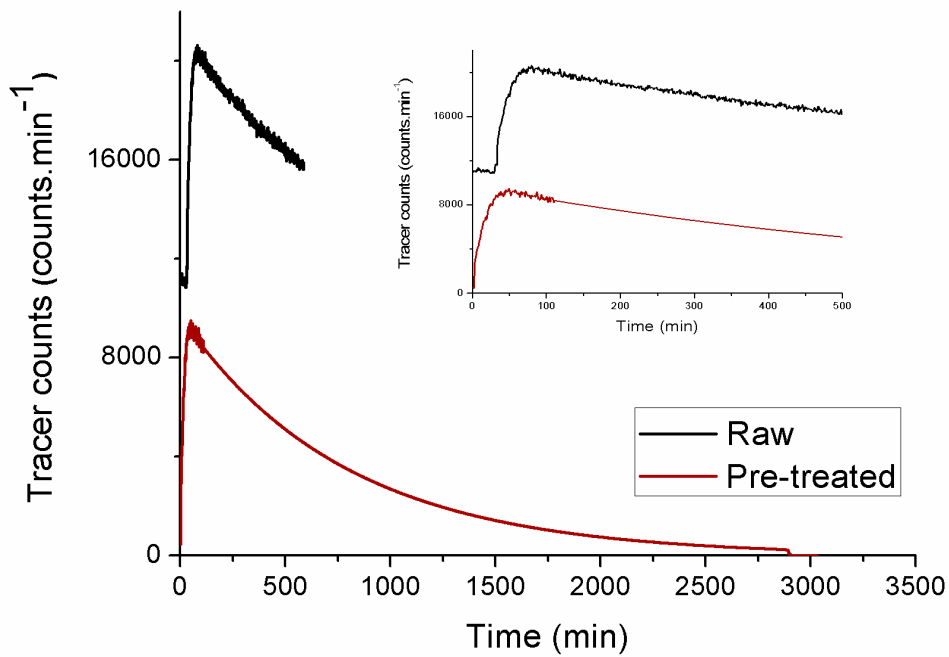


Fig. 4.8 Raw and pre-treated tracer counts for detector D5 (Run 3)

4.3. RTD analysis

The tracer concentration data recorded at the inlet and outlet of the reactors and other locations were corrected for starting point, background radiation, decay, and extrapolation and were finally normalized. The curve recorded at the inlet of the reactor R1 showed a very sharp peak indicating that the tracer was injected as an impulse. Therefore, the normalized tracer concentration (gamma count) curves obtained at the outlets of the reactor R1 and R2 directly provided the RTD of the reactor R1 and the reactor system1 respectively. The radiotracer concentration at the outlet of the reactors could not be recorded for a very long time and thus the incomplete curves were extrapolated using exponential regression method [16]. The extrapolated tracer concentration curves were normalized by dividing each data point by the area under the tracer concentration-time curves [5] using Eq. 4.2.

$$E(t) = \frac{n_c(t)}{\int_0^t n_c(t)dt} \quad (4.2)$$

where, $E(t)$ is normalized experimental tracer concentration, $n_c(t)$ is the experimental tracer concentration and t is the time variable. The first moment i.e. the centroid of the output curves provides the MRT of the fluid in the reactor [5] using Eq. 4.3.

$$\bar{t} = \frac{\int_0^{\infty} t n_c(t)dt}{\int_0^{\infty} n_c(t)dt} \quad (4.3)$$

where, \bar{t} is the experimental mean residence time, $n_c(t)$ is the experimental tracer concentration at any particular time t .

In order to investigate the flow behavior in the reactors, a suitable combination of RTD models was used to map the experimentally measured RTD curves. The models were proposed after careful examination of the experimental tracer concentration curves and considering the available information about the reactors. The tracer balance equations and the respective solutions of basic building blocks such as plug flow reactor (PFR), continuously stirred tank reactor (CSTR), CSTR with stagnant volume with exchange, etc. used in the proposed conceptual models are well-described elsewhere [5]. RTD analysis software DTSPRO V4.21 was used to simulate the measured RTD data using the suitably proposed RTD model. The software numerically solves the tracer balance equations of the proposed

model and can be tuned to fit the experimentally measured tracer concentration curves. RTD model parameters corresponding to the best fit between experimental and model RTD curves were estimated, which mapped with the sub-objective 4 of the thesis. In this study, the radiotracer was injected in a very short span of time in the fresh feed line of reactor R1 which approximated an idealized impulse function (Dirac's pulse). The tracer count measured at the outlet of reactor R1 directly provided the RTD of the reactor R1 after pre-treatment and normalization. The measured RTD could be directly fitted to the model simulated RTD curve. However, in case of reactor R2, the tracer concentration measured at the outlet of R2 was not the RTD of reactor R2 as the input to the reactor was not an impulse function. The radiotracer concentration measured at the outlet of reactor R1 acted as an input to the reactor R2. In such situations, the RTD of the reactor R2 could be obtained by convoluting the input tracer concentration with the impulse response of the proposed model [5] using Eq. 4.4.

$$Y(t) = \int_0^t X(t) \times E(t-T) dt \quad (4.4)$$

where, $X(t)$ is the input tracer concentration curve $Y(t)$ is the output tracer concentration curve, $E(t)$ is the impulse response of the proposed model and T is a random time variable.

4.4 Reactor R1

Reactor R1 was the first reactor in the series of the two ethyl acetate reactors and it received the fresh feed along with the recycle streams from the bottom of the distillation columns.

4.4.1 Model conceptualization

The RTD curves obtained at the outlet of the reactor R1 exhibited a sharp peak close to the origin of the curves and a long tail (Figures 4.10-4.12). The sharp peak at the beginning of the curves could be due to bypassing of a fraction of the fluid that exited the reactor without spending adequate time within the reactor and thus not taking part in the reaction. Whereas, the long tail in the curve could be contributed by either recycle of the tracer or by the presence of stagnant volume with exchange or both. Therefore, based on the measured RTD, the plant layout and other information available, the reactor R1 was represented by a CSTR with stagnant volume exchanging flow with the active volume, a CSTR in the bypass stream, and a recycle stream consisting of a plug flow component and a CSTR. The plug flow component represented the pipeline section whereas the CSTR represented the distillation

columns in the recycle path. The conceptual representation of the reactor R1 is shown in Fig. 4.9. Simulations were performed and values of the model parameters corresponding to the best fit were obtained and are shown in Table 4.1.

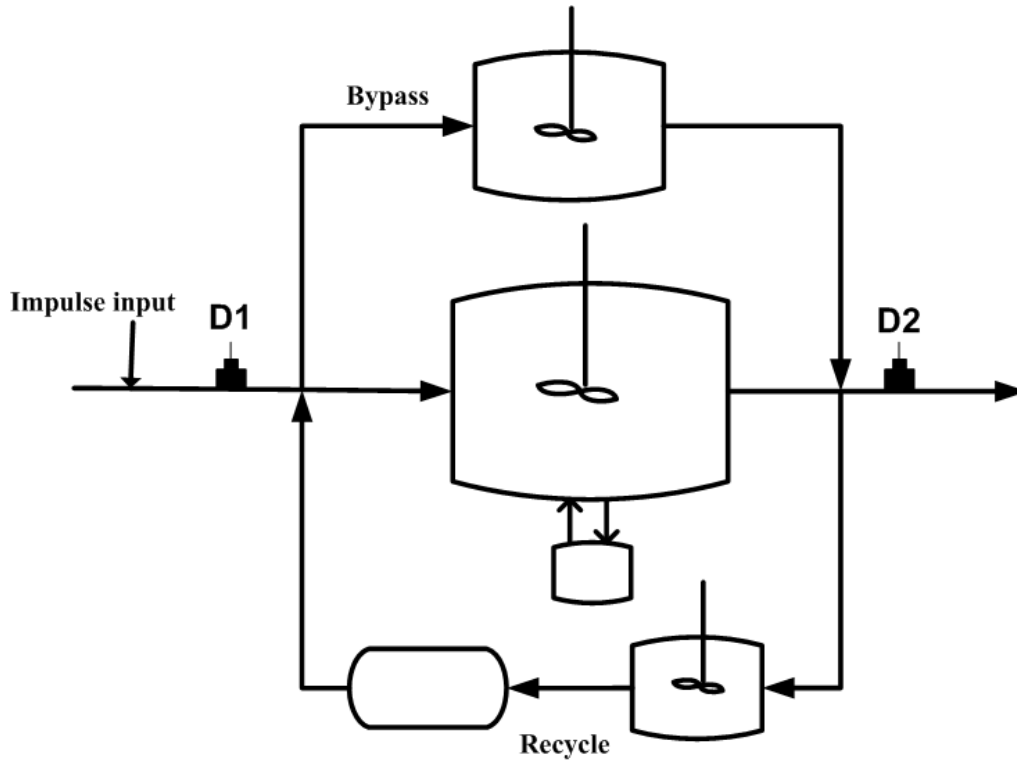


Fig. 4.9 Conceptual model of reactor R1

4.4.2 Effect of recirculation on MRT, bypassing and stagnant volume

It was observed that MRT of the fluid in reactor R1 decreased from 896 min to 505 min as the recirculation flow decreased (100% to 0%). This could be due to the increase in the bypassing of the input flow from 12% to 22% as can be seen from experimental RTD curves. In run 3, the MRT of fluid in the reactor was minimum because of the increased bypassing of the flow in the absence of recirculation flow in the reactor R1. The recirculation flow would have kept the tracer in the recirculation loop leading to an increased MRT as observed in the case of run 1 and 2. Also, operating the recirculation pump at lower capacity i.e. 50% (run 2) caused only a small increase in the bypass as compared to the bypass in run 1, but the MRT was significantly reduced. The model predicted RTD curves were found to fit very well with the experimental RTD curves as shown in Figures 4.10-4.12. The results of the model simulation corresponding to the best fit between experimental and model predicted RTD curves are shown in Table 4.1. A stagnant volume of 40% exchanging fluid with the active volume gave

the best fit between experimental and model predicted RTD curves for different operating conditions. Decrease in the bypass flow from 22% to 12% could be due to an increase in the recirculation rate which increased the experimental MRT from 505 min to 896 min.

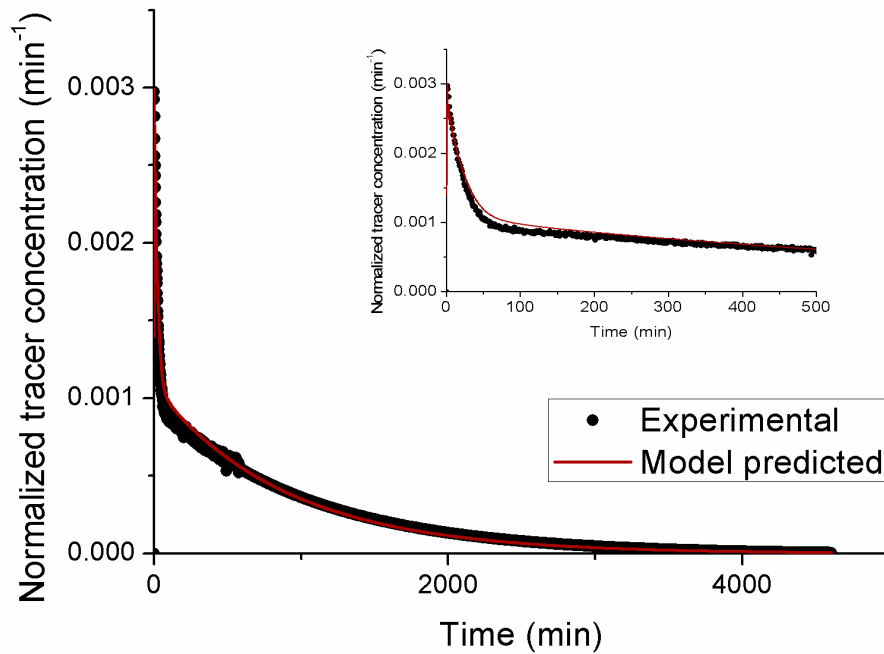


Fig. 4.10 Comparison of experimental and model predicted RTD curves for reactor R1 (Run 1)

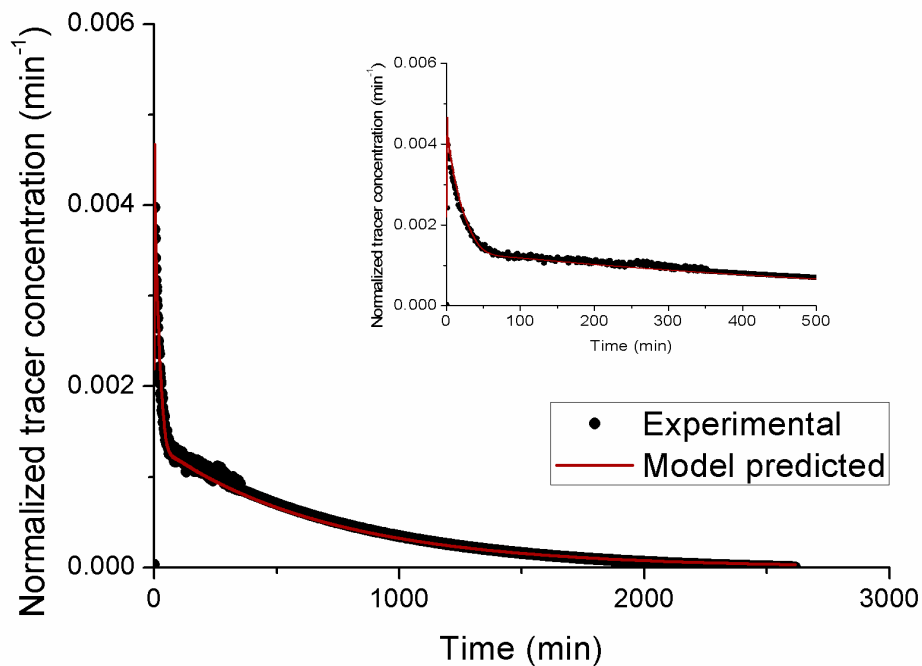


Fig. 4.11 Comparison of experimental and model predicted RTD curves for reactor R1

(Run 2)

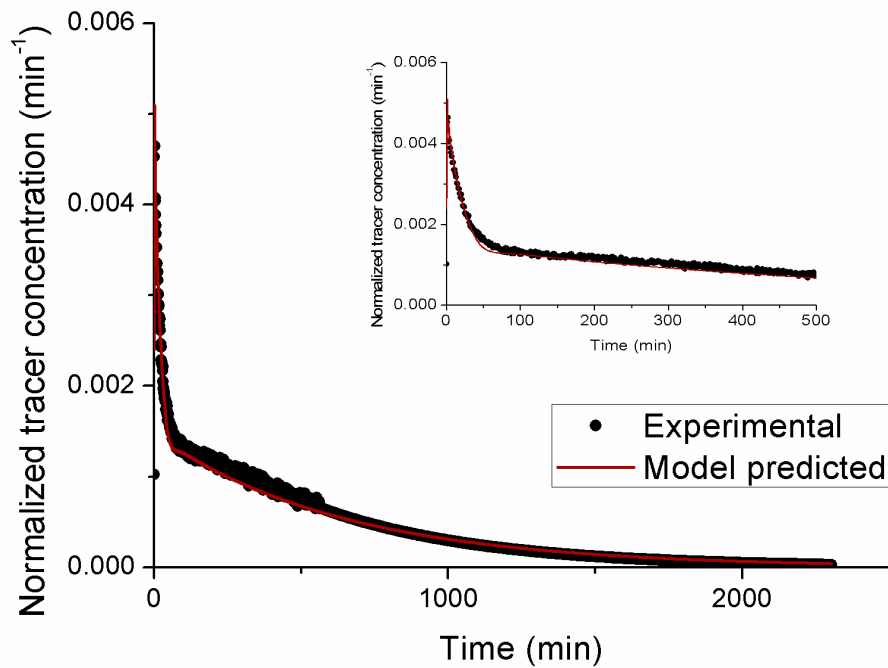


Fig. 4.12 Comparison of experimental and model predicted RTD curves for reactor R1 (Run 3)

Table 4.1 Results of the RTD model of reactor R1

Run	MRT		Bypass fraction	Stagnant volume		Recycle		
	Expt. (min)	Model (min)		Fraction	MRT (min)	Recycle ratio	PFR MRT (min)	CSTR MRT (min)
1	896	834	0.12	0.4	30	3.57	40	60
2	569	596	0.15	0.4	30	3.57	40	55
3	505	545	0.22	0.4	30	3.57	40	50

4.5. Reactor R2

Reactor R2 was the second reactor in the series of the two reactors. The reactor R2 did not receive any recycle flow and only received the output of reactor R1 as its feed. The output from the reactor R2 was fed to the distillation columns.

4.5.1 Model conceptualization

The proposed conceptual model that described the flow in reactor R2 is shown in Fig. 4.13. The model consisted of a CSTR having stagnant volume exchanging flow with the active volume of the reactor and was used to predict the RTD of the reactor.

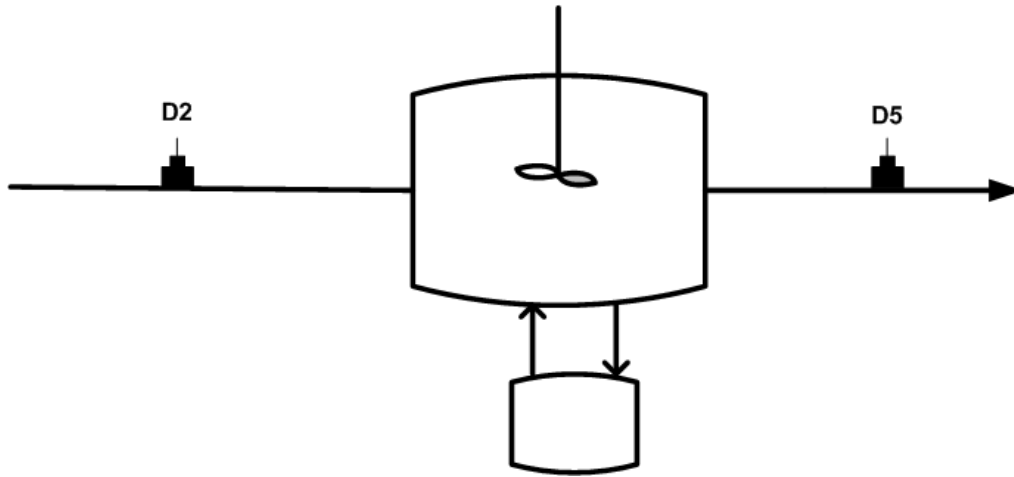


Fig. 4.13 Conceptual model of reactor R2

4.5.2 Data convolution

The output from the reactor R1 was fed directly to the reactor R2 and thus the radiotracer concentration curve recorded at the outlet of R1 ($X(t)$) served as an input to reactor R2. As $X(t)$ was not an impulse input, the RTD of reactor R2 was determined by the process of convolution (Eq. 4.4). $X(t)$ was convoluted with the impulse response of the proposed model and the $Y(t)$ was fitted to the experimental RTD curve measured at the outlet of R2 at different operating conditions.

4.5.3 Effect of recirculation on MRT, bypassing and stagnant volume

It was observed that the model predicted MRT marginally decreased from 50 min to 45 min with a decrease in recirculation rate. This indicated that the effect of the recirculation in reactor R2 was not as dominant as in the case of reactor R1. Also, no bypass flow was predicted during the model simulation. A low stagnant volume (1%) with exchange was predicted corresponding to the best fit of experimental RTD curves, was also not affected by the recirculation rate. The marginal change in the model predicted MRT of the reactor could be due to the negligible stagnant volume (1%) inside the reactor as well as the absence of bypass flow. The comparison of experimental and model predicted RTD for different operating conditions are shown in Figures 4.14-4.16. The excellent fitting of model predicted RTD curves to the experimentally measured RTD curves indicate that the proposed model was suitable to describe the flow of reactor R2. The results of the model simulation are shown in Table 4.2.

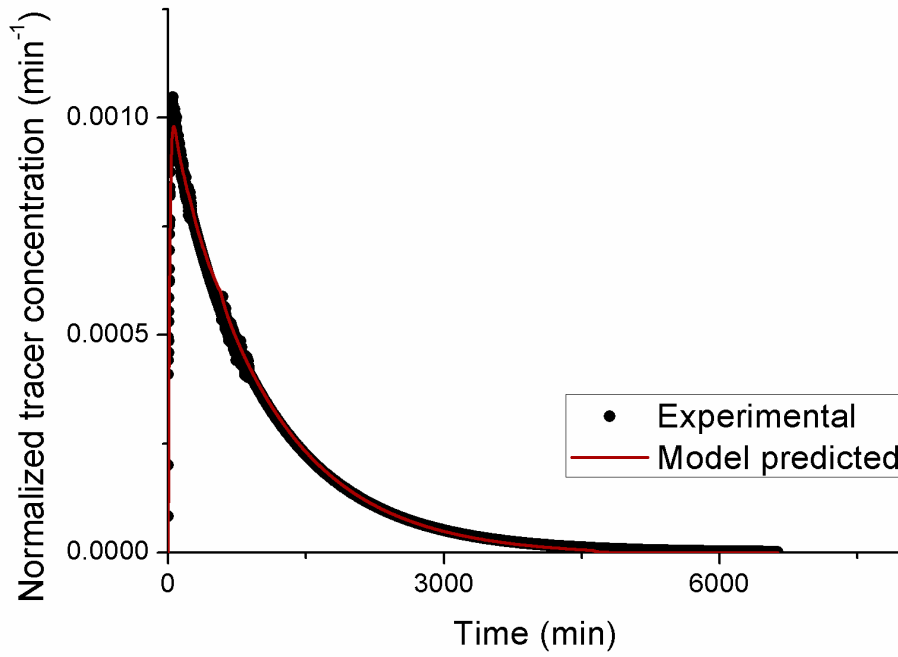


Fig. 4.14 Comparison of experimental and model predicted RTD curves for reactor R2 (Run 1)

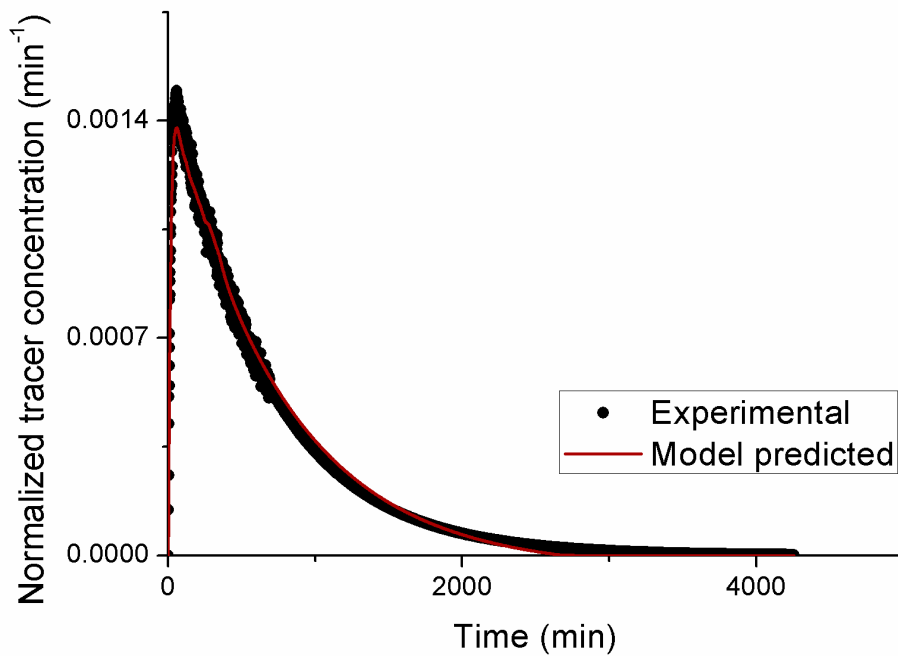


Fig. 4.15 Comparison of experimental and model predicted RTD curves for reactor R2 (Run 2)

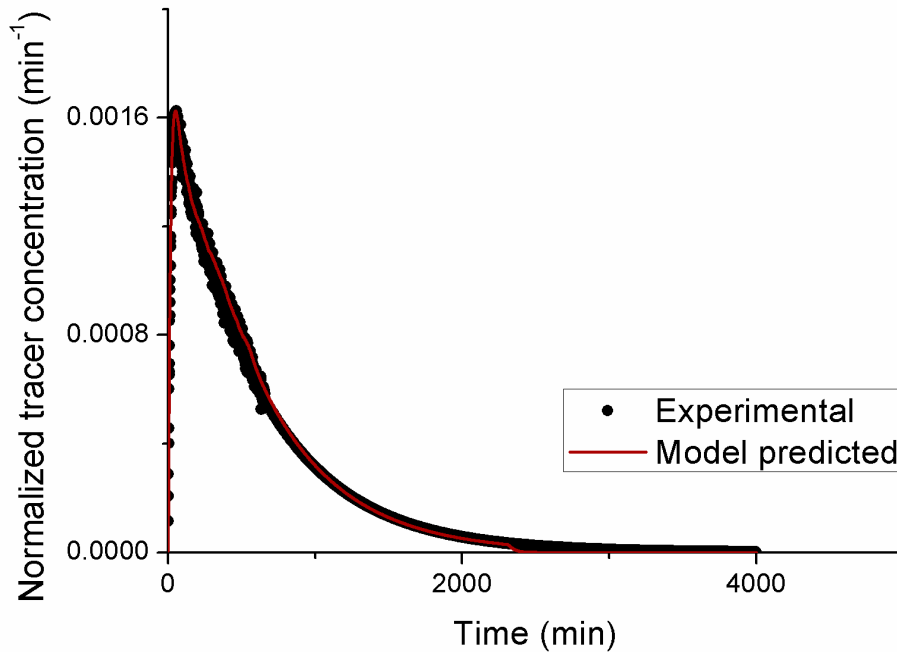


Fig. 4.16 Comparison of experimental and model predicted RTD curves for reactor R2 (Run 3)

Table 4.2 Results of the RTD model of reactor R2

Run	MRT		Stagnant Volume	
	Theoretical (min)	Model(min)	Fraction	MRT (min)
1	60	50	0.01	5
2	60	45	0.01	5
3	60	40	0.01	5

4.6 Reactor system 1

The reactor system 1 comprised of both the ethyl acetate reactors R1 and R2 in series.

4.6.1 Model conceptualization

The flow behavior of reactor system 1 (reactor R1 connected in series with reactor R2) was modeled. The entire reactor system was modeled as a combination of the conceptual models of reactors R1 and R2. The conceptual model proposed for the reactor system 1 is shown in Fig. 4.17. The model consisted of two CSTR with stagnant volume (with exchange) connected in series. The reactor R1 had a bypass stream represented by a CSTR and a recycle stream from outlet of the reactor R2 to the inlet of the reactor R1 represented by a plug flow component. The response of the reactor system 1 to an impulse injection at the inlet of R1 provided the RTD of the reactor system 1. The proposed model was used to predict the RTD

of the reactor system 1 and was fitted to the experimental RTD curves at the outlet of the reactor R2. The values of the MRT in the plug flow component that represented the recycle loop was predicted to be 40 min for all the three runs and was unaffected by the variation in recirculation flow. The parameters of the model were obtained and the results of the model simulation corresponding to the best fit are shown in Table 4.3. The comparison of the experimental and model predicted RTD showed an excellent match as shown in Figures 4.18-4.20 for the model parameters reported in Table 4.3.

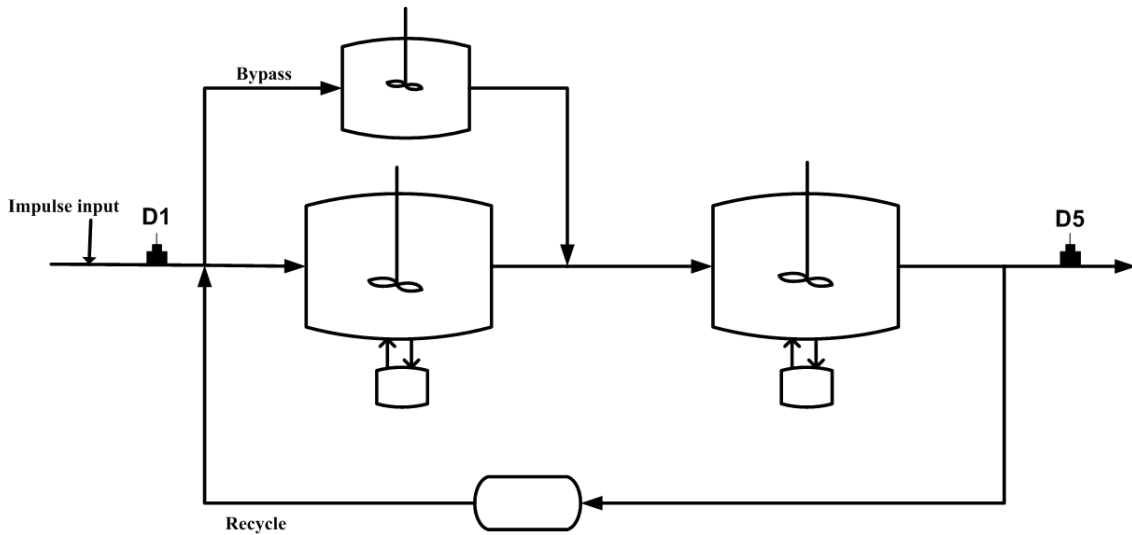


Fig. 4.17 Conceptual model of reactor system 1

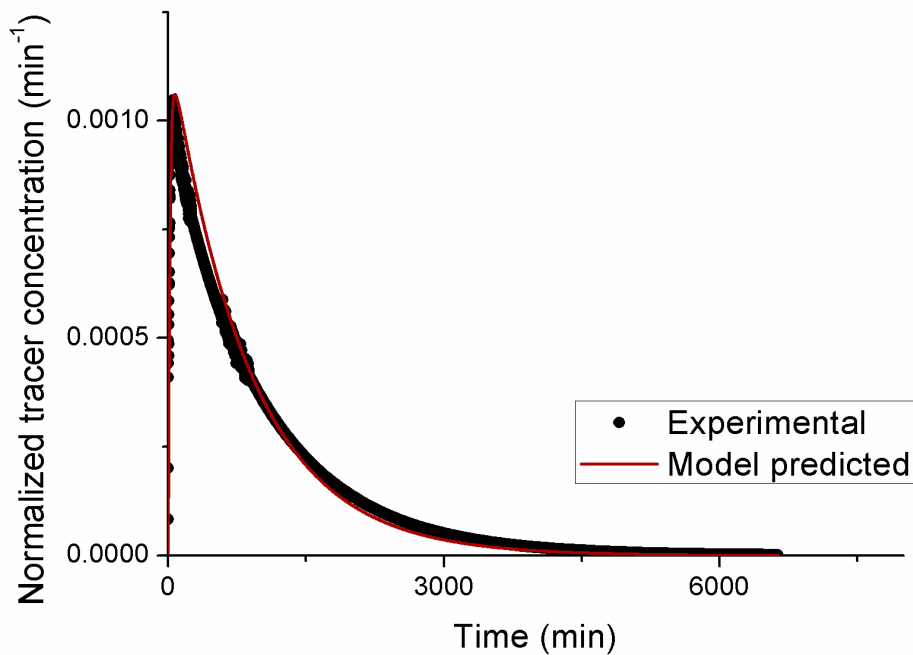


Fig. 4.18 Comparison of experimental and model predicted RTD curves for reactor system 1 (Run 1)

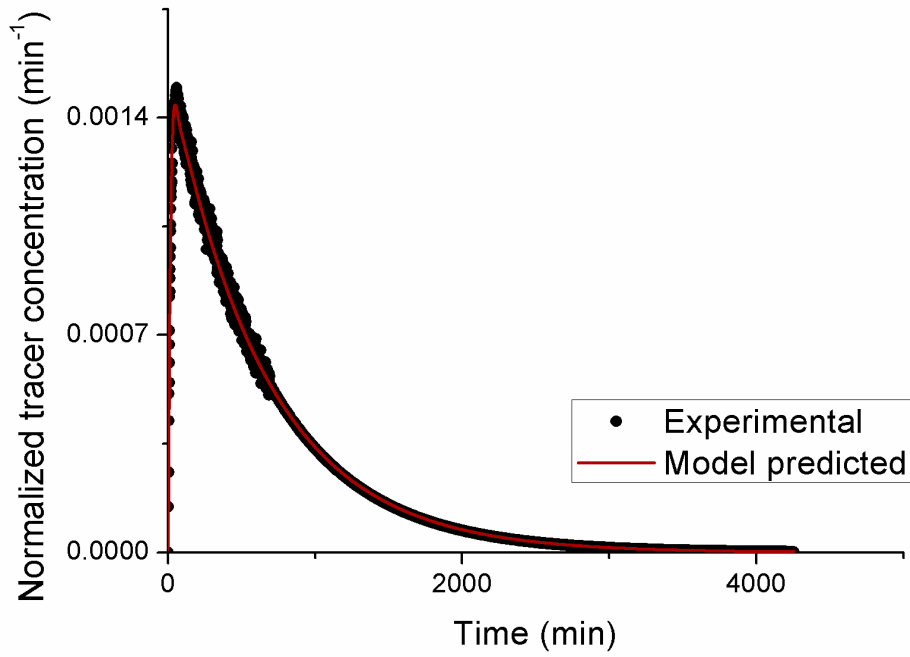


Fig. 4.19 Comparison of experimental and model predicted RTD curves for reactor system 1 (Run 2)

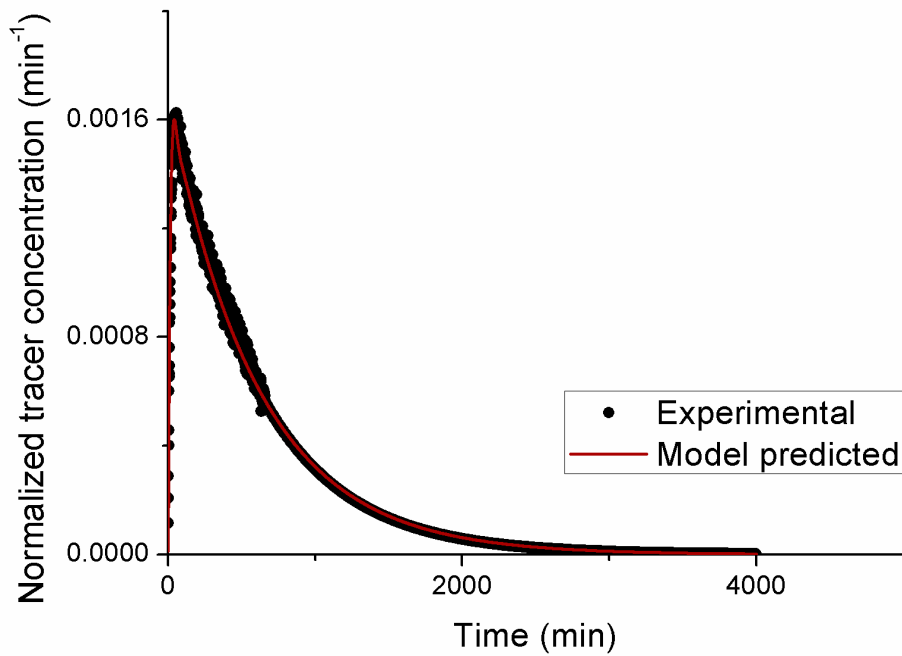


Fig. 4.20 Comparison of experimental and model predicted RTD curves for reactor system 1 (Run 3)

Table 4.3 Results of RTD model of the reactor system 1

Run	MRTs			Bypass fraction	Stagnant Volume				Recycle PFR MRT, (min)
	Theo. (min)	Expt. (min)	Model (min)		Reactor R1		Reactor R2		
					Fraction	MRT (min)	Fraction	MRT (min)	
1	1003	1010	873	0.12	0.4	30	0.01	5	40
2	771	650	661	0.15	0.4	30	0.01	5	40
3	617	594	611	0.22	0.4	30	0.01	5	40

4.7 Uncertainty analysis

During the experimentation and analysis of any experimental data, certain errors may creep into the data and cause uncertainty in the results which needs to be quantified [94]. In the present work, three kinds of uncertainties i.e. uncertainty in estimated values of theoretical MRT, in measured values of the MRT and in model parameters obtained after model simulation were studied. The uncertainties in the results were quantified using the root sum squared (RSS) method covering 95% of the true value [95].

The uncertainty in theoretical MRT depended on errors in the volume of the fluids in the reactors and flow rate through them. The values of these two quantities were continuously measured using well-calibrated instrumentation installed in the plant with associated uncertainties of $\leq 5\%$. Using the theory of propagation of error [96], the uncertainty in the values of the theoretical mean MRTs were estimated to be about 5% for different runs.

Similarly, the uncertainty in experimentally measured MRT due to extrapolation of incomplete measurement of RTD curves was also estimated. In the present work, the experimentally measured RTD curves were extrapolated by regressing the final 40% of the data points of the experimental data set with an exponentially decaying function. The regression coefficient (R^2) corresponding to the extrapolation was found to be $\geq 95\%$ for all the runs. This indicates that the uncertainty in the experimental MRT values was within 5%.

Uncertainties in the model predicted parameters were also estimated by studying the effect of varying magnitudes of the model parameters on the simulated RTD curve and its deviation from the experimentally measured curve. The analysis showed that the uncertainties in the obtained model parameters ranged from 5-25% for reactor R1 and 1-15% for reactor R2 corresponding to an acceptable fit between experimental and model predicted RTD curves.

CHAPTER-5

Chapter-5 RTD experiments on industrial reactor system 2

After the first set of RTD studies at the ethyl acetate plant of IOLCP Ltd., Barnala, India, the reactor system was replaced by a new set of reactors to accommodate any future increase in the production capacity of the plant. Reactor R1 was replaced with a new vessel, whereas, an existing vessel in the plant was used as reactor R2. The reactor R1 had a horizontal orientation with an internal diameter of 4 m and a height of 7.7 m. The horizontal orientation of the reactor R1 helped with proper distribution of feed and recycle products compared to a vertical orientation. The reactor R2 had vertical orientation and an internal diameter and height of 4 and 7.8 m, respectively. The working volume of the reactor R1 and R2 was 37% and 47% of their respective geometric volumes. In order to understand the flow behavior inside the new reactors, the second set of industrial RTD studies were performed. The schematic of the plant and detector setup for the industrial reactor system 2 is shown in Fig. 5.1. The reactor R1 and R2 are shown in Fig. 5.2.

In the second set of industrial RTD experiments, detector D1 was installed at the inlet of reactor R1 at a position just next to the injection point to record the entry time. Detector D2 and D5 were installed at the outlet of the reactor R1 and reactor R2 respectively to detect and record the output tracer counts from the reactors. Detector D3 and D4 were respectively positioned at the bottom product of the columns 1A and 1B entering reactor R1. Detector D6 was mounted at the inlet of column 1B from reactor R2. Detectors D7 and D8 were installed on the top product of column 1B and the reflux stream to the column respectively. D9 and D10 detectors were respectively mounted at the organic and aqueous stream output from the decanter.

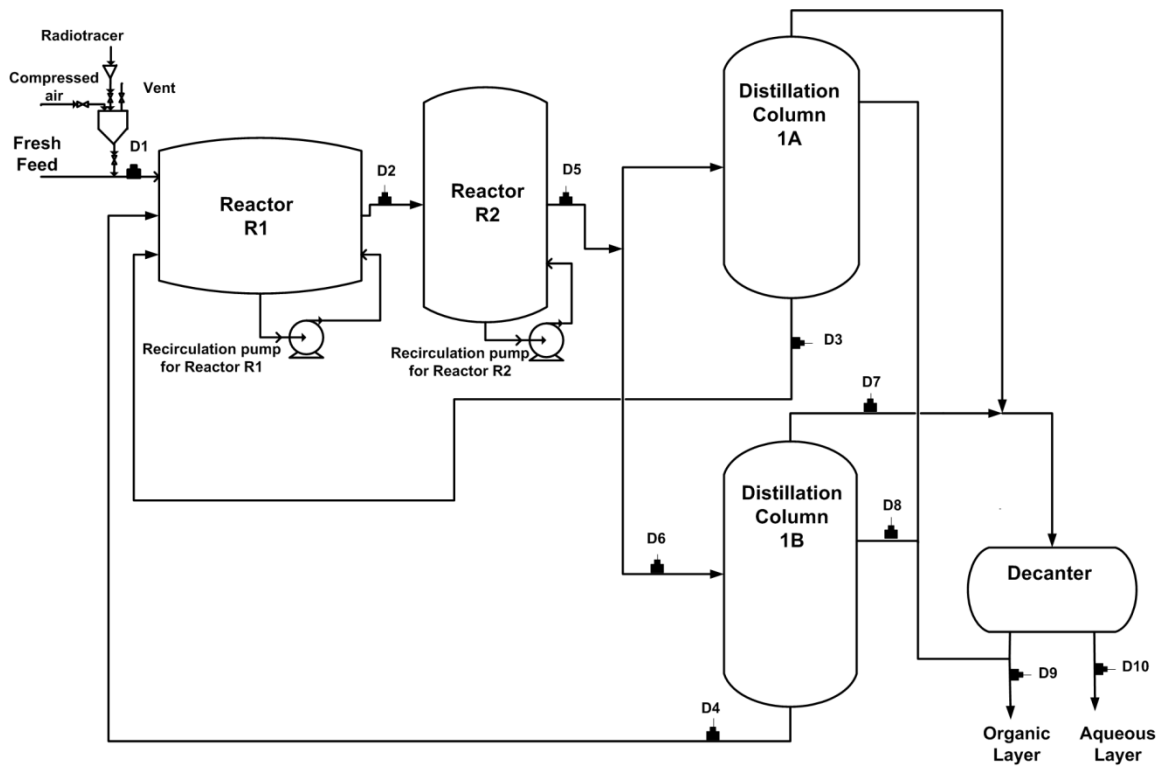


Fig. 5.1 Schematic of industrial reactor system 2 showing the detector positioning



Fig. 5.2 Reactor R1 (a) and reactor R2 (b) of industrial reactor system 2

Three experiments with different recirculation rate were performed as shown in Table 3.2. These experiments mapped with the sub-objective 3 of the thesis. After the RTD experiments pre-treatment of the radiotracer data was performed.

5.1 Pre-treatment of the radiotracer data

Similar to the first set of industrial RTD experiments, the raw output tracer count data obtained in the second set of industrial RTD experiments was corrected for starting point, background radioactivity, and radioactive decay before extrapolating the tail of the tracer count curve. In the second set of industrial RTD experiments, the tracer data was collected for a longer duration as compared to the first set data. Also, in the first set of industrial RTD experiments, high background radiation was observed. This could be due to the presence of radiotracer station, where the radiotracer was handled, in close vicinity of the detectors D2 (mounted in the outlet of reactor R1) and D5 (mounted in the outlet of reactor R2). Hence, in the second set of industrial RTD experiments, the radiotracer station was set up at a remote place from where it couldn't unnecessarily add to the background radiation detected by the detectors D2 and D5. Figures 5.3-5.8 shows the comparison between the output tracer curves before and after pre-treatment for detector D2 and D5 for different runs.

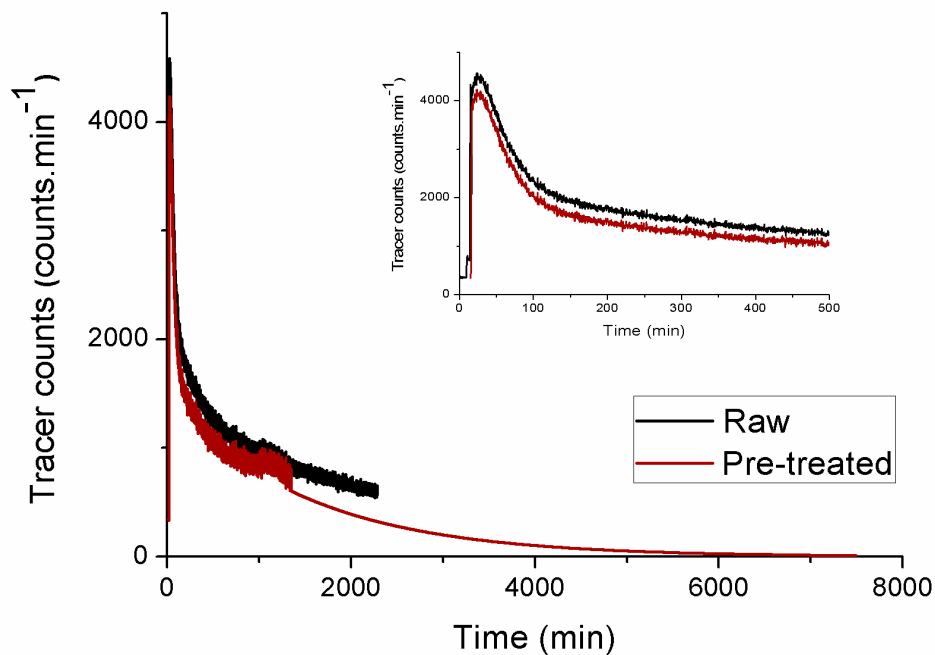


Fig. 5.3 Raw and pre-treated tracer counts for detector D2 (Run 1)

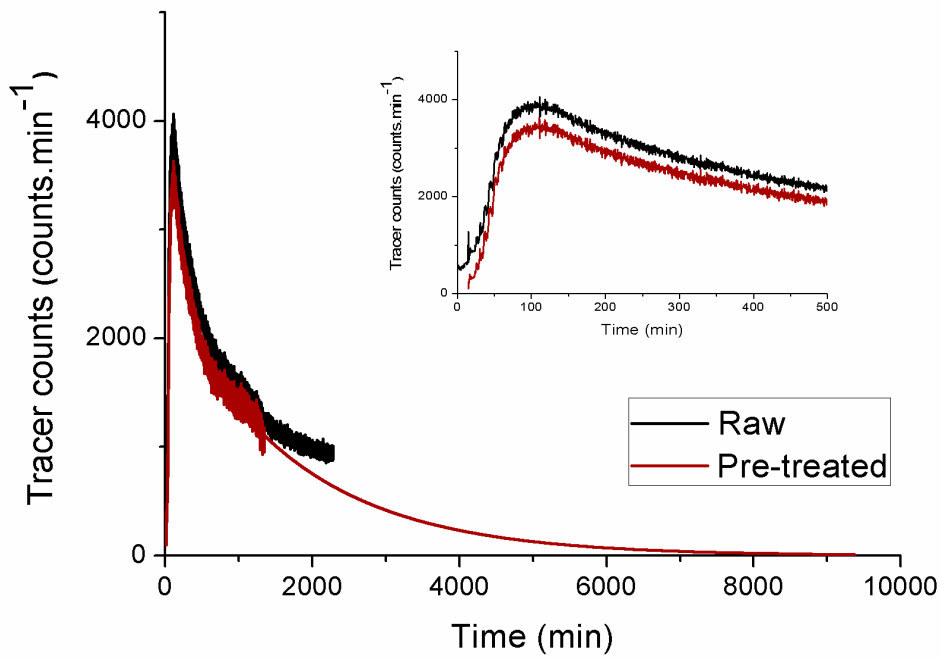


Fig. 5.4 Raw and pre-treated tracer counts for detector D5 (Run 1)

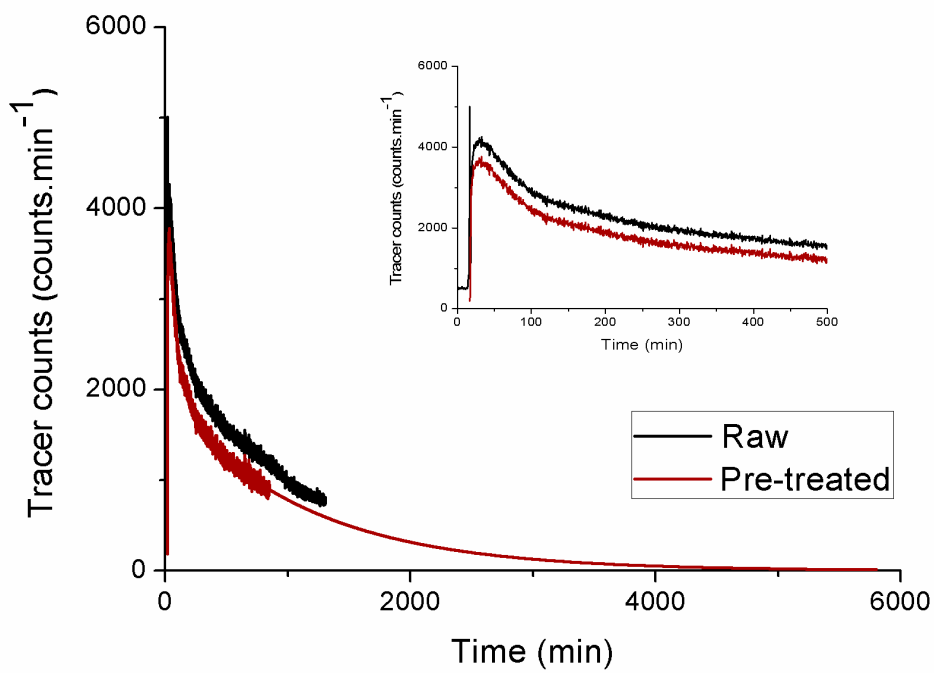


Fig: 5.5 Raw and pre-treated tracer counts for detector D2 (Run 2)

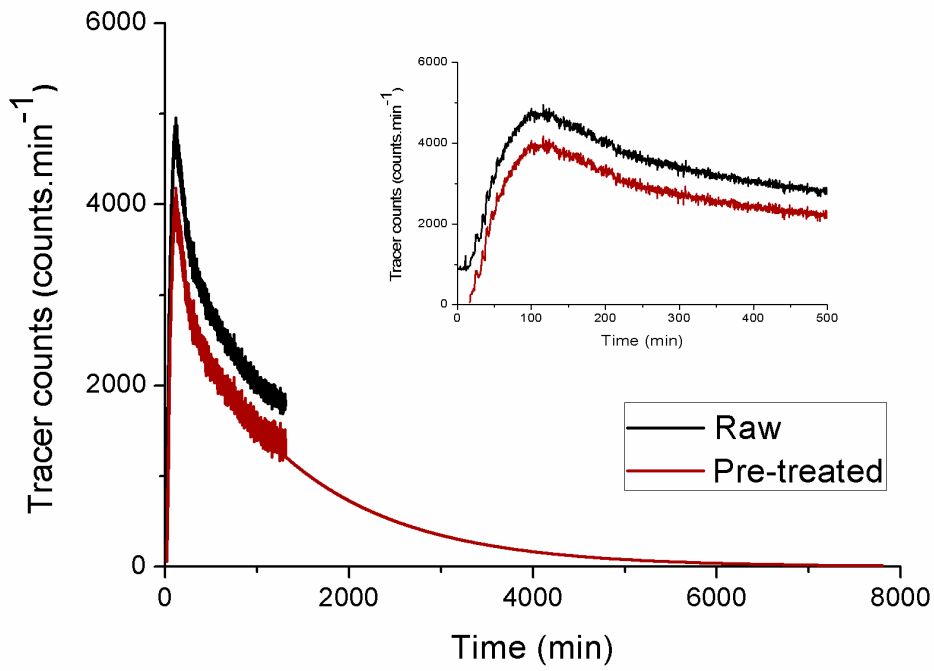


Fig. 5.6 Raw and pre-treated tracer counts for detector D5 (Run 2)

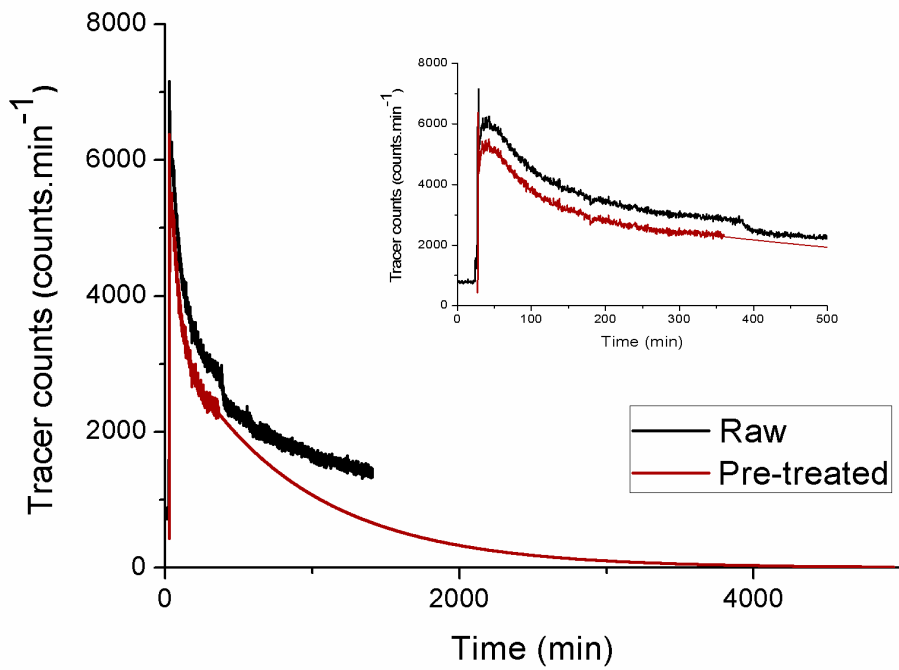


Fig: 5.7 Raw and pre-treated tracer counts for detector D2 (Run 3)

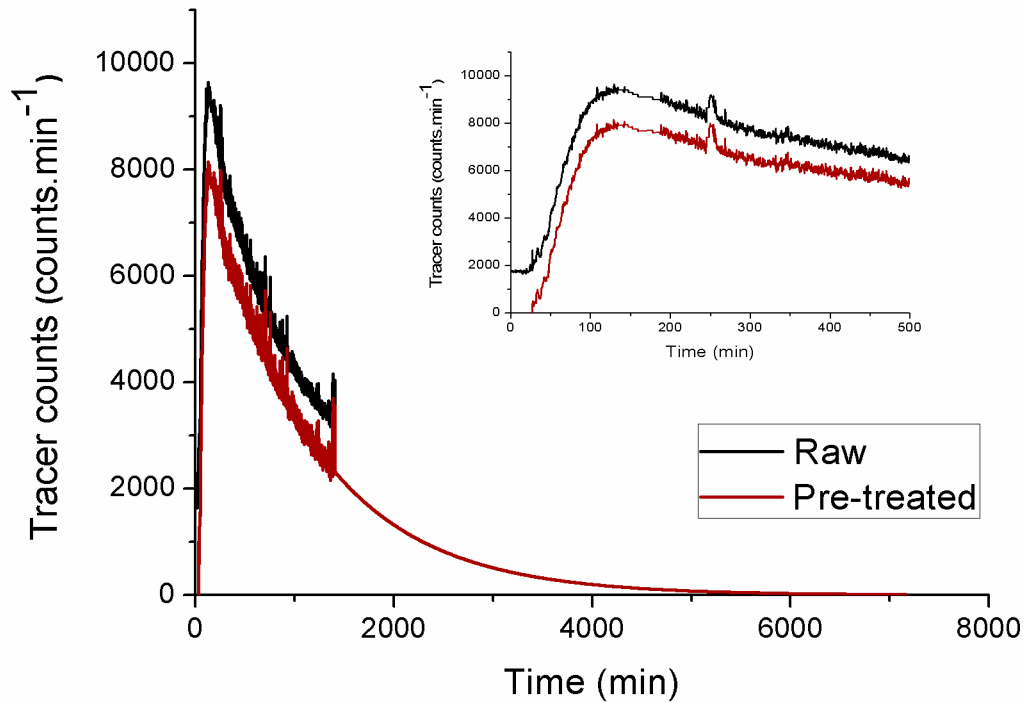


Fig: 5.8 Raw and pre-treated tracer counts for detector D5 (Run 3)

5.2 RTD analysis

After the radiotracer data was pre-treated, it was normalized following the Eq. 4.2. Also, MRT for the experimental RTD data was calculated using Eq. 4.3. RTD model parameters corresponding to the best fit between experimental and model RTD curves were estimated, which mapped the sub-objective 4 of the thesis.

The conceptualized models for the reactors were proposed using basic models of RTD namely CSTR, PFR, CSTR with stagnant zone exchanging fluid with active volume, etc. As compared to the first set of industrial RTD experiments, more physical compartments were added to the conceptual model of the reactor system in the second set of industrial RTD experiments to mimic the system more accurately.

5.3 Reactor R1

Reactor R1 was the first reactor in the series of the two ethyl acetate reactors. It received the fresh feed and the bottom product of distillation columns. The output of reactor R1 was fed to reactor R2.

5.3.1 Model conceptualization

The experimental RTD curves showed the presence of bypass flow (sharp peak at the beginning of the curve) and stagnant volume exchanging flow with active volume (long tail). Thus, reactor R1 was modeled as a CSTR (named as CSTR A in Fig. 5.9) with stagnant volume exchanging tracer with the rest (active volume) of the reactor volume, a well-mixed bypass and a recycle stream with a plug flow unit representing the pipelines and series of CSTR representing the stages of distillation columns. Reactor R2 was also represented as a simple CSTR (named as CSTR B in Fig. 5.9) in the recycle path of the conceptual model of reactor R1 as it was a part of the recycle for reactor R1. The conceptual model of reactor R1 is shown in Fig. 5.9.

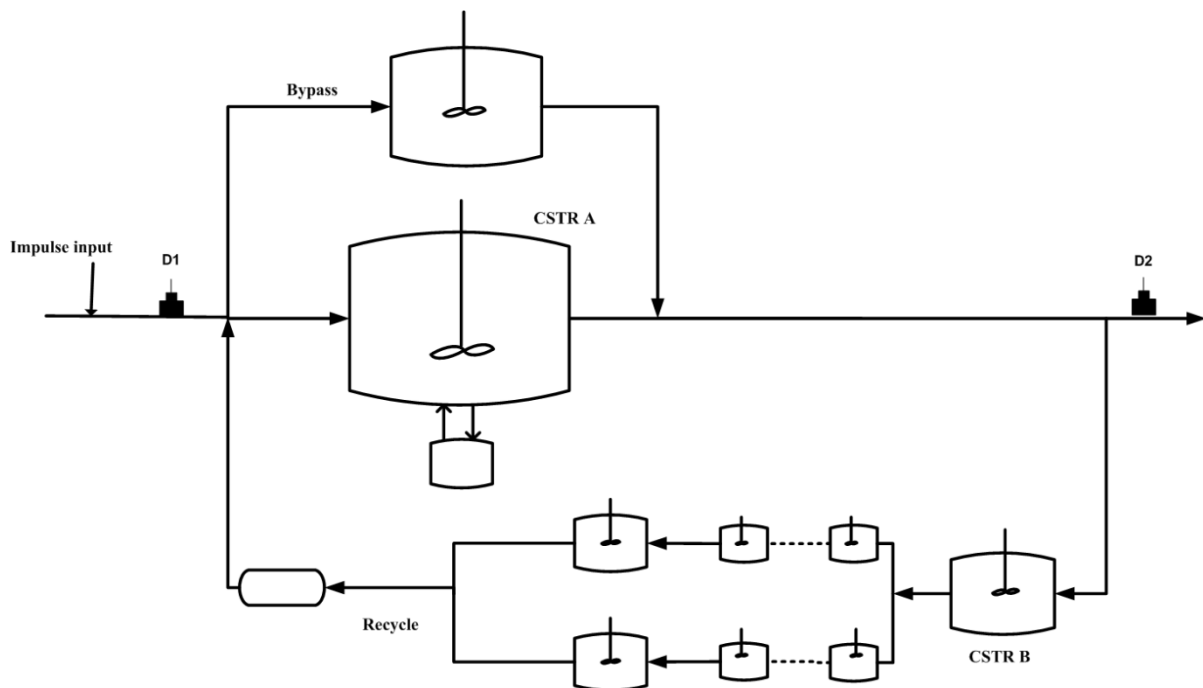


Fig. 5.9 Conceptual model of reactor R1

5.3.2 Effect of recirculation on MRT, bypass and stagnant volume

It can be seen from the results that MRT (experimental) was the highest (22.17 h) for run 1 and the lowest (13.21 h) for run 3. In run 1, the recirculation pump at its 100% capacity, held the tracer in a continuous circuit which in turn raised the MRT. In run 3, the recirculation pump was turned off, and a lower value of MRT was obtained. Bypass of 18% to 32% was observed from the experimental RTD curves for the three runs. A large amount of recycle entering reactor R1 may have caused bypassing. Also, the absence of recirculation (run 3)

leads to less turbulence inside the reactor which in turn might have resulted in the short-circuiting of fluid to the reactor outlet causing a low value of MRT as well. The experimentally observed value of bypass flow (obtained from RTD curves) served as an input parameter for the simulation. Corresponding to the best fit of experimental RTD curves, an increase in stagnant volume (exchanging fluid with the active volume) from 5% to 15% was predicted with decrease in the recirculation rates. Increase in the experimental MRT (13.21 h to 22.17 h) with an increase in the recirculation flow for reactor R1 could be due to simultaneous decrease in the bypass flow (32% to 18%) and stagnant volume (15% to 5%). The model predicted RTD curves fitted well to the experimental RTD curves and are shown in Figures 5.10-5.12. The best-fit values of the model parameters predicted by the simulation are shown in Tables 5.1-5.4.

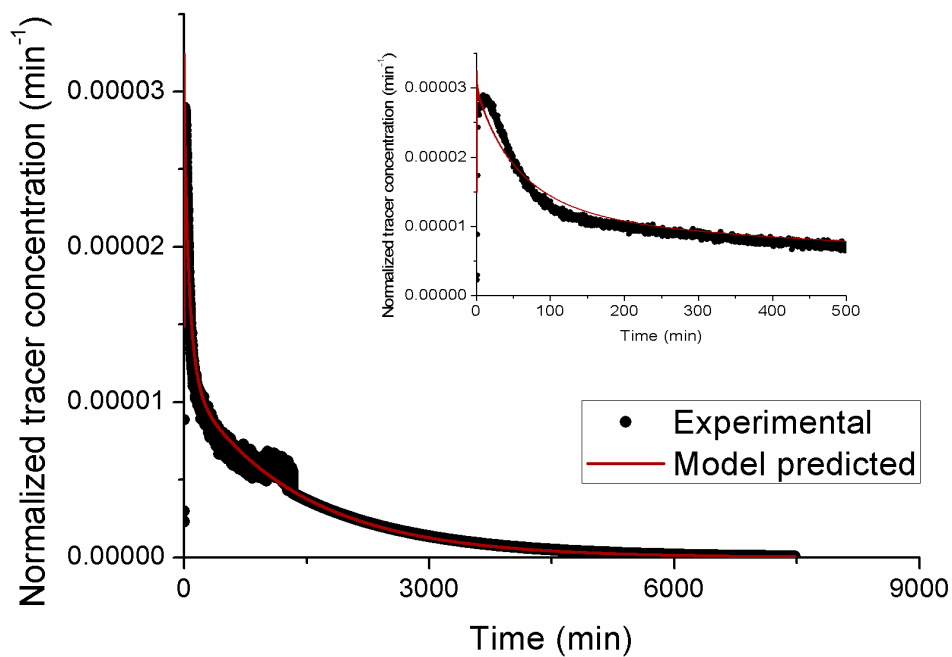


Fig. 5.10 Comparison of experimental and model predicted RTD curves for reactor R1 (Run 1)

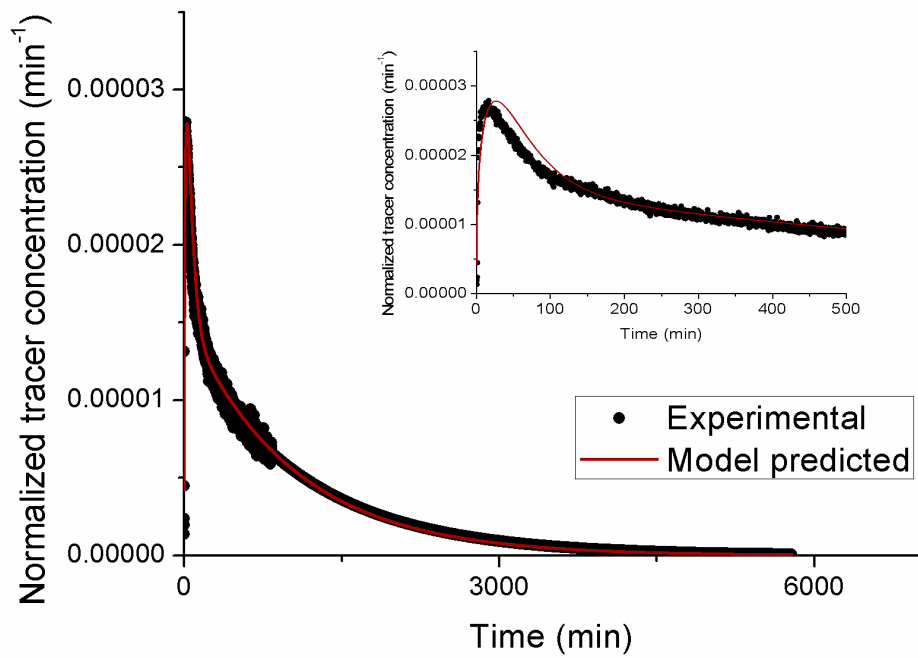


Fig. 5.11 Comparison of experimental and model predicted RTD curves for reactor R1 (Run 2)

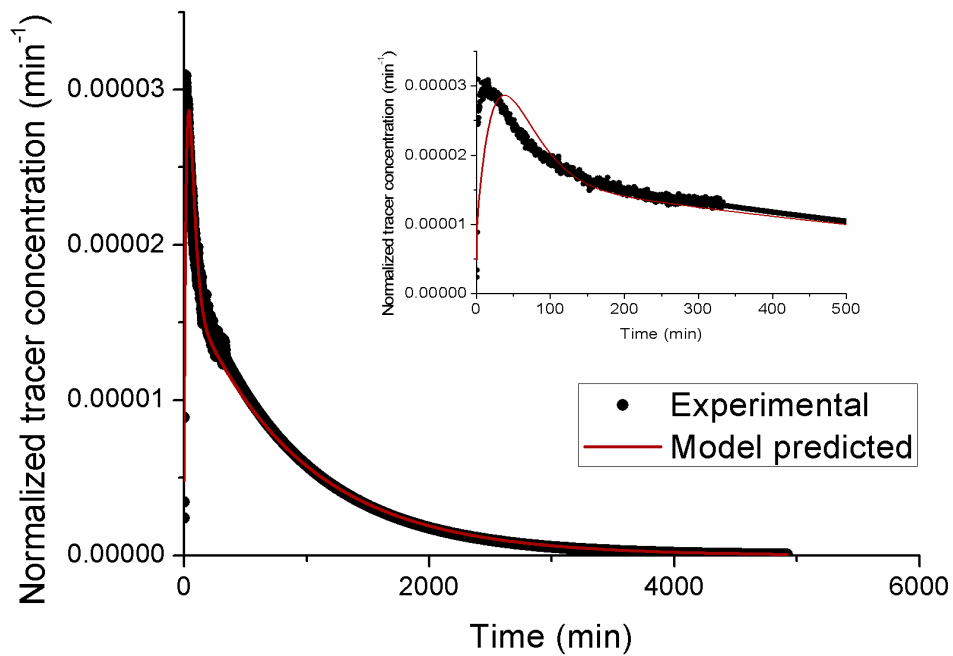


Fig. 5.12 Comparison of experimental and model predicted RTD curves for reactor R1 (Run 3)

Table 5.1 Experimental and model predicted MRT for reactor R1

Run	Experimental MRT (h)	Model MRT (h)
1	22.17	20.71
2	16.62	14.54
3	13.21	12.25

Table 5.2 Model predicted bypass parameters for reactor R1

Run	Fraction	MRT (h)
1	0.18	0.67
2	0.29	0.56
3	0.32	0.44

Table 5.3 Model predicted stagnant volume parameters for CSTR A

Run	MRT (h)	No. of CSTR in series	Stagnant volume	
			Fraction	MRT (h)
1	2.22	1	0.05	0.28
2	1.58	1.5	0.10	0.83
3	1.47	2	0.15	1.11

Table 5.4 Model predicted recycle parameters for reactor R1

Run	Recycle ratio	CSTR B MRT (h)	Distillation columns			PFR MRT(h)
			Stage MRT (h)	No. of stages	Reboiler MRT (h)	
1	3.57	2.78	0.006	48	0.25	0.03
2	3.57	2	0.006	48	0.25	0.03
3	3.57	1.92	0.006	48	0.25	0.03

5.4 Reactor R2

Reactor R2 was the second reactor in the series of the two reactors. The reactor R2 did not receive any recycle flow and only received the output of reactor R1 as its feed. The output from the reactor R2 was fed to the distillation columns.

5.4.1 Model conceptualization

Reactor R2 was conceptualized as a CSTR having stagnant volume (exchanging fluid with the active volume) and a CSTR in the bypass flow as shown in Fig. 5.13.

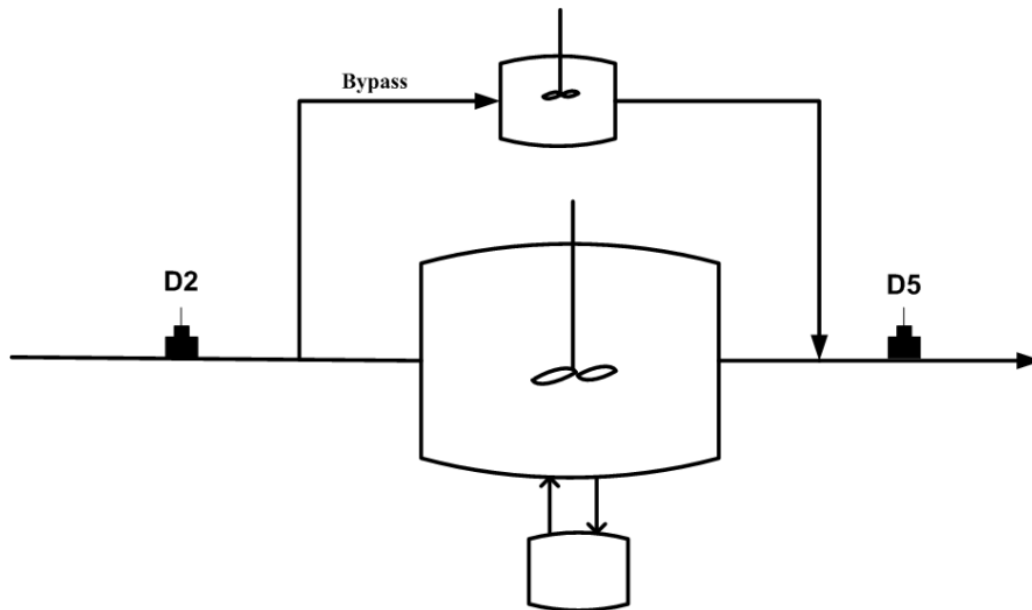


Fig. 5.13 Conceptual model of reactor R2

5.4.2 Data convolution

Similar to the first set of industrial RTD experiments, as the output from the reactor R1 was not an ideal impulse function, the RTD of reactor R2 was obtained by convolution (Eq. 4.4).

5.4.3 Effect of recirculation on MRT, bypassing and stagnant volume

Corresponding to the best fit of experimental RTD curves, the highest bypass fraction of 15% was predicted for 100% recirculation (run 1) and lowest bypass of 2% was predicted in the absence of recirculation (run 3). Reduction in bypass with reduction in recirculation rate indicated that the recirculation flow on reactor R2 had the opposite effect as compared to reactor R1. Reactor R2 had higher L/D ratio compared to reactor R1 and this may have lead to the promotion of channeling from flow distributors to the outflow by the recirculation flow. Also, an increase in the predicted MRT from 1.25 h to 1.80 h with a decrease in recirculation flow was also observed. At high recirculation rates, increased bypassing of the process fluid could have helped the tracer particles to escape the reactor without spending adequate time inside the reactor which resulted in a decrease in the MRT of the reactor. Model predicted stagnant volume of 5% exchanging fluid with the active volume gave the best fit to experimental RTD curves and was not affected by the recirculation flow to reactor R2. The increase in the MRT from 1.25 h to 1.80 h of the reactor R2 with the decrease in recirculation flow could be attributed to the decrease in bypass flow (15% to 2%). The comparison of experimental and model predicted RTD curves for different operating

conditions are shown in Figures 5.14-5.16. The model parameters corresponding to the best fit between experimental and model predicted RTD curves are shown in Table 5.5.

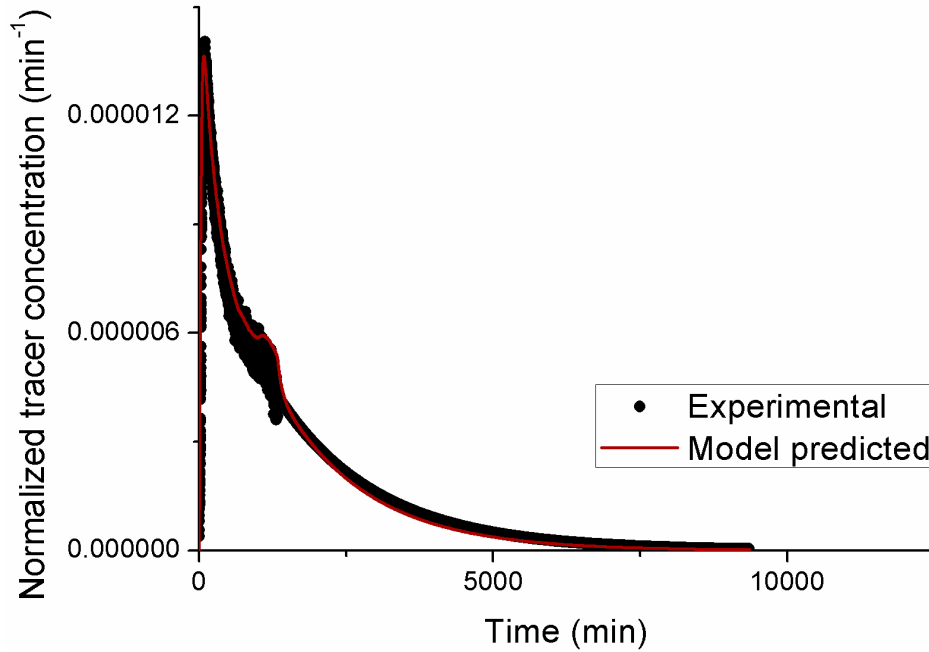


Fig. 5.14 Comparison of experimental and model predicted RTD curves for reactor R2 (Run 1)

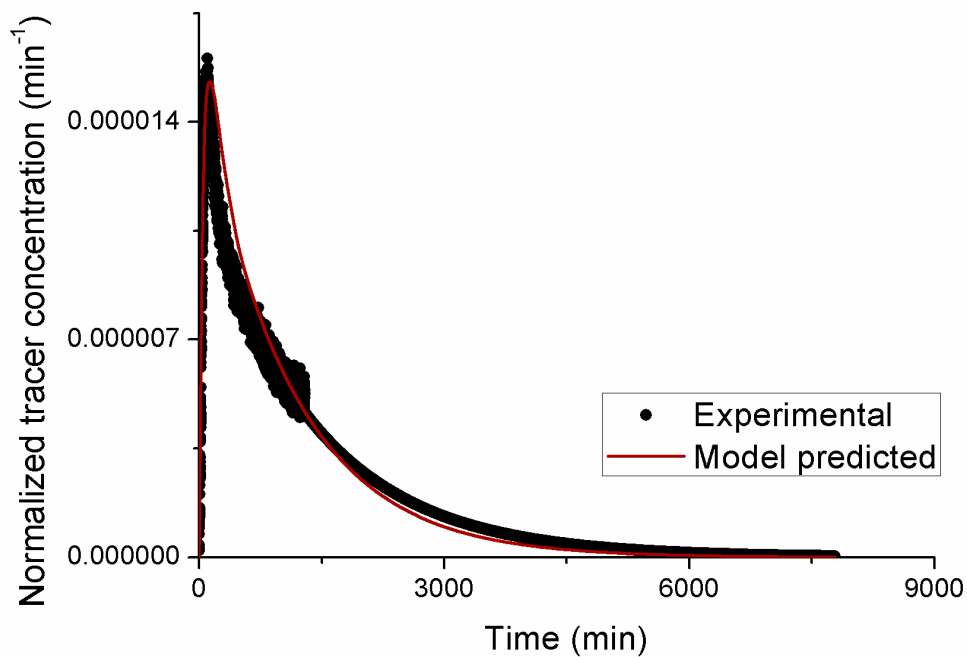


Fig. 5.15 Comparison of experimental and model predicted RTD curves for reactor R2 (Run 2)

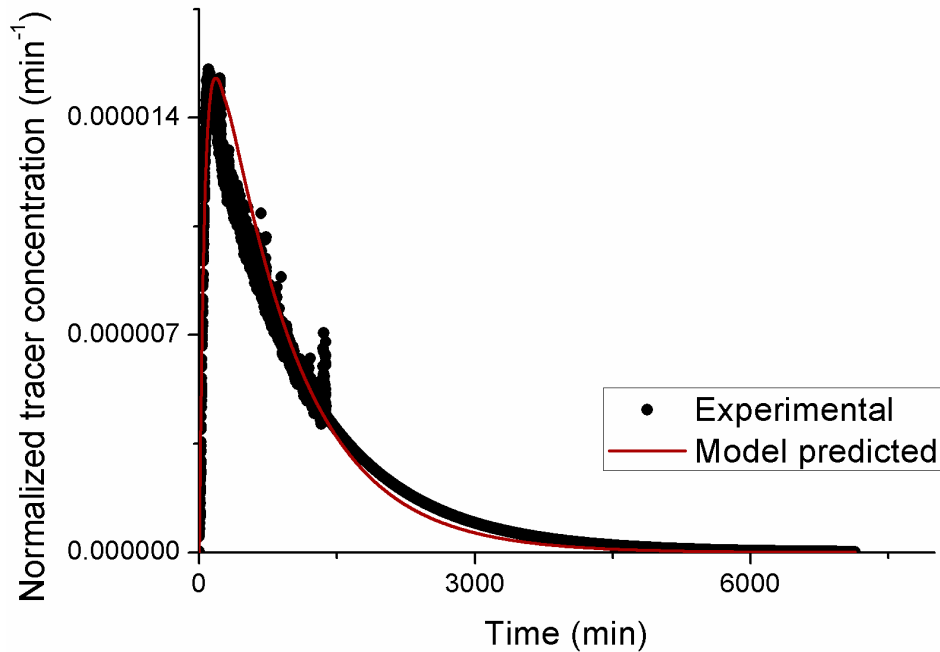


Fig. 5.16 Comparison of experimental and model predicted RTD curves for reactor R2 (Run 3)

Table 5.5 Model predicted parameters for reactor R2

Run	Active volume MRT (h)	Bypass		Stagnant volume	
		Fraction	MRT (h)	Fraction	MRT (h)
1	1.25	0.15	0.56	0.05	0.83
2	1.39	0.1	0.56	0.05	0.83
3	1.80	0.02	0.56	0.05	0.83

5.5 Reactor system 2

The reactor system 2 comprised of reactors R1 and R2 in series. Fresh feed and bottom product of the distillation columns as recycle were fed to reactor R1 and output of reactor R1 was fed to reactor R2.

5.5.1 Model conceptualization

The normalized output tracer count at the outlet of reactor R2 provided the RTD of the reactor system 2 in response to the impulse function provided at the feed of reactor R1. The reactor system 2 was modeled as a combination of the individual conceptual models of reactors R1 and R2 as shown in Fig. 5.17. The conceptual model of the reactor system 2 consisted of two CSTR in series, each having stagnant volume exchanging tracer with the

active volume, and bypass flow. The recycle flow line was modeled as plug flow, and two columns 1A and 1B in the recycle path were modeled as CSTR in series. The comparison between the experimentally measured and model predicted RTD curves for the reactor system 2 shows a good match (Figures 5.18-5.20). The results of the model simulation corresponding to the best fit are shown in Tables 5.6-5.9.

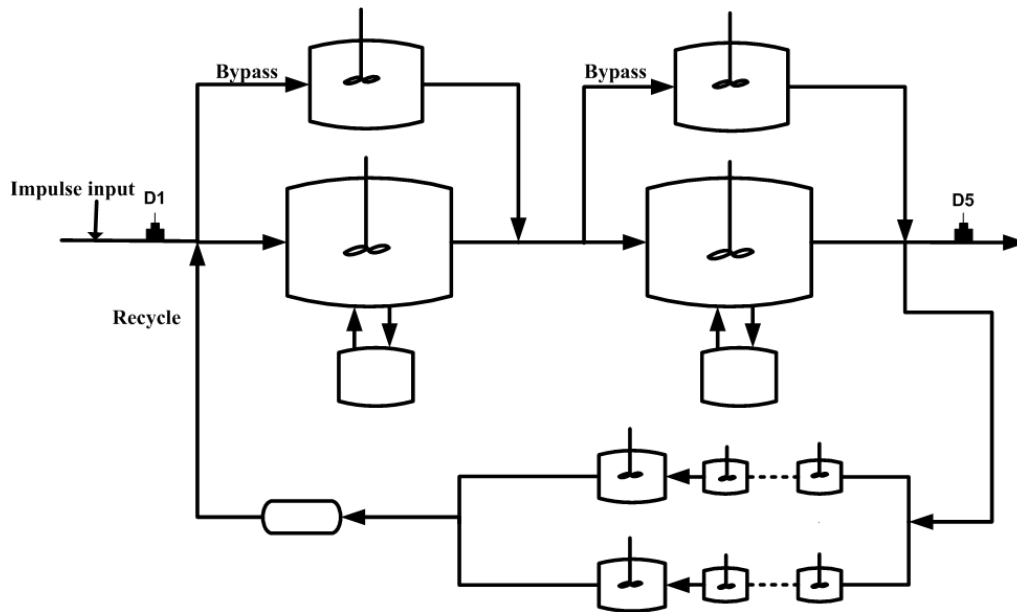


Fig. 5.17 Conceptual model of reactor system 2

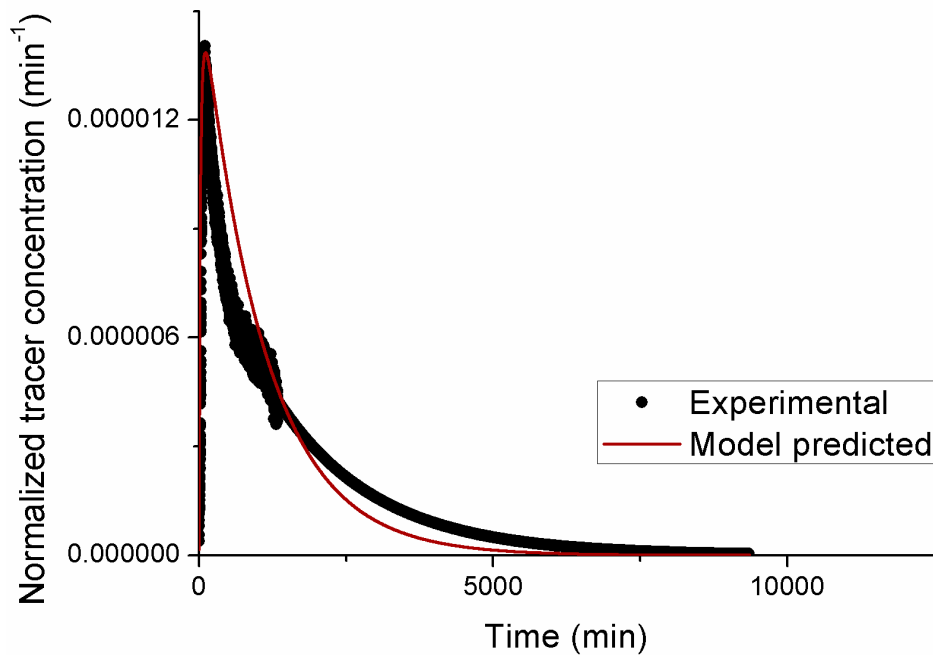


Fig. 5.18 Comparison of experimental and model predicted RTD curves for reactor system 2 (Run 1)

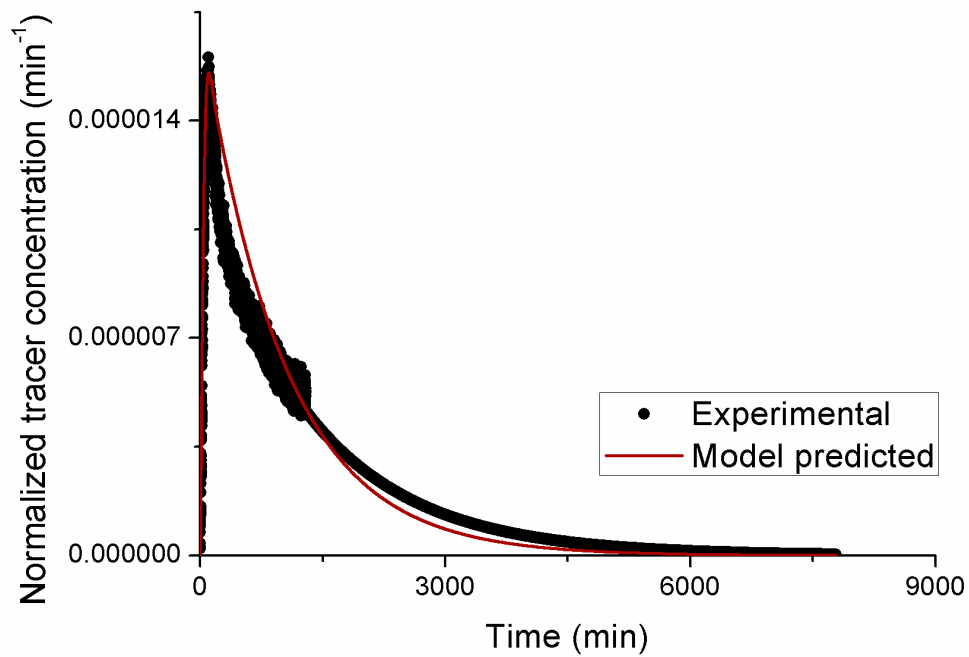


Fig. 5.19 Comparison of experimental and model predicted RTD curves for reactor system 2 (Run 2)

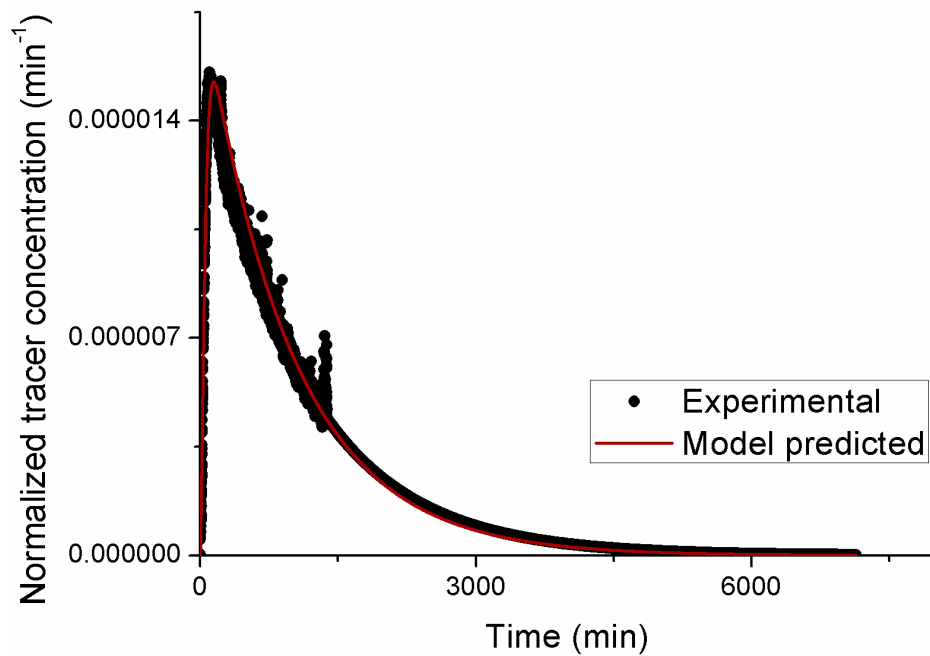


Fig. 5.20 Comparison of experimental and model predicted RTD curves for reactor system 2 (Run 3)

Table 5.6 Experimental and model predicted MRT for reactor system 2

Run	Overall MRT (h)	
	Expt.	Model
1	26.64	18.11
2	21.80	17.10
3	18.06	16.81

Table 5.7 Model predicted bypass parameters for reactor system 2

Run	Reactor R1		Reactor R2	
	Fraction	MRT (h)	Fraction	MRT (h)
1	0.18	0.67	0.15	0.56
2	0.29	0.56	0.1	0.56
3	0.32	0.44	0.02	0.56

Table 5.8 Model predicted stagnant volume parameters for reactor system 2

Run	Stagnant volume					
	Reactor R1			Reactor R2		
	No. of CSTR in series	Fraction	MRT (h)	No. of CSTR in series	Fraction	MRT (h)
1	1	0.05	0.28	1	0.05	0.83
2	1.5	0.10	0.83	1	0.05	0.83
3	2	0.15	1.11	1	0.05	0.83

Table 5.9 Model predicted recycle parameters for reactor system 2

Run	Recycle				
	Recycle Ratio	Distillation column			PFR MRT (h)
		Stage MRT (h)	No. of Stages	Reboiler MRT (h)	
1	3.57	0.006	48	0.25	0.03
2	3.57	0.006	48	0.25	0.03
3	3.57	0.006	48	0.25	0.03

5.6 Uncertainty analysis

Similar to the first set of industrial RTD experiments, three kinds of uncertainties were studied in the second set of industrial RTD experiments namely, uncertainty in estimated values of theoretical MRT, in measured values of the MRT and in model parameters obtained after model simulation.

The uncertainty in the measurement of flows at different parts of the plant had an uncertainty <5%. Also, the uncertainty in the measurement of experimental MRT due to the extrapolation of the experimental data to completion was less than 5%. The uncertainties in the model parameter were around 5-20% and 1-10% respectively for reactors R1 and R2 corresponding to an acceptable fit between experimental and model predicted curve.

CHAPTER-6

Chapter-6 RTD experiments on laboratory system

Two sets of industrial RTD experiments were performed on a reactor system with high recycle and recirculation as a mean of mixing. However, the effect of recycle on reactor behavior could not be studied in those experiments due to some plant limitations. The laboratory-scale RTD experiments were performed to study the effect of recirculation and recycle on the flow behavior in the reactor.

6.1 Process flow description

The laboratory-scale reactor system consisted of a main reactor and a reactor in the recycle line. The main reactor was a cylindrical vessel with a height of 0.54 m and a diameter of 0.51 m. The working volume of the reactor was 0.08 m³. The reactor, placed in the recycle line to the main reactor, had 0.55 m height and 0.35 m diameter with a working volume of 0.05 m³. A centrifugal feed pump (0.37 kW) provided feed at a constant rate of 30 l/h to the main reactor. A centrifugal recirculation pump (0.47 kW) was used to recirculate the contents of the main reactor (0-150 l/h) to cause turbulence inside the main reactor. The recirculation by the pump causes turbulence inside the reactor thus promoting fluid mixing. A part of the output stream from the main reactor was recycled back (0-120 l/h) to the main reactor through a well-mixed reactor with the help of a centrifugal recycle pump (0.47 kW). The laboratory-scale reactor system is shown in Fig. 6.1 and the line diagram is shown in Fig. 6.2. Tracer was instantaneously injected into the fresh feed of the main reactor (close to an ideal impulse function) and the normalized output concentration of the tracer provided the RTD of the reactor system. Detector (conductivity meter probe) D1 was mounted on the feed line to record the time of the entry of the tracer into the main reactor and detector D2 was mounted at the outlet to record the tracer concentration curves.



Fig. 6.1 Laboratory-scale reactor system

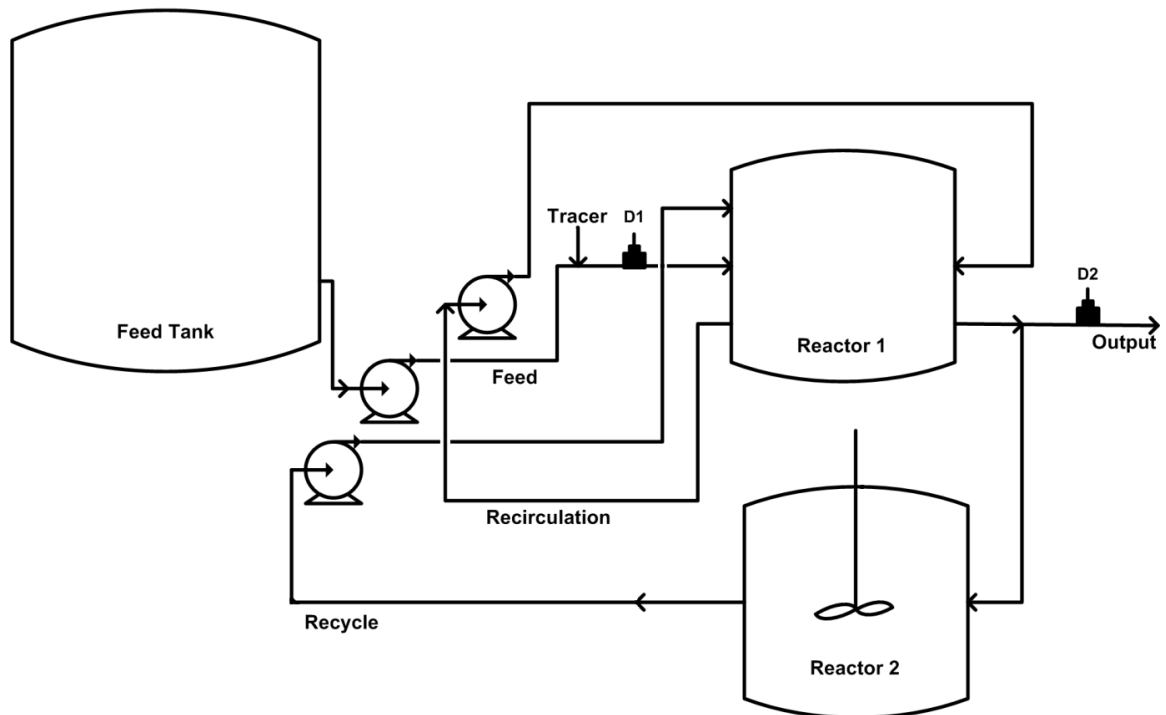


Fig. 6.2 Schematic of the laboratory-scale reactor system

Sixteen experiments with different recirculation and recycle rates were performed as shown in Table 3.3. These experiments mapped the sub-objective 1 of the thesis. After the experiments, RTD analysis was performed.

6.2 RTD analysis

In order to get the concentration data from the output conductivity of NaCl, a calibration curve (Fig. 6.3) was prepared and used. The calibration curve was prepared by plotting NaCl conductivity and its corresponding concentration in tap water at ambient temperature after making the correction for tap water conductivity.

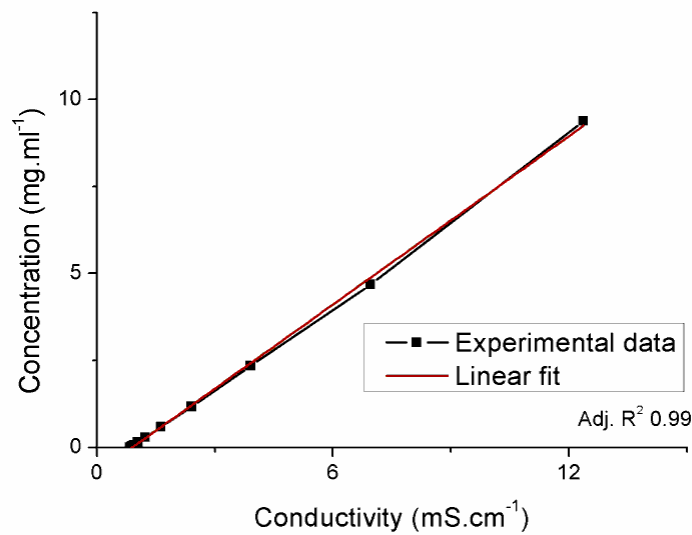


Fig. 6.3 Calibration curve for sodium chloride

The output tracer concentration data thus obtained was normalized using the Eq. 4.1. The experimental mean residence time was evaluated by Eq. 4.2. Theoretical residence time (τ) was calculated using the volume of the reactor system (V) and the steady feed flow rate (v_0) using the Eq. 6.1.

$$\tau = \frac{V}{v_0} \quad (6.1)$$

6.3 Model development

Experimental RTD curves (Figures 6.5-6.8) showed an abrupt and sharp peak close to the origin (detail in the inset) of the experimental curves was observed indicating bypassing from the reactor. Bypass flow fraction was determined by calculating the ratio between the area

under the initial sharp peak of the output tracer concentration curve and the area under the total curve.

Also, an extended tail seen in the experimental RTD curves of all the runs suggested the presence of a stagnant volume exchanging flow with the rest of the reactor. Stagnant volume fraction in the reactor system was calculated from experimental mean residence time (\bar{t}) and theoretical mean residence time (τ) following the Eq. 6. 2.

$$\text{Stagnant volume fraction} = 1 - \frac{\bar{t}}{\tau} \quad (6.2)$$

These observations along with information about the experimental parameters and combinations of ideal flow behavior (mixed flow and plug flow) in a particular arrangement lead to the development of the conceptual model shown in Fig. 6.4. The main reactor was, thus, modeled as a CSTR exchanging process fluid with the stagnant region. Bypass flow was modeled as a CSTR parallel to the main reactor. The reactor in the recycle line was modeled as a CSTR with a stagnant volume exchanging flow with the active volume. The recirculation flow was modeled as a CSTR exchanging flow with the main reactor of the reactor system.

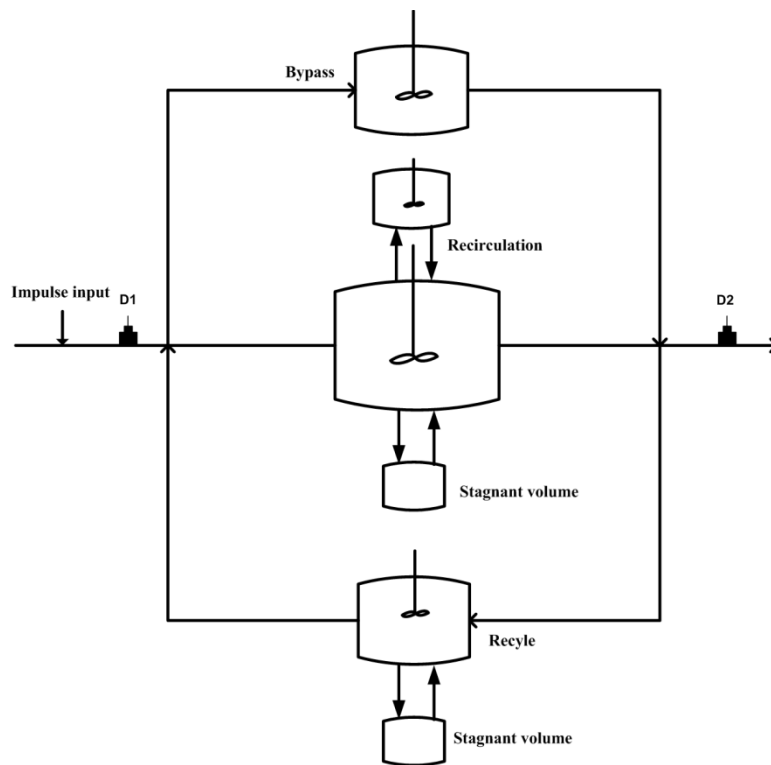


Fig. 6.4 Conceptual model of laboratory-scale reactor system

6.3.1 Model equations and solution

A computer program was developed to solve unsteady state tracer balance equations (first-order ODEs) for the model using fourth-order Runge-Kutta method with a time step of 10^{-4} seconds. The computer program was developed to help in the better conceptual understanding of the physical system and flexibility of data input which was limited in the DTSPro 4.1. The unsteady state tracer material balance equations for the RTD model are shown in Equations 6.3-6.24.

$$\alpha c_z + \pi c_d + \omega c_{rc} - (\alpha + \gamma + \omega)c_m = \tau \varepsilon \frac{dc_m}{dt} \quad (6.3)$$

$$\omega c_m - \omega c_{rc} = \tau \mu \frac{dc_{rc}}{dt} \quad (6.4)$$

$$\gamma c_m - \pi c_d = \tau \theta \frac{dc_d}{dt} \quad (6.5)$$

$$\beta c_y - \beta c_b = \tau \eta \frac{dc_b}{dt} \quad (6.6)$$

$$\delta c_1 + \rho c_{rd} - (\rho + \delta)c_r = \tau \lambda \frac{dc_r}{dt} \quad (6.7)$$

$$\rho c_r - \rho c_{rd} = \tau \phi \frac{dc_{rd}}{dt} \quad (6.8)$$

$$c_0 + \delta c_r = \beta c_y + \alpha c_z \quad (6.9)$$

where,

$$\alpha = \frac{v_a}{v_0} \quad (6.10)$$

$$\beta = \frac{v_b}{v_0} \quad (6.11)$$

$$\delta = \frac{v_r}{v_0} \quad (6.12)$$

$$\gamma = \frac{v_d}{v_0} \quad (6.13)$$

$$\pi = \frac{v_d'}{v_0} \quad (6.14)$$

$$\rho = \frac{v_{rd}}{v_0} \quad (6.15)$$

$$\omega = \frac{v_{rc}}{v_0} \quad (6.16)$$

$$\varepsilon = \frac{V_A}{V} \quad (6.17)$$

$$\eta = \frac{V_B}{V} \quad (6.18)$$

$$\theta = \frac{V_D}{V} \quad (6.19)$$

$$\lambda = \frac{V_R}{V} \quad (6.20)$$

$$\varphi = \frac{V_{RD}}{V} \quad (6.21)$$

$$\mu = \frac{V_{RC}}{V} \quad (6.22)$$

$$\tau = \frac{V}{v_0} \quad (6.23)$$

$$\varepsilon + \eta + \theta + \lambda + \varphi + \mu = 1 \quad (6.24)$$

where, v_0 is the fresh feed flow rate, v_a is the flow rate of the stream entering the active volume of main reactor, v_b is the flow rate of the stream entering the bypass CSTR, v_r is the recycle flow rate, v_d is the flow rate of the stream from active volume to the stagnant volume of the main reactor, v_d' is the flow rate of the stream from the stagnant volume to the active

volume of main reactor, v_{rd} is the flow exchange rate between stagnant volume and active volume of the reactor in recycle line and v_{rc} is the recirculation flow rate. V_A is the volume of the active region of the main reactor, V_B is the bypass CSTR volume, V_D is the stagnant volume of main reactor, V_R is the active volume of the reactor in recycle line, V_{RD} is the stagnant volume of the reactor in recycle line, V_{RC} is the volume of the recirculation CSTR and V is the total volume of the reactor system. c_0 is the fresh feed tracer impulse input concentration, c_y is the concentration of the input stream to bypass CSTR, c_b is the concentration of the output stream from bypass CSTR, c_z is the concentration of the input stream to the active volume of main reactor, c_m is the output concentration from the active volume of main reactor, c_d is the output concentration of flow from stagnant volume entering active volume of the main reactor, c_r is the concentration of the output stream of active volume of the reactor in recycle line, c_{rd} is the output concentration of the flow from stagnant volume to active volume of the reactor in recycle line, c_{rc} is the output concentration of flow from recirculation pump volume entering the active volume of the main reactor and c_l is the output concentration of the reactor system and also input to active volume of the reactor in recycle line. τ is the mean residence time of the reactor system.

The developed model has 14 process parameters and 6 initial values for concentrations. There are five input parameters in this model namely, ε (active volume of main reactor/total reactor volume), η (bypass volume of main reactor/total reactor volume), γ (flow rate from active volume to stagnant volume of main reactor/fresh feed flow rate), π (flow rate from stagnant volume to active volume of main reactor/fresh feed flow rate and lastly, ρ (flow exchange rate between active volume and stagnant volume in reactor in recycle line/ fresh feed flow rate). All the other parameters were calculated from the experimental information about the reactor system e.g. reactor volumes, flow rates, experimental bypass percentage and total stagnant volume of the reactor system. Different concentration values used to initialize the fourth-order Runge-Kutta method in solving tracer balance equations, were calculated from the process parameters and input tracer concentration. Analysis of experimental RTD data and subsequently developing a model along-with estimating model parameters corresponding to the best fit between experimental and model RTD curves mapped with the sub-objective 2 of the thesis. The model predicted tracer concentration data was fitted with the experimental data. Figures 6.5-6.8 show model predicted curves matched with the experimental data. The values of model parameters are reported in Tables 6.1-6.7.

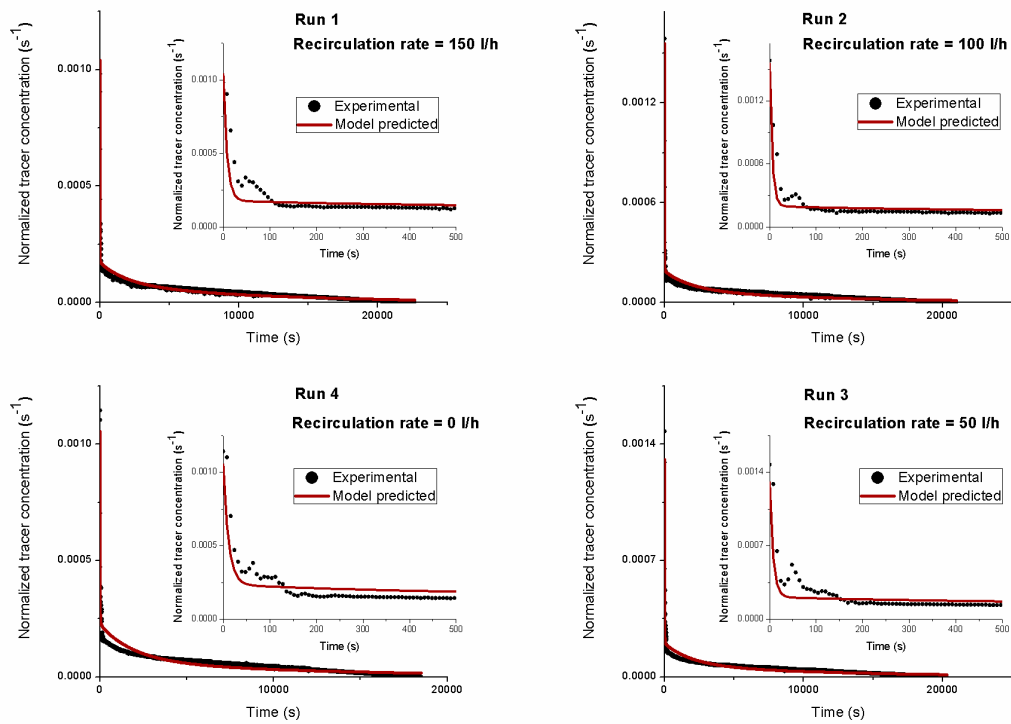


Fig. 6.5 Comparison between experimental and model predicted RTD curves for run 1-4 at recycle rate of 120 l/h

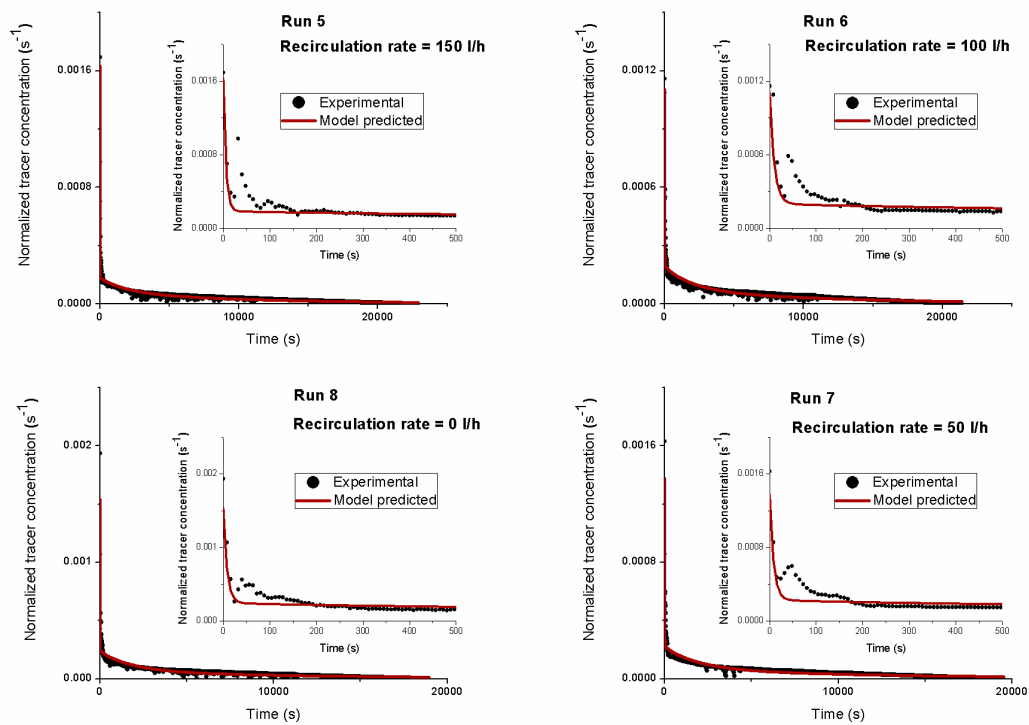


Fig. 6.6 Comparison between experimental and model predicted RTD curves for run 5-8 at recycle rate of 80 l/h

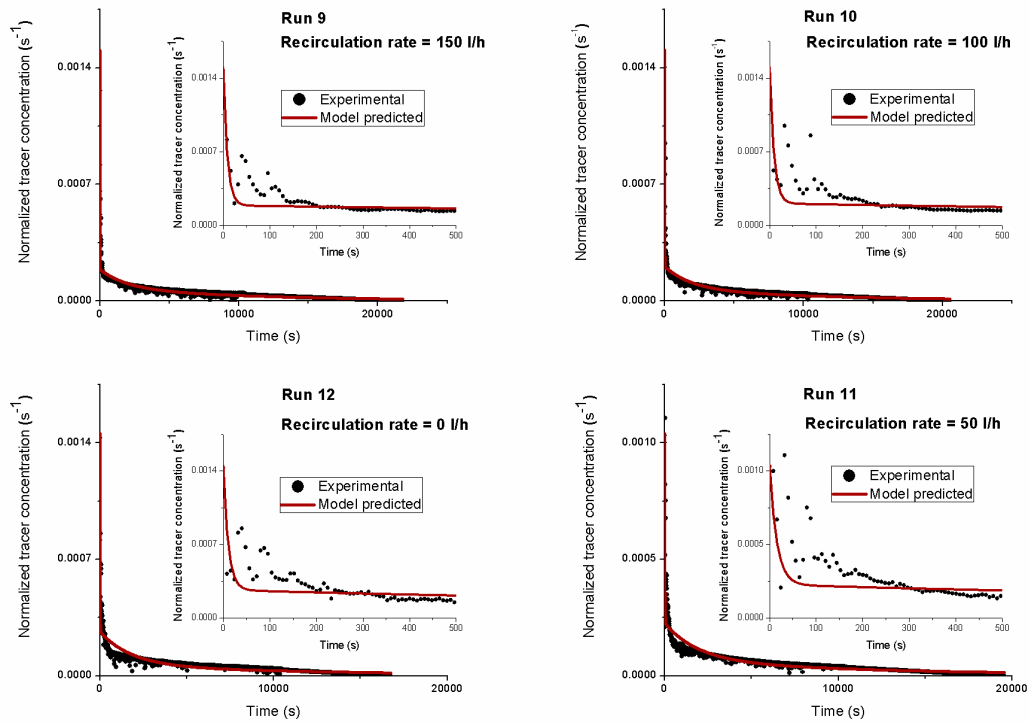


Fig. 6.7 Comparison between experimental and model predicted RTD curves for run 9-12 at recycle rate of 40 l/h

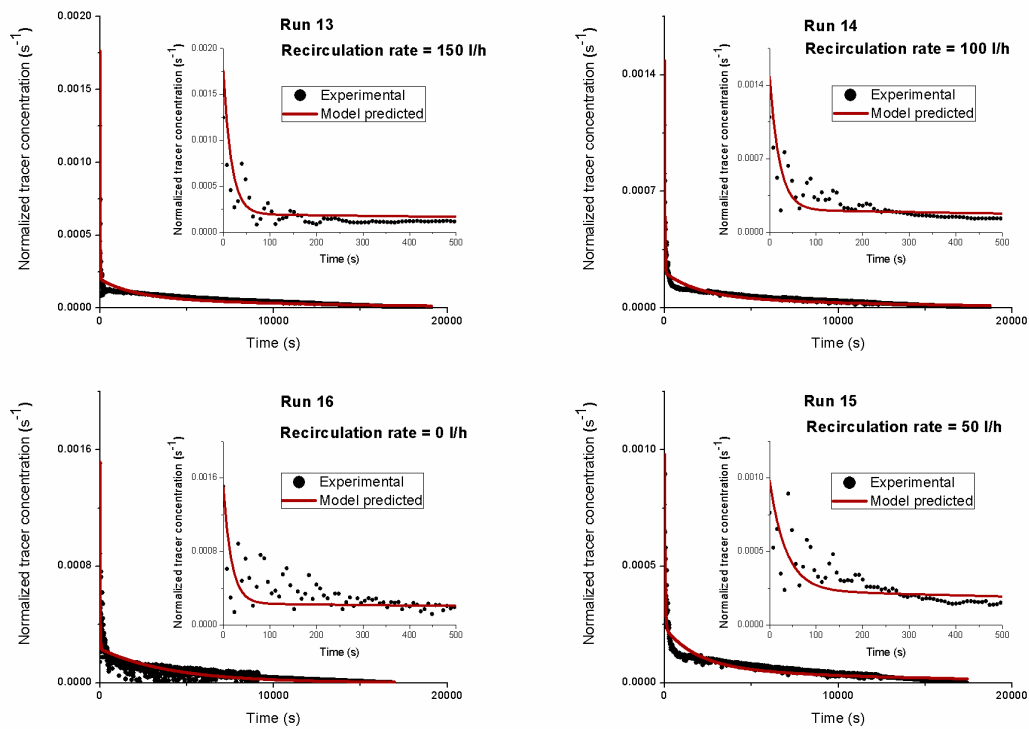


Fig. 6.8 Comparison between experimental and model predicted RTD curves for run 13-16 at recycle rate of 0 l/h

Table 6.1 Comparison of experimental, model predicted and theoretical MRT for reactor system

Run	Theoretical MRT (s)	Experimental MRT (s)	Model MRT (s)
1	15600	6638	6712
2	15600	6187	6218
3	15600	5871	5974
4	15600	5427	5428
5	15600	6366	6623
6	15600	6046	6244
7	15600	5478	5646
8	15600	5185	5407
9	15600	5993	6295
10	15600	5569	5898
11	15600	5199	5575
12	15600	4666	4764
13	9600	5628	5622
14	9600	5272	5433
15	9600	4919	5036
16	9600	4479	3849

Table 6.2 Model predicted bypass parameters for reactor system

Run	β	MRT (s)
1	3.04	8.02
2	3.21	5.43
3	3.43	7.36
4	3.78	11.27
5	2.58	5.48
6	2.78	9.68
7	2.94	8.31
8	3.11	7.88
9	2.31	8.58
10	2.39	9.15
11	2.45	15.29
12	2.40	10.75
13	2.31	17.4
14	2.24	21
15	2.15	35.30
16	2.04	17.54

where,

β is bypass flow percentage

Table 6.3 Model predicted parameters for stagnant volume in main reactor

Run	θ	κ	γ	π	MRT (s)
1	0.22	0.37	1	1	3585
2	0.25	0.42	1	1	4036
3	0.27	0.45	1	1	4352
4	0.30	0.49	1	1	4795
5	0.24	0.39	1	1	3786

6	0.26	0.42	1	1	4106
7	0.29	0.48	1	1	4674
8	0.31	0.51	1	1	4967
9	0.24	0.40	1	1	3843
10	0.27	0.44	1	1	4267
11	0.29	0.48	1	1	4637
12	0.33	0.53	1	1	5169
13	0.41	0.41	1	1	3972
14	0.45	0.45	1	1	4328
15	0.48	0.48	1	1	4680
16	0.53	0.53	0	0	N/A

where,

θ is stagnant volume in main reactor / total reactor volume

κ is stagnant volume in the main reactor/main reactor volume

γ is flow rate of stream from active volume to stagnant volume of main reactor/ fresh feed flow rate

π is flow rate of stream from stagnant volume to active volume of main reactor/ fresh feed flow rate

Table 6.4 Model predicted parameters for active volume in main reactor

Run	ϵ	α	MRT (s)
1	0.38	4.96	1210
2	0.35	4.96	1119
3	0.33	4.96	1057
4	0.30	4.96	968
5	0.37	3.64	1597
6	0.35	3.63	1509
7	0.31	3.63	1354
8	0.29	3.63	1274
9	0.36	2.31	2491
10	0.34	2.30	2309
11	0.31	2.30	2149
12	0.28	2.30	1918
13	0.58	0.97	5761
14	0.54	0.97	5393
15	0.51	0.97	5027
16	0.46	0.97	4573

where,

ϵ is active volume of main reactor/ total reactor volume

α is flow rate of stream entering active volume of main reactor/fresh feed flow rate

Table 6.5 Model predicted parameters for recirculation in main reactor

Run	ω	MRT (s)
1	5	1.20
2	3.33	1.80
3	1.66	3.60
4	0	0
5	5	1.20
6	3.33	1.80

7	1.66	3.60
8	0	0
9	5	1.20
10	3.33	1.80
11	1.66	3.60
12	0	0
13	5	1.20
14	3.33	1.80
15	1.66	3.60
16	0	0

where,

ω is flow exchange rate between recirculation CSTR and active volume of main reactor/ fresh feed flow rate

Table 6.6 Model predicted parameters for stagnant volume of reactor in recycle line

Run	ρ	MRT (s)
1	1	5377.1
2	1	5377.1
3	1	5377.1
4	1	5377.1
5	1	5447.8
6	1	5447.8
7	1	5447.8
8	1	5447.8
9	1	5764.4
10	1	5764.4
11	1	5764.4
12	1	5764.4
13	N/A	N/A
14	N/A	N/A
15	N/A	N/A
16	N/A	N/A

where,

ρ is flow exchange rate between stagnant volume and active volume of reactor in recycle line/ fresh feed flow rate

Table 6.7 Model predicted parameters for active volume of reactor in recycle line

Run	δ	MRT (s)
1	4	156
2	4	156
3	4	156
4	4	156
5	2.66	207
6	2.66	207
7	2.66	207
8	2.66	207
9	1.33	177
10	1.33	177
11	1.33	177

12	1.33	177
13	N/A	N/A
14	N/A	N/A
15	N/A	N/A
16	N/A	N/A

where,

δ is recycle flow rate/ fresh feed flow rate

6.4. Effect of recirculation and recycle on MRT

Fig. 6.9 shows the variation in the experimental MRT for different recirculation rates at a fixed recycle rate. It could be observed that an increase in the recirculation rate increased the MRT of the reactor system. This could be due to improved mixing inside the reactor at a higher recirculation rate. It lead to an increase in the volume of the reactor where the tracer particle couldn't reach at lower recirculation rates. As the active volume of the reactor increased with the increase in recirculation, the mean residence time of the reactor also increased. Also, it was observed from Fig. 6.9 that for a particular recirculation rate the MRT also increased with an increase in the recycle rate. It could be due to the reason that the recycle stream also assisted the recirculation system in increasing the active volume of the reactor and thereby increasing the MRT of the reactor system.

The maximum MRT observed was 6638 seconds for run 1 when the recirculation rate was 150 l/h and the recycle rate was 120 l/h. The lowest MRT observed was 4479 seconds for run 16 when the recirculation and recycle flows were both absent.

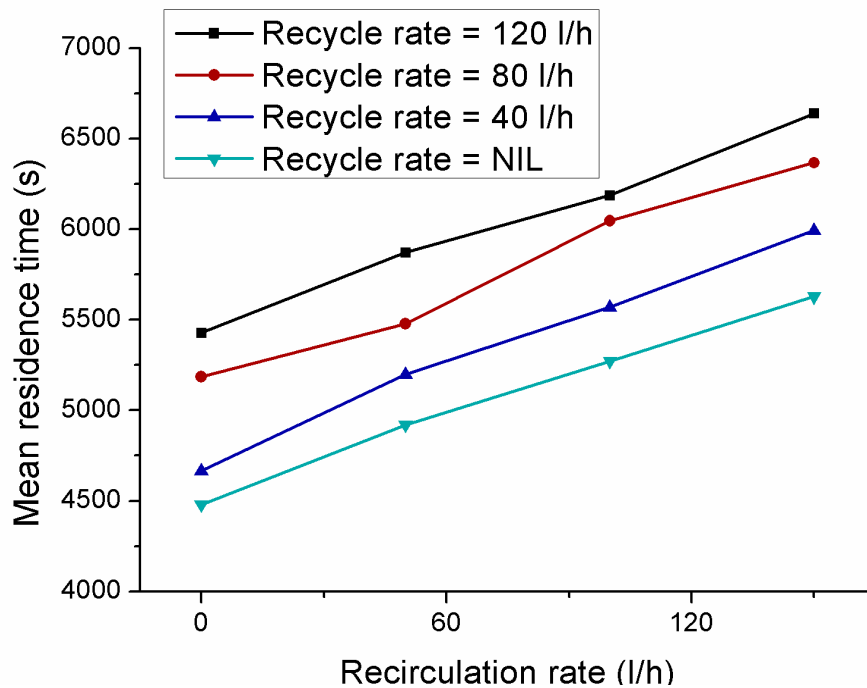


Fig. 6.9 Effect of recirculation rate on MRT of reactor system at different recycle rates

6.5. Effect of recirculation and recycle on bypassing

A small bypass was observed for all the runs. The highest bypass of 3.8% was observed for the recycle rate of 120 l/h and in the absence of recirculation. The lowest bypass percentage of approximately 2% was observed in the absence of the recycle and recirculation flows. Fig. 6.10 showed that at all recycle flows, bypass flow decreased with the increase in the recirculation rate. However, in the absence of recycle flow, an increase in the recirculation flow promoted bypassing.

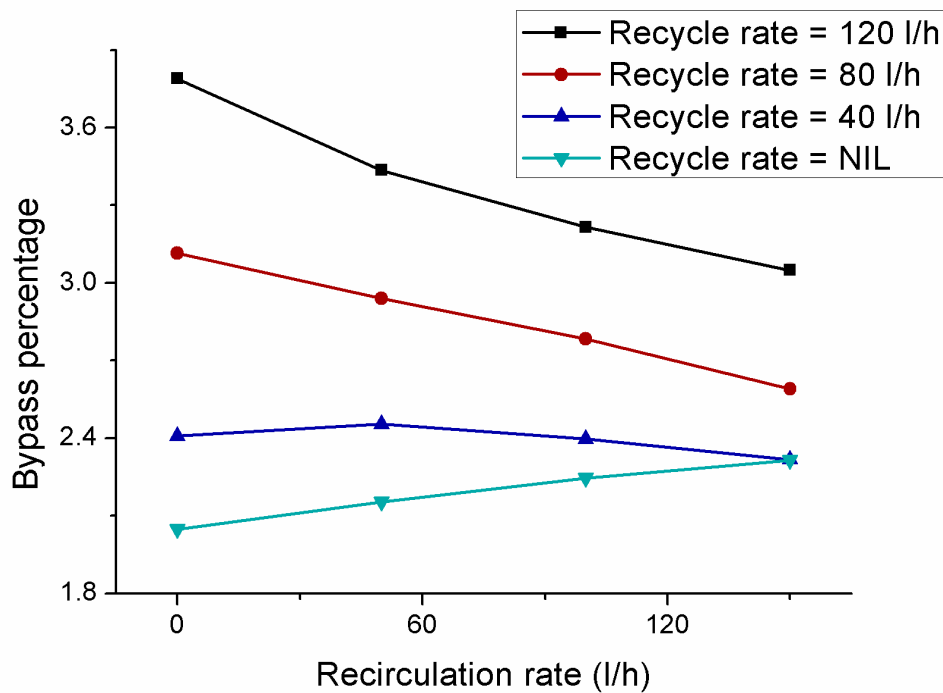


Fig. 6.10 Effect of recirculation rate on bypass percentage of reactor system at different recycle rates

6.6. Effect of recirculation and recycle on stagnant volume

The total stagnant volume fraction of the reactor system was calculated using Eq. 6.4. Assuming $55 \pm 5\%$ of the total stagnant volume was in the recycle line reactor and gave the best fit for the experimental RTD curves. Recycle flow helped in inducing turbulence and minimizing the stagnant volume inside the main reactor. It could be observed from Fig. 6.11 that for a fixed recirculation rate, stagnant volume fraction in the main reactor decreased with the increase in recycle rate. The highest stagnant volume of 53% was predicted in the main reactor, when the recycle and recirculation flow were absent. On the other hand, the lowest stagnant volume of 37% was predicted in the main reactor when the recycle and the recirculation flow rate were highest at 120 l/h and 150 l/h respectively.

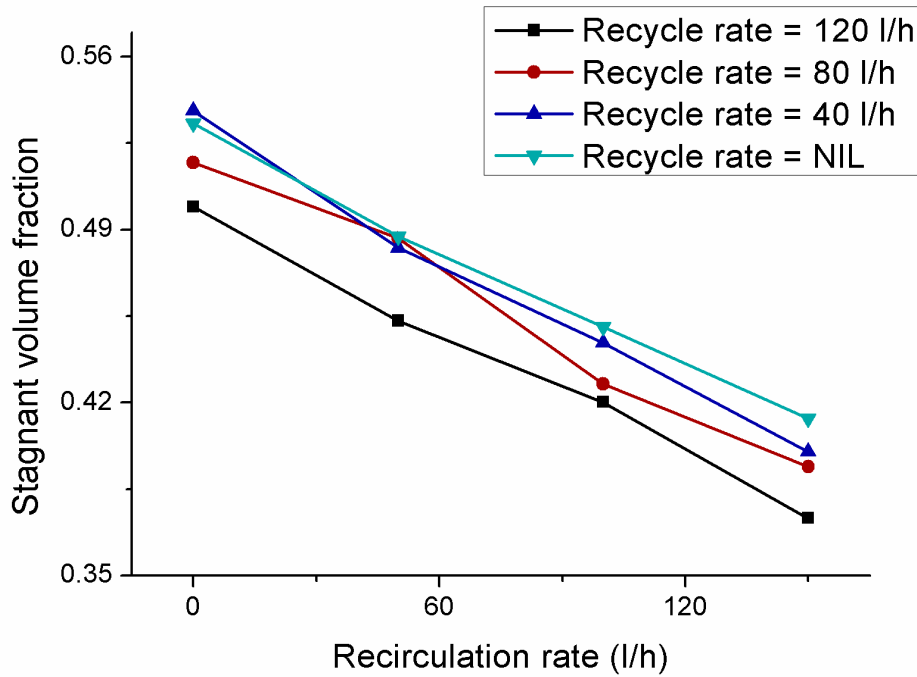


Fig. 6.11 Effect of recirculation rate on stagnant volume fraction of main reactor at different recycle rates

6.7. Statistical analysis

In the laboratory-scale RTD study, there were two controllable factors namely, recirculation rate and recycle rate. The individual and interaction effect of these two factors in the three response variables namely bypass flow, stagnant volume and mean residence time were studied. With four levels of each factor, this study was an example of a two-factor four-level experiment without replication [93]. Tukey [97] developed a test to find out whether an interaction is present between factors, in cases of experiments without replication like the present study. ANOVA including Tukey's test was performed in order to see the effect of the two factors on the three responses. The results from the ANOVA are shown in Tables 6.8-6.10. From the analysis, it could be seen that the recirculation and recycle rate had a significant individual effect on all three responses. But, a significant interaction effect between recirculation and recycle was seen for only the bypass flow of the reactor system.

Table 6.8 Statistical analysis of MRT (s) for reactor system

Recycle					
	<i>120 l/h</i>	<i>80 l/h</i>	<i>40 l/h</i>	<i>0 l/h (NIL)</i>	
Recirculation					
<i>150 l/h</i>	6638	6366	5993	5628	
<i>100 l/h</i>	6187	6046	5569	5271	
<i>50 l/h</i>	5871	5478	5199	4919	
<i>0 l/h (NIL)</i>	5427	5185	4666	4479	
Descriptives					
Recirculation	Count	Sum	Average	Variance	
<i>150 l/h</i>	4	24625	6156	194096	
<i>100 l/h</i>	4	23074	5768	179583	
<i>50 l/h</i>	4	21467	5367	164786	
<i>0 l/h (NIL)</i>	4	19758	4939	194923	
Recycle	Count	Sum	Average	Variance	
<i>120 l/h</i>	4	24123	6031	260976	
<i>80 l/h</i>	4	23076	5768	286359	
<i>40 l/h</i>	4	21425	5356	317227	
<i>0 l/h (NIL)</i>	4	20299	5075	240935	
ANOVA					
Source of Variation	SS	df	MS	F	F-Crit
<i>Recirculation rate</i>	3284731	3	1094910.3	276.2	3.86
<i>Recycle rate</i>	2168403	3	722801.1	182.3	3.86
<i>Interaction between recirculation rate and recycle rate</i>	49.19	1	49.19	0.012	5.31
<i>Error</i>	31709	8	3964		
Remarks					
<i>Recirculation rate</i>			F>F-Crit		Significant
<i>Recycle rate</i>			F>F-Crit		Significant
<i>Interaction between recirculation and recycle rate</i>			F<F-Crit		Not-Significant

Table 6.9 Statistical analysis of the bypass percentage for reactor system

Recycle				
	<i>120 l/h</i>	<i>80 l/h</i>	<i>40 l/h</i>	<i>NIL</i>
Recirculation				
<i>150 l/h</i>	3.04	2.58	2.31	2.31
<i>100 l/h</i>	3.21	2.78	2.39	2.24
<i>50 l/h</i>	3.43	2.94	2.45	2.15
<i>0 l/h (NIL)</i>	3.78	3.11	2.40	2.04
Descriptives				
Recirculation	Count	Sum	Average	Variance
<i>150 l/h</i>	4	10.27	2.56	0.11
<i>100 l/h</i>	4	10.64	2.66	0.18
<i>50 l/h</i>	4	10.98	2.74	0.31
<i>0 l/h (NIL)</i>	4	11.36	2.84	0.59
Recycle	Count	Sum	Average	Variance
<i>120 l/h</i>	4	13.48	3.37	0.10

80 l/h	4	11.42	2.85	0.05	
40 l/h	4	9.57	2.39	0.003	
0 l/h (NIL)	4	8.76	2.19	0.01	
ANOVA					
Source of Variation	SS	df	MS	F	F-Crit
Recirculation rate	0.16	3	0.054	11.59	3.86
Recycle rate	3.31	3	1.10	235.86	3.86
Interaction between recirculation rate and recycle rate	0.30	1	0.30	65.53	5.31
Error	0.037	8	0.004		
Remarks					
Recirculation rate			F>F-Crit	Significant	
Recycle rate			F>F-Crit	Significant	
Interaction between recirculation and recycle rate			F>F-Crit	Significant	

Table 6.10 Statistical analysis of the fraction of stagnant volume of main reactor to the total volume of main reactor

Recycle	120 l/h	80 l/h	40 l/h	0 l/h (NIL)	
	Recirculation				
150 l/h	0.37	0.39	0.40	0.41	
100 l/h	0.42	0.42	0.44	0.45	
50 l/h	0.45	0.48	0.48	0.48	
0 l/h (NIL)	0.49	0.51	0.53	0.53	
Descriptives					
Recirculation	Count	Sum	Average	Variance	
150 l/h	4	1.58	0.39	28.19E-05	
100 l/h	4	1.74	0.43	20.12E-05	
50 l/h	4	1.91	0.47	26.74E-05	
0 l/h (NIL)	4	2.08	0.52	30.94E-05	
Recycle	Count	Sum	Average	Variance	
120 l/h	4	1.74	0.66	28.31E-04	
80 l/h	4	1.82	0.45	31.07E-04	
40 l/h	4	1.86	0.46	34.42E-04	
0 l/h (NIL)	4	1.88	0.47	26.14E-04	
ANOVA					
Source of Variation	SS	df	MS	F	F-Crit
Recirculation rate	0.035	3	0.011	276.9	3.86
Recycle rate	0.002	3	9.45E-04	22.03	3.86
Interaction between recirculation rate and recycle rate	1.45E-06	1	1.45E-06	0.033	5.31
Error	3.43E-04	8	4.28E-05		
Remarks					
Recirculation rate			F>F-Crit	Significant	
Recycle rate			F>F-Crit	Significant	
Interaction between recirculation and recycle rate			F<F-Crit	Not-Significant	

6.8. Uncertainty analysis

In the present work, three types of uncertainties were studied namely, uncertainty in the measurement of flow rate (experimental uncertainty), uncertainty in the experimental MRTs (extrapolation uncertainty) and uncertainty in the model variables (parametric variability) [98].

The uncertainty in the measurement of feed, recycle and recirculation flows were based on the uncertainty associated with the measuring equipment was <5%. Uncertainty in calculating the experimental MRT was measured to be < 5% (coefficient of determination $\geq 95\%$).

Uncertainty in the model output because of variation in the values of input parameters was found out by the one-factor-at-a-time (OFAT) principle [99]. It involved varying one input keeping other input parameters constant and observing the effect on the output parameter(s). It was one of the easiest ways to observe the effect of variation in the input parameter(s) on the output parameter(s). This process was repeated for all the input parameters after the last input parameter varied was returned to its initial baseline value. In this study, there were five input parameters namely ε (active volume of main reactor/total reactor volume), η (bypass volume of main reactor/total reactor volume), γ (flow rate from active volume to stagnant volume of main reactor/fresh feed flow rate), π (flow rate from stagnant volume to active volume of main reactor/fresh feed flow rate) and lastly, ρ (flow exchange rate between stagnant volume and active volume in reactor in recycle line/ fresh feed flow rate). Their values were varied 50% of their initial values and the corresponding change in the MRT (output parameter) of the reactor system was observed. The study showed that a 50% change in the value of ρ and ε lead to a change of 18.7% and 10.5% change in the mean residence time of the reactor system respectively. These were the most sensitive input parameters in the model developed. The least sensitive parameters in the model were γ , π , and η where a 50% change in their values lead to a change of 5.7%, 2.3% and 0.2% in the mean residence time of the reactor system respectively.

CHAPTER-7

Chapter-7 Conclusions and recommendations

7.1 Conclusions

RTD studies conducted on industrial reactor systems using radiotracers and the studies conducted on laboratory reactor setup provided interesting information about the flow behavior of these systems. Some information about the mixing in the reactors was obtained from the experimental RTD curves, whereas, some other information was obtained by the simulation of the conceptual models used to map the RTD curves of these systems.

Experimental RTD curves obtained from industrial reactor system 1 showed an increase in the bypass from 12% to 22% with a decrease in recirculation flow from 100% to 0% for reactor R1. MRT of the reactor system 1 decreased from 17h to 10h when the recirculation to both the reactors (R1 & R2) decreased from 100% to 0%. Model parameters obtained by fitting the experimental RTD curves showed 40% stagnant volume (exchanging fluid with the active volume) for reactor R1 and 1% stagnant volume (exchanging fluid with the active volume) for reactor R2 at all recirculation rates.

Experimental RTD curves of reactor system 2 showed an increase in bypass flow from 18% to 32% with a decrease in recirculation flow from 100% to 0% for reactor R1. Experimental MRT for the reactor system 2 decreased from 26h to 18h when the recirculation to both the reactors decreased from 100% to 0%. Model parameters obtained by fitting the experimental RTD curves showed an increase in the stagnant volume (exchanging fluid with the active volume) from 5 to 15% as the recirculation flow decreased from 100% to 0% for reactor R1. However, for reactor R2 a constant stagnant volume (exchanging fluid with the active volume) of 5% was obtained at all recirculation rates.

After the first industrial RTD experiments, it was concluded based on the high stagnant volume present in reactor R1 that it needed some design modifications. Reactor R2, however, behaved very close to an ideal mixed reactor. Due to the absence of bypass and a very low stagnant volume at all recirculation rates, it was concluded that reactor R2 could operate at a minimum recirculation rate, thus saving energy. In the second set of industrial RTD experiments, replaced reactor R1 showed design improvement in terms of low stagnant volume than the old reactor at all recirculation rates. This was also explained by an increase

in the MRT of reactor R1 from 15 h to 22 h (100 % recirculation rate). However, reactor R2 did not show any improvements in flow behavior over the old reactor.

In laboratory experiments, both recirculation and recycle were varied. Experimental RTD curves of laboratory-scale reactor setup showed a flow bypass of 3.8% when the recycle flow was 120 l/h (highest in the study range) and recirculation flow was 0 l/h. The lowest bypass of 2% was observed in the absence of both recirculation and recycle flow. It was also observed at a higher recycle flow, bypass decreased with an increase in the recirculation flow. However, at lower recycle flow, increase in recirculation flow promoted bypassing. The highest MRT of 1.8h for the highest recycle rate (120 l/h) and highest recirculation flow (150 l/h) in the study range was obtained from experimental RTD curves. The lowest MRT of 1.2h was obtained in the absence of recycle and recirculation flow. Both the recirculation and recycle flows increased the MRT of the reactor system by increasing the active volume of the reactor. A computer program developed to solve the tracer equations of the conceptual model predicted a stagnant volume (exchanging fluid with the active volume) of 37% at the 120 l/h recycle flow and 150 l/h recirculation flow. Stagnant volume (exchanging fluid with the active volume) of 53% was obtained in the absence of recycle and recirculation flow. For a fixed recirculation rate, stagnant volume in the reactor decreased with an increase in the recycle rate. Also, the stagnant volume in the reactor decreased with an increase in the recirculation rate at a fixed recycle flow.

Similar trends in the variation of experimental MRT and bypass flow were observed as the recirculation was changed in the industrial-scale as well as the laboratory-scale RTD experiments. In both kinds of studies, an increase in the recirculation flow caused an increase in the MRT. In the laboratory-scale experiments, at high recycle flow rates, bypass flow was also observed to decrease with an increase in recirculation rate as was observed during industrial RTD experiments. Also, the stagnant volume (with fluid exchange) decreased with an increase in recirculation. Similar trend was observed in the laboratory-scale RTD experiments.

7.2 Recommendations for future work

- Radiotracers provide an excellent opportunity in studying the flow behavior in operational industrial systems without disturbing the process. RTD studies using

radiotracers can be performed on similar industrial reactor systems to get valuable information about their flow behavior and also to conduct real-time equipment diagnosis.

- CFD analyses are a very important source of information to design new and improved reactor systems. The RTD of recycle reactors with recirculation can be obtained from CFD analysis and the results can be compared with the experimental data. It will provide a deeper insight into the process and the hydrodynamics of recycle reactors.

References

1. Aftalion, F., 1986. *A History of the International Chemical Industry*. 2nd ed. Philadelphia: Chemical Heritage Press.
2. Nagiev, M.F., 2014. *The Theory of Recycle Processes in Chemical Engineering: International Series of Monographs on Chemical Engineering*, vol 3. London: Pergamon Press Limited.
3. Pant, H., Yelgoankar, V., 2002. Radiotracer investigations in aniline production reactors. *Applied Radiation and Isotopes*, 57 (3), 319-325.
4. Othman, N., Kamarudin, S.K., 2014. Radiotracer technology in mixing processes for industrial applications. *The Scientific World Journal*, Article I.D 768604, 15 pages.
5. Levenspiel, O., 1998. *Chemical Reaction Engineering*. 3rd ed. New Jersey: John Wiley & Sons Inc.
6. Dutia, P., 2004. Ethyl acetate: A techno-commercial profile. *Chemical Weekly-Bombay*, 49,179-186.
7. Singh, D., Gupta, R.K., Kumar, V., 2015. Simulation of a plant scale reactive distillation column for esterification of acetic acid. *Computers & Chemical Engineering*, 73, 70-81.
8. Revill, B.K., 1992. Chapter 9 - Jet mixing. In: Harnby, N., Edwards, M.F., Nienow, A.W., 2nd ed. *Mixing in the Process Industries*. Oxford: Butterworth-Heinemann, 159-183.
9. Kennedy, S., Bhattacharjee, P.K., Bhattacharya, S.N., Eshtiaghi, N., Parthasarathy, R., 2018. Control of the mixing time in vessels agitated by submerged recirculating jets. *Royal Society Open Science*, 5 (1), Article I.D 171037.
10. Patwardhan, A., Gaikwad, S., 2003. Mixing in tanks agitated by jets. *Chemical Engineering Research and Design*, 81 (2), 211-220.
11. Fogler, H.S., 2004. *Elements of Chemical Reaction Engineering*. 3rd ed. New Jersey: Prentice Hall Inc.
12. Antoine, B., Leclerc, J., Claudel, S., Lintz, H., Potier, O., 2000. Theoretical interpretation of residence-time distribution measurements in industrial processes. *Oil & Gas Science and Technology*, 55 (2), 159-169.
13. Sheoran, M., Chandra, A., Bhunia, H., Bajpai, P.K., Pant, H.J., 2018. Residence time distribution studies using radiotracers in chemical industry—a Review. *Chemical Engineering Communications*, 205 (6), 739-758.
14. Hills, A.E., 2001. *Practical Guidebook for Radioisotope-Based Technology in Industry*. IAEA/RCA RAS/8/078.
15. IAEA, 2001. *Radiotracer Technology as Applied To Industry*. IAEA: Vienna, IAEA-TECDOC-1262.

16. IAEA, 2008. *Residence Time Distribution Method for Industrial and Environmental Applications*. IAEA: Vienna, Training course series 31.
17. IAEA, 1982. *Tracer Methods in Isotope Hydrology*. IAEA: Vienna.
18. IAEA, 1999. *Safety Assessment Plans for authorization and Inspection of Radiation Sources*. IAEA: Vienna, IAEA-TECDOC-1113.
19. IAEA, 1996. *Radiation Protection and the Safety of Radiation Sources: A Safety Fundamental*. IAEA: Vienna, Series-120 IS.
20. Hua, L., Zhao, H., Li, J., Zhu, Q., Wang, J., 2019. Solid residence time distribution in a cross-flow dense fluidized bed with baffles. *Chemical Engineering Science*, 200, 320-335.
21. Anitha, D., Narsaiah, T., Bala, Rao, V.B., 2017. RTD studies in liquid–solid tapered fluidized bed. *International Journal of Engineering Technology Science and Research*, 4 (9), 221-229.
22. Bachmann, P., Tsotsas, E., 2015. Analysis of residence time distribution data in horizontal fluidized beds. *Procedia Engineering*, 102, 790-798.
23. Goswami, S., Biswal, J., Samantray, J., Gupta, D., Pant, H.J. 2014 Measurement of mixing time and holdup of solids in gas–solid fluidized bed using radiotracer technique. *Journal of Radioanalytical and Nuclear Chemistry*, 302 (2), 845-850.
24. Rao, J., Ramani, N., Pant, H.J., Reddy, D., 2012. Measurement of residence time distributions of coal particles in a pressurized fluidized bed gasifier (PFBG) using radio tracer technique. *Indian Journal of Science And Technology*, 5 (12), 3746-3752.
25. Pant, H.J, Sharma, V.K, Nair, A., Tomar, B., Nathaniel, T., Reddy, A., Singh, G., 2009. Application of ¹⁴⁰La and ²⁴Na as intrinsic radiotracers for investigating catalyst dynamics in FCCUs. *Applied Radiation and Isotopes*, 67 (9), 1591-1599.
26. Pant, H.J., Sharma, V.K., Kamudu, M.V., Prakash, S., Moorthy, S.K., Anandam, G., Ramani, N., Singh, G., 2009. Measurement of circulation rates of coal particles in standpipe of a circulating fluidized bed system (CFBS) using radiotracer technique. *Journal of Radioanalytical and Nuclear Chemistry*, 280 (1), 47-56.
27. Pant, H.J., Sharma, V.K., Kamudu, M.V, Prakash, S., Krishnamoorthy, S., Anandam, G., Rao, P.S., Ramani, N., Singh, G., Sonde, R., 2009. Investigation of flow behaviour of coal particles in a pilot-scale fluidized bed gasifier (FBG) using radiotracer technique. *Applied Radiation and Isotopes*, 67 (9), 1609-1615.
28. Santos, V., Dantas, C., 2004. Transit time and RTD measurements by radioactive tracer to assess the riser flow pattern. *Powder Technology*, 140 (1), 116-121.
29. Gauthier, D., Flamant, G., 1991. Residence time distribution in a series of three tanks with bypass and back-mixing. Application to multistage fluidized-bed. *Chemical Engineering Communications*, 100 (1), 77-94.

30. Wolf, D., Resnick, W., 1965. Experimental study of residence time distribution in multistage fluidized bed. *Industrial & Engineering Chemistry Fundamentals*, 4 (1), 77-81.
31. Veluswamy, G.K., Upadhyay, R.K., Utikar, R.P., Tade, M.O., Evans, G., Glenny, M.E., Roy, S., Pareek, V.K., 2013. Hydrodynamic study of fluid catalytic cracker unit stripper. *Industrial & Engineering Chemistry Research*, 52 (12), 4660-4671.
32. Veluswamy, G.K., Upadhyay, R.K., Utikar, R.P., Evans, G.M., Tade, M.O., Glenny, M.E., Roy, S., Pareek, V.K., 2011. Hydrodynamics of a fluid catalytic cracking stripper using γ -ray densitometry. *Industrial & Engineering Chemistry Research*, 50 (10), 5933-5941.
33. Abdulmohsin, R.S., Al-Dahhan, M.H., 2016. Axial dispersion and mixing phenomena of the gas phase in a packed pebble-bed reactor. *Annals of Nuclear Energy*, 88, 100-111.
34. Gupta, R., Bansal, A., 2012. Axial dispersion in packed bed reactors involving viscoelastic and viscoelastic non-Newtonian fluids. *Bioprocess and Biosystems Engineering*, 36 (8), 1011-1018.
35. Gupta, R., Bansal, A., 2010. Effect of bed configuration on dispersion in a packed-bed reactor. *Industrial & Engineering Chemistry Research*, 49 (19), 9525-9528.
36. Furman, L., Leclerc, J.P., Stegowski, Z., 2005. Tracer investigation of a packed column under variable flow. *Chemical Engineering Science*, 60 (11), 3043-3048.
37. van Gelder, K.B., Westerterp, K.R. 1990. Residence time distribution and hold-up in a cocurrent upflow packed bed reactor at elevated pressure. *Chemical Engineering & Technology*, 13 (1), 27-40.
38. Van Swaaij, W., Charpentier, J., Villermaux, J., 1969. Residence time distribution in the liquid phase of trickle flow in packed columns. *Chemical Engineering Science*, 24 (7), 1083-1095.
39. Blet, V., Berne, P., Chaussy, C., Perrin, S., Schweich, D., 1999. Characterization of a packed column using radioactive tracers. *Chemical Engineering Science*, 54 (1), 91-101.
40. Upadhyay, R.K., Kaim, J., Roy, S., 2009. Investigation of downflow bubble columns: experiments and modeling. *Journal of Chemical Engineering of Japan*, 42(1), s156-s161.
41. Pant, H.J, Sharma, V.K., 2016. Investigation of flow dynamics of liquid phase in a pilot-scale trickle bed reactor using radiotracer technique. *Applied Radiation and Isotopes*, 116, 163-173.
42. Bittante, A., García-Serna, J., Biasi, P., Sobrón, F., Salmi, T., 2014. Residence time and axial dispersion of liquids in trickle bed reactors at laboratory-scale. *Chemical Engineering Journal*, 250:99-111.
43. Srivastava, V.C., 2012. An evaluation of desulfurization technologies for sulfur removal from liquid fuels. *RSC Advances*, 2 (3), 759-783.

44. Prokešová, A., Tukač, V., Zbuzek, M., 2012. Hydrodynamics characteristics of HDS trickle bed test reactor. *Procedia Engineering*, 42, 885-891.
45. Wanchoo, R., Kaur, N., Bansal, A., Thakur, A., 2007. RTD in trickle bed reactors: Experimental study. *Chemical Engineering Communications*, 194 (11), 1503-1515.
46. Kulkarni, R., Natividad, R., Wood, J., Stitt, E., Winterbottom, J., 2005. A comparative study of residence time distribution and selectivity in a monolith CDC reactor and a trickle bed reactor. *Catalysis Today*, 105 (3-4), 455-463.
47. Pant, H.J., Saroha, A., Nigam, K., 2000. Measurement of liquid holdup and axial dispersion in trickle bed reactors using radiotracer technique. *Nukleonika*, 45 (4), 235-241.
48. Bošković, D., Loebbecke, S., 2008. Modelling of the residence time distribution in micromixers. *Chemical Engineering Journal*, 135, S138-S146.
49. Bošković, D., Löbbecke, S., 2006. Measurement and modelling of the residence time distribution in microfluidic devices. In: *ASME 4th International Conference On Nanochannels, Microchannels, and Minichannels*, American society of mechanical engineers, 795-801.
50. Commenge, J-M., Obein, T., Genin, G., Framboisier, X., Rode, S., Schanen, V., Pitiot, P., Matlosz, M., 2006. Gas-phase residence time distribution in a falling-film microreactor. *Chemical Engineering Science*, 61 (2), 597-604.
51. Trachsel, F., Günther, A., Khan, S., Jensen, K.F., 2005. Measurement of residence time distribution in microfluidic systems. *Chemical Engineering Science*, 60 (21), 5729-5737.
52. Sarkar, M., Sangal, V.K., Bhunia, H., 2020. Hydrodynamics and parametric study of an activated sludge process using residence time distribution technique. *Environmental Engineering Research*, 25(3), 400-408.
53. Sievers, D.A., Kuhn, E.M., Stickel, J.J., Tucker, M.P., Wolfrum, E.J., 2016. Online residence time distribution measurement of thermochemical biomass pretreatment reactors. *Chemical Engineering Science*, 140, 330-336.
54. Royaeae, S.J., Sohrabi, M., 2012. Comprehensive study on wastewater treatment using photo-impinging streams reactor: Residence time distribution and reactor modeling. *Industrial & Engineering Chemistry Research*, 51 (11), 4152-4160.
55. Pant, H.J., Sharma, V.K., Singh, G., Raman, V., Bornare, J., Sonde, R., 2012. Radiotracer investigation in a rotary fluidized bioreactor. *Journal of Radioanalytical and Nuclear Chemistry*, 294 (1), 59-63.
56. Borroto, J., Dominguez, J., Griffith, J., Fick, M., Leclerc, J., 2003. Technetium-99m as a tracer for the liquid RTD measurement in opaque anaerobic digester: Application in a sugar wastewater treatment plant. *Chemical Engineering and Processing: Process Intensification*, 42 (11), 857-865.

57. Shin, S., Kim, J., Jung, S., Jin, J., 2003., The RTD measurement on a submerged bio-reactor using a radioisotope tracer and the RTD analysis. *International Journal of Control, Automation, and Systems*,1, 201-215.
58. Prokop, A., Erickson, L., Fernandez, J., Humphrey, A., 1969., Design and physical characteristics of a multistage, continuous tower fermentor. *Biotechnology and Bioengineering*, 11 (5), 945-966.
59. Bogatykh, I., Osterland, T., 2019. Characterization of residence time distribution in a plug flow reactor. *Chemie Ingenieur Technik*, 91 (5), 668-672.
60. Onyemelukwe, I.I., Parsons, A.R., Wheatcroft, H.P., Robertson, A., Nagy, Z.K., Rielly, C.D., 2018. The role of residence time distribution in the continuous steady-state mixed suspension mixed product removal crystallization of glycine. *Crystal Growth & Design*,19 (1), 66-80.
61. Pant, H.J., Goswami, S., Biswal, J., Samantaray, J.S., Sharma, V.K., Singhal, S., 2016. Radiotracer investigation in a glass production unit. *Applied Radiation and Isotopes*,116, 41-50.
62. Puaux, J., Bozga, G., Ainser, A., 2000. Residence time distribution in a corotating twin-screw extruder. *Chemical Engineering Science*, 55 (9), 1641-1651.
63. Hornsby, P., Singh, D., Sothern, G., 1985. Determination of residence time distribution in polymer processing apparatus using tracer techniques. *Polymer Testing*, 5 (2), 77-97.
64. Sharma, V.K., Pant, H.J., Tandon, D., Garg, M.O., 2016. Radiotracer investigations in pilot-scale soakers. *Applied Radiation and Isotopes*, 107, 57-63.
65. Pant, H.J., Goswami, S., Samantray, J., Sharma, V., Maheshwari, N., 2015. Residence time distribution measurements in a pilot-scale poison tank using radiotracer technique. *Applied Radiation and Isotopes*,103, 54-60.
66. Pant, H.J., Sharma, V., Shenoy, K., Sreenivas, T., 2015. Measurements of liquid phase residence time distributions in a pilot-scale continuous leaching reactor using radiotracer technique. *Applied Radiation and Isotopes*,97, 40-46.
67. Jafari, M., Soltan, M.J.S., 2005. Mixing time, homogenization energy and residence time distribution in a gas-induced contactor. *Chemical Engineering Research and Design*,83 (5), 452-459.
68. Burkhardt, T., Verstraete, J., Galtier, P., Kraume, M., 2002. Residence time distributions with a radiotracer in a hydrotreating pilot plant: Upflow versus downflow operation. *Chemical Engineering Science*,57 (11), 1859-1866.
69. Emami-Meibodi, M., Soleimani, M., Bani-Najarian, S., 2018. Toward enhancement of rotating packed bed (RPB) reactor for CaCO₃ nanoparticle synthesis. *International Nano Letters*, 8 (3), 189-199.
70. Sánchez, F., Viedma, A., Kaiser, A., 2016. Hydraulic characterization of an activated sludge reactor with recycling system by tracer experiment and analytical models. *Water Research*, 101, 382-392.

71. Martinov, M., Hadjiev, D., Vlaev, S., 2010. Liquid flow residence time in a fibrous fixed bed reactor with recycle. *Bioresource Technology*, 101 (4), 1300-1304.
72. Haddad, A., Wolf, D., Resnick, W., 1964. Residence time distribution in multi-stage systems with recycle. *The Canadian Journal of Chemical Engineering*, 42 (5), 216-218.
73. Sinclair, C., McNaughton, K., 1965. The residence time probability density of complex flow systems. *Chemical Engineering Science*, 20 (4), 261-264.
74. Rippin, D., 1967. Recycle reactor as a model of incomplete mixing. *Industrial & Engineering Chemistry Fundamentals*, 6 (4), 488-492.
75. Hopkins, M., Sheppard, A., Eisenklam, P., 1969. The use of transfer functions in evaluating residence time distribution curves. *Chemical Engineering Science*, 24 (7), 1131-1137.
76. Hochman, J.M., McCord, J.R., 1970. Residence time distributions in recycle systems with crossmixing. *Chemical Engineering Science*, 25 (1), 97-107.
77. Fu, B., Weinstein, H., Bernstein, B., Shaffer, A., 1971. Residence time distributions of recycle systems - Integral equation formulation. *Industrial & Engineering Chemistry Process Design and Development*, 10 (4), 501-508.
78. Mah, R., 1971. Residence time distributions in discrete recycle systems with crossmixing. *Chemical Engineering Science*, 26 (2), 201-210.
79. Dohan, L.A., Weinstein, H., 1973. Generalized recycle reactor model for micro-mixing. *Industrial & Engineering Chemistry Fundamentals*, 12 (1), 64-69.
80. Mann, U., Crosby, E., 1973. Cycle time distribution in circulating systems. *Chemical Engineering Science*, 28 (2), 623-627.
81. Nauman, E., 1974. Residence times and cycle times in recycle systems. *Chemical Engineering Science*, 29 (9), 1883-1888.
82. Buffham, B., Nauman, E., 1975. On the limiting form of the residence-time distribution for a constant-volume recycle system. *Chemical Engineering Science*, 30 (12), 1519-1524.
83. Nauman, B., Buffham, B., 1977. Limiting forms of the residence time distribution for recycle system. *Chemical Engineering Science*, 32 (10), 1233-1236.
84. Rubinovitch, M., Mann, U., 1979. The limiting residence time distribution of continuous recycle systems. *Chemical Engineering Science*, 34 (11), 1309-1317.
85. Mann, U., Rubinovitch, M., Crosby, E.J., 1979. Characterization and analysis of continuous recycle systems. *AIChE Journal*, 25 (5), 873-882.
86. Mathur, V.K., Weinstein, H., 1980. Residence time distribution of the TRAM recycle reactor system. *Chemical Engineering Science*, 35 (6), 1449-1452.

87. Mann, U., Rubinovitch, M., 1981. Characterization and analysis of continuous recycle systems: Part II. Cascade. *AIChE Journal*, 27 (5), 829-836.
88. Buffham, B., Nauman, E., 1984. Residence-time distributions at high recycle ratios: Limiting forms obtained by increasing the recycle and by reducing the throughput. *Chemical Engineering Science*, 39 (5), 841-849.
89. Fan, L., Too, J., Nassar, R., 1985. Stochastic simulation of residence time distribution curves. *Chemical Engineering Science*, 40 (9), 1743-1749.
90. Waldram, S., 1987. Some general observations on the recycle flow model. *Chemical Engineering Science*, 42 (11), 2741-2744.
91. Battaglia, A., Fox, P., Pohland, F.G., 1993. Calculation of residence time distribution from tracer recycle experiments. *Water Research*, 27 (2), 337-341.
92. Pant, H.J., Kundu, A., Nigam, K., 2001. Radiotracer applications in chemical process industry. *Reviews in Chemical Engineering*, 17 (3), 165-252.
93. Montgomery, D.C., 2012. *Design and Analysis of Experiments*, 8th ed. New Jersey: John Wiley & Sons.
94. Stern, F., Muste, M., Beninati, M., Eichinger, W.E., 1999. *Summary of Experimental Uncertainty Assesment Methodolgy with Example*. IIHR: Iowa, Technical Report No. 406.
95. Coleman, H.W., Steele, W.G., 2009. *Experimentation, Validation, and Uncertainty Analysis for Engineers*, 3rd ed. New Jersey: John Wiley & Sons.
96. Bevington, P.R., Robinson, D.K., Blair, J.M., Mallinckrodt, A.J., McKay, S., 1993. Data reduction and error analysis for the physical sciences. *Computers in Physics*, 7 (4), 415-416.
97. Tukey, J.W., 1949. One degree of freedom for non-additivity. *Biometrics*, 5 (3), 232-242.
98. Kennedy, M.C., O'Hagan, A., 2001. Bayesian calibration of computer models. *Journal of the Royal Statistical Society: Series b (statistical methodology)*, 63 (3), 425-464.
99. Daniel, C., 1973. One-at-a-time plans. *Journal of the American Statistical Association*, 68 (342), 353-360.

List of publications

I. In peer reviewed (SCI) journals

Published

1. **Arghya Datta**, Raj Kumar Gupta, Sunil Goswami, Vijay Kumar Sharma, Haripada Bhunia, Damandeep Singh, Harish Jagat Pant, **“Residence time distribution measurements in an ethyl acetate reactor using radiotracer technique”**. *Journal of Radioanalytical and Nuclear Chemistry*, 320 (2019) 711-723(Impact Factor: 1.137)
2. **Arghya Datta**, Raj Kumar Gupta, Sunil Goswami, Vijay Kumar Sharma, Haripada Bhunia, Damandeep Singh, Harish Jagat Pant, **“Radiotracer investigation for measurement of residence time distribution in an ethyl acetate reactor system with large recycle ratio”**. *Applied Radiation and Isotope*, 130 (2017) 245–251 (Impact Factor: 1.270)

Under review

1. **Arghya Datta**, Haripada Bhunia, Raj Kumar Gupta, **“Residence time distribution studies on recycle reactor with recirculation”**. *International Journal of Chemical Reactor Engineering*, (Manuscript ID - IJCRE-2021-0024)

II. Presentations in conferences

International conferences

1. **Arghya Datta**, Raj Kumar Gupta, Sunil Goswami, Vijay Kumar Sharma, Haripada Bhunia, Damandeep Singh, Harish Jagat Pant, **“Residence time distribution studies on plant scale recycle reactor”** *International Conference on Advanced Applications of Radiation Technology*, March 5-7, 2018, Mumbai, India
2. **Arghya Datta**, Raj Kumar Gupta, Sunil Goswami, Vijay Kumar Sharma, Haripada Bhunia, Damandeep Singh, Harish Jagat Pant, **“Residence time distribution measurements in industrial scale reactors with recycle using radiotracer technique”** *International Conference on Applications of Radiation and Technology*, April 24-28, 2017, Vienna, Austria.

National Conferences

1. **Arghya Datta**, Raj Kumar Gupta, Sunil Goswami, Vijay Kumar Sharma, Haripada Bhunia, Damandeep Singh, Harish Jagat Pant, “**Residence time distribution studies in reactors with recirculation**” *CHEMCON 2018*, December 27-30, 2018, Dr. B. R. Ambedhkar NIT Jalandhar, Punjab
2. **Arghya Datta**, Raj Kumar Gupta, Sunil Goswami, Vijay Kumar Sharma, Haripada Bhunia, Damandeep Singh, Harish Jagat Pant, “**Radiotracer Studies on Industrial Scale Ethyl Acetate Reactor**” *Application of Radiation and Radioisotope Technology in Industry, Healthcare and Agriculture*, November 28-29, 2016, Thapar University, Patiala, Punjab



Residence time distribution measurements in an ethyl acetate reactor using radiotracer technique

Arghya Datta¹ · Raj Kumar Gupta¹ · Sunil Goswami² · Vijay Kumar Sharma² · Haripada Bhunia¹ · Damandeep Singh³ · Harish Jagat Pant²

Received: 27 January 2019
© Akadémiai Kiadó, Budapest, Hungary 2019

Abstract

In the present study, residence time distribution measurements were carried out in an industrial-scale ethyl acetate reactors using Bromine-82 as radiotracer. The process fluid is re-circulated into the reactor at a high flow instead of mechanical agitation inside the reactor to facilitate the mixing. The objective of the study was to measure the effect of recirculation rate on the mean residence time and flow pattern process of material in the reactor. The results showed that recirculation significantly affects the flow characteristics and mean residence time of the reactors. A bypass stream and stagnant fluid zones present in the system and their fraction affected by recirculation in both the reactors.

Keywords Residence time distribution · Mean residence time · Bypassing · Stagnant volume · Radiotracer · Bromine-82

Introduction

Chemical process reactors are designed to have either of the ideal flow patterns i.e. well-mixed flow or plug-flow pattern. However, the flow behavior of real reactors always deviates

from these ideal flow conditions. Non-ideality in their flow behaviour occurs due to one or more of the flow abnormalities such as bypassing, stagnant zones, channeling etc. occurring inside the reactors [1, 2]. Nonideal flow patterns can lead to significant deterioration in product quality and loss of process efficiency leading to significant economic losses to the concerned industry. These can also be detrimental to the industrial plant and the environment [3, 4]. Measurement of residence time distribution (RTD) of process material and its analysis is an imperative approach for distinguishing the irregularity in the process reactors in the chemical industry. The RTD in industrial reactors is measured using stimulus–response technique and used to identify/quantify several flow abnormalities [2]. In this method an impulse of tracer (dye, salt or radioactivity) is injected at inlet of the system and their response is measured at inlet and outlet of the reactor. Conventional tracers such as dyes (change in color), chemicals (change in concentration) and salts (change in conductivity) are used to measure the RTD of the process material in laboratory-scale systems. However, conventional tracers cannot be used for measurement of process material in large-scale industrial systems. Therefore, radiotracers are the only alternative to measure RTD of process material in industrial scale reactor [5–7]. The radiotracer have various advantages over conventional tracer such as high detection sensitivity, in situ detection, online detection, physical chemical compatibility, limited memory

✉ Harish Jagat Pant
hjgant@barc.gov.in
Arghya Datta
arghya.datta@thapar.edu
Raj Kumar Gupta
rk Gupta@thapar.edu
Sunil Goswami
gsunil@barc.gov.in
Vijay Kumar Sharma
vksharma@barc.gov.in
Haripada Bhunia
hbhunias@thapar.edu
Damandeep Singh
damandeep@iolcp.com

¹ Department of Chemical Engineering, Thapar Institute of Engineering and Technology, Patiala, Punjab 147001, India

² Isotope and Radiation Application Division, Bhabha Atomic Research Centre, Mumbai 400085, India

³ IOL Chemicals and Pharmaceuticals Limited, Barnala 148101, India



Radiotracer investigation on the measurement of residence time distribution in an ethyl acetate reactor system with a large recycle ratio



Arghya Datta^a, Raj Kumar Gupta^a, Sunil Goswami^b, Vijay Kumar Sharma^b, Haripada Bhunia^a, Damandeep Singh^c, Harish Jagat Pant^{b,*}

^a Department of Chemical Engineering, Thapar University, Patiala, Punjab 147001, India

^b Isotope and Radiation Application Division, Bhabha Atomic Research Centre, Mumbai 400085, India

^c IOL Chemicals and Pharmaceuticals Limited, Barnala, India

HIGHLIGHTS

- A radiotracer investigation was carried out in an ethyl acetate reactor system.
- RTDs were measured at different operating conditions and MRTs were determined.
- Measured RTDs were treated and simulated using suitable mathematical models.
- Stagnant volumes and bypass fractions of the flow were estimated.

ARTICLE INFO

Keywords:

Ethyl acetate reactor
Radiotracer
Bromine-82
Residence time distribution
Mean residence time
Bypassing
Stagnant volume
Continuously stirred tank reactor

ABSTRACT

A radiotracer investigation was carried out on the measurement of residence time distribution (RTD) of process fluid in an industrial-scale ethyl acetate reactor system, which consists of two independent reactors with recirculation and connected in series with each other. Bromine-82 as ammonium bromide was used as the radiotracer for the RTD experiments at different operating conditions. The individual reactors and the overall reactor system were modelled using physically representative phenomenological models comprising of continuously stirred tank reactors (CSTRs). The results showed that the recirculation rate considerably affected the flow mixing behaviour and mean residence time of the process fluid in the reactor system. The results also showed that there was bypassing of the fluid in the first reactor that ranged from 12% to 22% and 40% dead volume at different operating conditions, whereas the second reactor behaved closely as an ideal CSTR. The results of the investigation can be used to optimise the process parameters and design new improved reactor systems for the production of ethyl acetate.

1. Introduction

In chemical engineering, an equipment is designed to behave as either an ideal plug flow reactor (PFR) or an ideal continuously stirred tank reactor (CSTR) depending upon the process requirement. However, in actual operating systems, the flow patterns deviate from the designed ideal flow patterns because of the occurrence of one or more abnormalities such as bypassing, dead zones and channelling (Fogler, 2004). These abnormalities cause deviation in the flow patterns and eventually lead to deterioration in product quality and decrease in process efficiency, thereby causing significant economic loss for the industry and even posing a threat to the manufacturing plants and the environment (Pant and Yelgoankar, 2002; Othman and Kamarudin,

2014). Measurement and analysis of residence time distribution (RTD) of process material is an important approach to identify abnormalities, if any, and to investigate the hydrodynamics of process equipment in the chemical process industry. The approach is very reliable and provides valuable information about the performance of process equipment such as reactors and columns (Levenspiel, 1998). This is also used for the evaluation and optimisation of the design of laboratory and pilot-scale systems at the design stage.

Conventional tracer techniques using dyes, chemicals and salts are often used to measure the RTD of process fluid in laboratory-scale systems; however, they cannot be applied to pilot-scale and large-scale industrial systems because of their many disadvantages (van Gelder and Westerterp, 1990; Jafari and Soltan Mohammadzadeh, 2005; Le

* Corresponding author.

E-mail address: hjpant@barc.gov.in (H. Jagat Pant).

<http://dx.doi.org/10.1016/j.apradiso.2017.09.039>

Received 21 February 2017; Received in revised form 3 September 2017; Accepted 22 September 2017

Available online 25 September 2017

0969-8043/© 2017 Elsevier Ltd. All rights reserved.